The United Nations University

GEOLOGY, HYDROTHERMAL ALTERATION AND FLUID INCLUSION STUDIES OF OLKARIA DOMES GEOTHERMAL FIELD, KENYA

MSc Thesis
Department of Geology and Geography
University of Iceland

by

John Kipng'etich Lagat
Kenya Electricity Generating Co., Ltd.
Olkaria Geothermal Project
P.O. Box 785, Naivasha
KENYA

This MSc thesis has also been published in April 2004 by the
Department of Geology and Geography,
University of Iceland

INTRODUCTION

The Geothermal Training Programme of the United Nations University (UNU) has operated in Iceland since 1979 with six months annual courses for professionals from developing countries. The aim is to assist developing countries with significant geothermal potential to build up groups of specialists that cover most aspects of geothermal exploration and development. During 1979-2004, 318 scientists and engineers from 39 countries have completed the six months courses. They have come from Asia (44%), Africa (26%), Central America (14%), and Central and Eastern Europe (16%). There is a steady flow of requests from all over the world for the six months training and we can only meet a portion of the requests. Most of the trainees are awarded UNU Fellowships financed by the UNU and the Government of Iceland.

Candidates for the six months specialized training must have at least a BSc degree and a minimum of one year practical experience in geothermal work in their home countries prior to the training. Many of our trainees have already completed their MSc or PhD degrees when they come to Iceland, but several excellent students who have only BSc degrees have made requests to come again to Iceland for a higher academic degree. In 1999, it was decided to start admitting one or two outstanding UNU Fellows per year to continue their studies and study for MSc degrees in geothermal science or engineering in co-operation with the University of Iceland. An agreement to this effect was signed with the University of Iceland. The six months studies at the UNU Geothermal Training Programme form a part of the graduate programme.

It is a pleasure to introduce the fourth UNU Fellow to complete the MSc studies at the University of Iceland under the co-operation agreement. Mr. John K. Lagat, geologist of the Kenya Electricity Generating Co. Ltd., completed the six months specialized training at the UNU Geothermal Training Programme in October 1995. His research report was entitled "Borehole geology and hydrothermal alteration of well OW-30 Olkaria geothermal field, Kenya". After seven years of research work as borehole geologist in Olkaria, he came back to Iceland for MSc studies at the Faculty of Science of the University of Iceland in September 2002. He defended his MSc thesis presented here, entitled "Geology, hydrothermal alteration and fluid inclusion studies of Olkaria Domes geothermal field, Kenya" in April 2004. His studies in Iceland were financed by a fellowship from the Government of Iceland through the UNU Geothermal Training Programme. We congratulate him on his achievements and wish him all the best for the future. We thank the Faculty of Science of the University of Iceland for the co-operation, and his supervisors for the dedication.

With warmest wishes from Iceland,

Ingvar B. Fridleifsson, director,
United Nations University
Geothermal Training

ACKNOWLEDGEMENTS

ABSTRACT

Three geothermal exploration wells OW-901, OW-902 and OW-903 were drilled in Olkaria Domes field to evaluate its geothermal potential. The three wells were drilled to a depth of 2200 m and all encountered a high temperature system and discharged on test. The highest recorded measured temperatures in the wells are; 342˚C at -290 masl, 248˚C at 207 masl and 341˚C at -107 masl for wells OW-901, OW-902 and OW-903 m respectively. Rocks encountered in the wells include pyroclastics, rhyolite, tuff, trachyte, basalt and minor dolerite and microsyenite intrusives. Fractures, vesicles, spaces between breccia fragments, glassy rocks and primary minerals exhibit little or no hydrothermal alteration in the upper parts of the wells with mainly silica, calcite, zeolites, phyllosilicates, oxides and sulphides being the alteration minerals present. In the deeper parts of the wells, however, hydrothermal alteration to ranged from high to extensive. Hydrothermal zeolites, calcite, epidote, phyllosilicates, silica, sulphides, epidote, albite, adularia, biotite, garnet, fluorite, prehnite, oxides and titanite are the alteration minerals observed. The most important hydrothermal alteration controls in Olkaria Domes field are temperature, rock types and permeability. Four hydrothermal alteration zonations can be recognized in the field based on the distribution of the hydrothermal alteration minerals. They are in the order of increasing depth and temperature; the zeolite-chlorite, the illite-chlorite, the illite-chlorite-epidote and the garnet-biotite-actinolite zones. Hydrothermal alteration temperatures correlate well with the measured formation temperatures in wells OW-901 and OW-903 indicating probable equilibrium conditions with the geothermal system in that sector of the field. In well OW-902, however, a high temperature alteration mineral (garnet) was observed at depths where current measured formation temperature is 246˚C. This phase now exist where the present temperature is much lower than what would be expected from its thermal stability range, which is over 300˚C. This indicates that cooling must have occurred in that part of the field. Fluid inclusions in quartz and calcite veins from well OW-901 and quartz veins in OW-903 indicate that heating must have occurred in that sector of the field with present temperatures being higher than the average fluid inclusions homogenization temperatures by as much as 60˚C. In well OW-902, however, homogenization temperatures reflect more or less present condition with measured temperatures being close to the average fluid inclusion homogenization temperatures. Feeder zones in the wells are mainly confined to faults, fractures, joints and lithologic contacts. Observations from hydrothermal alteration mineralogy, pressure and temperature profiles indicate that well OW-901 is close to the upflow whereas well OW-903 is in the outflow zone and well OW-902 is in the outflow and also the marginal zone of the field.

TABLE OF CONTENTS

LIST OF FIGURES

LIST OF PLATES

LIST OF TABLES

PREFACE

Geothermal energy is a clean and reliable source for production of electricity, which is not affected by short-term fluctuations in the weather or world producer prices of oil. Once installed, maintenance costs are low and availability high as evident from the records for the Olkaria I power station in Kenya. Geothermal investigations in the Kenya rift started in 1956. Further work, which produced positive results, was carried out when two exploratory wells (OW-X1 and OW-X2) were drilled to a depth of 502 m and 942 m for OW-X1 and OW-X2 respectively at Olkaria in the late fifties. Between 1970 and 1972, investigations were carried out at Olkaria, Lake Bogoria and in the Eburru area. Intensive drilling at Olkaria started in 1973 and by 1975 four more wells had been drilled in the area. Today over 95 wells have been drilled for exploration, production, monitoring and re-injection with depths varying from between 180 and 2,600 meters deep. Of these, 89 wells are in the Greater Olkaria geothermal area while the remaining six are in the Eburru geothermal field.

The Least Cost Generation Expansion program has identified geothermal power to be the least cost source of power in Kenya. Based on this program, the National Power Development Plan requires 576 MWe of geothermal power to be installed by the year 2019. The known geothermal prospects occur within the Kenya rift valley where widespread volcanic activity and geothermal manifestations signify the existence of viable geothermal prospects. To meet the geothermal component in the next 15 or so years, it is necessary that detailed geothermal exploration is carried out in these prospect areas along the Kenya rift. Olkaria Domes is one of the fields in the Greater Olkaria geothermal area within the Kenya rift. Three exploration wells have been drilled in this field and appraisal drilling is expected to commence soon. Representative cuttings samples from the three wells were shipped to Iceland to be studied as part of a Master of Science project thesis at the University of Iceland.

This thesis is submitted to the University of Iceland (HÍ), as part of the requirements of a Master of Science degree in Geology. The thesis accounts for 30 of the 60 credits, required for the degree, 15 credits were earned at the United Nations University Geothermal Training Programme, Iceland and the remaining 15 credits were covered as course work at the University of Iceland.

1.0 INTRODUCTION

The Greater Olkaria geothermal area is situated south of Lake Naivasha on the floor of the southern segment of the Kenya rift (Figure 1). The Kenya rift is part of the East African rift system that runs from Afar triple junction at the Gulf of Eden in the north to Beira, Mozambique in the south. It is the segment of the eastern arm of the rift that extends from Lake Turkana to the North to Lake Natron, northern Tanzania to the south (Figure 1). The rift is part of a continental divergent zone where spreading occurs resulting to the thinning of the crust hence eruption of lavas and associated volcanic activities.

The Greater Olkaria geothermal area (Figure 2) is within the Greater Olkaria volcanic complex. It is subdivided into seven fields for geothermal development purposes namely Olkaria East, Olkaria Northeast, Olkaria Central, Olkaria Northwest, Olkaria Southwest, Olkaria Southeast and Olkaria Domes (Figure 3). Olkaria East field (Olkaria I) has been producing power since 1981 when the first
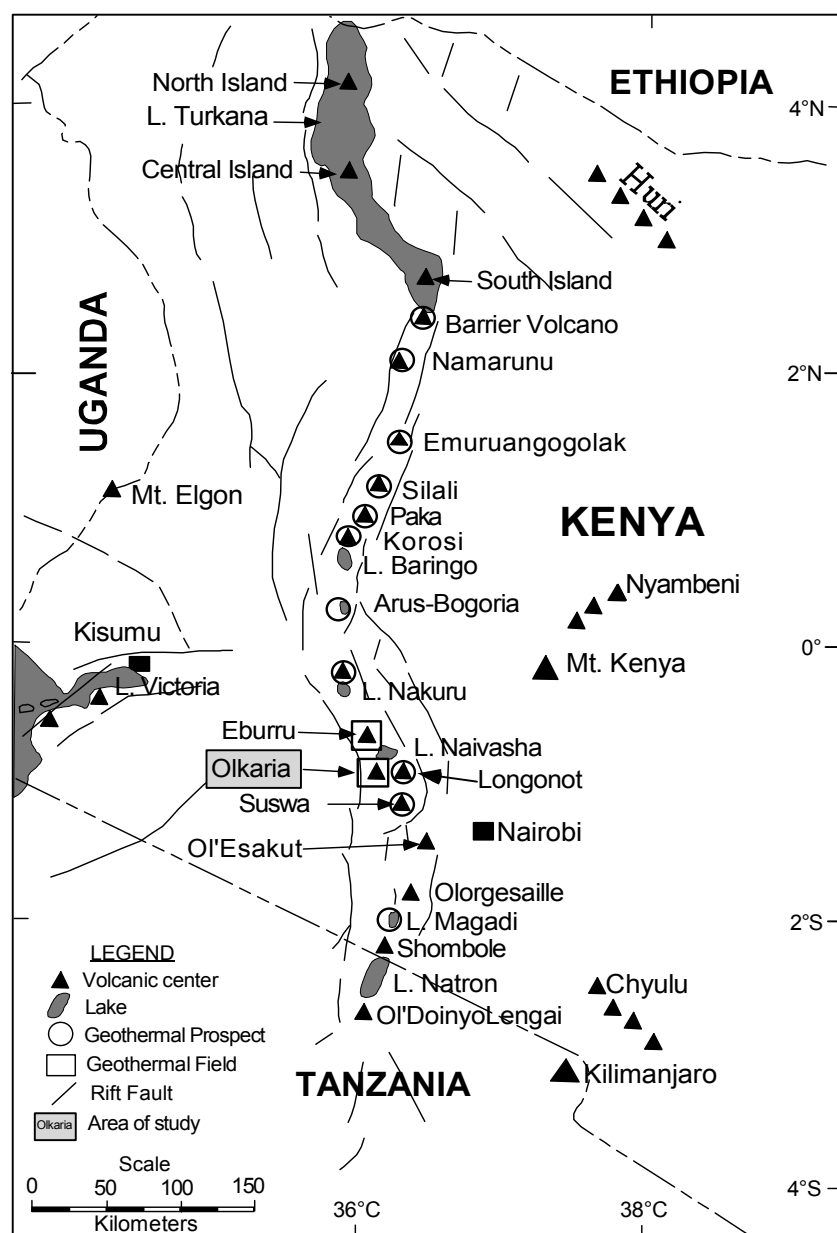
FIGURE 1: Map of the Kenya rift showing the location of Olkaria geothermal field and other Quaternary volcanoes along the rift axis

2

of the three 15 MWe units was commissioned. The current generating capacity of the field is 45 MWe. Olkaria Northeast field (Olkaria II) is generating 70 MWe and Olkaria Northwest field (Olkaria III) which is being developed by an Independent Power Producer (IPP) is currently producing 12 MWe and will have a capacity of 48 MWe when the construction of the power plant is completed in 2005. The rest of the fields are at various exploration stages.

Olkaria Domes, which is the field of focus in this study is the area approximately bound by the Hell's Gate – Ol'Njorowa gorge to the west and a ring of domes to the east and south of the area (Figure 2). Detailed surface investigations were conducted in the area in 1992/93, which led to the development of a basic working model, from which recommendations for drilling of exploration wells were made. Three exploration wells OW-901, OW-902 and OW-903 were drilled in the field between September 1998 and May 1999. All the three wells encountered a high temperature system and discharged on test. Appraisal drilling is to commence soon and therefore better understanding of the field is vital for best results to be achieved. The field is earmarked to be developed as Olkaria IV.
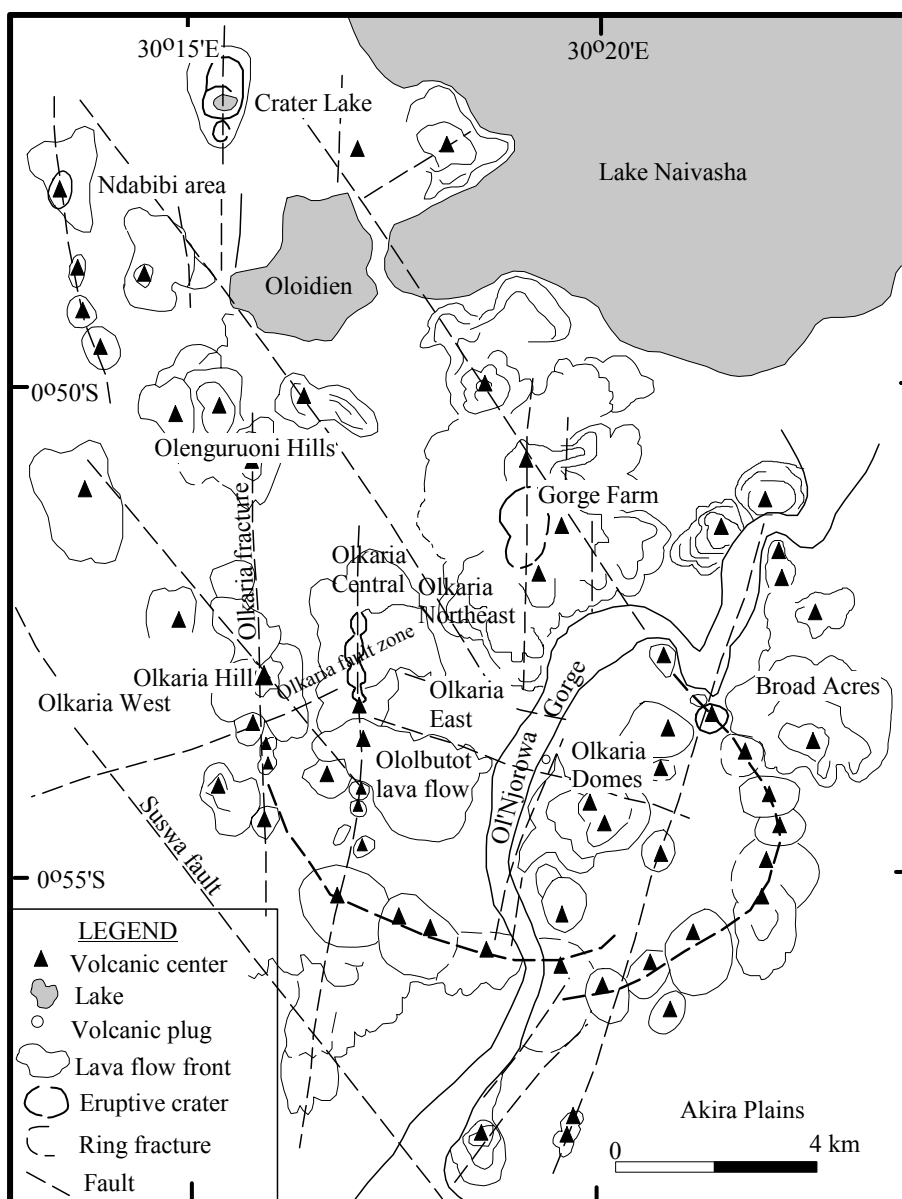
FIGURE 2: Volcano-tectonic map of the Greater Olkaria
volcanic complex (modified from Clarke et al., 1990)

FIGURE 3: Map of the Greater Olkaria geothermal area showing
the subdivisions of the fields (KenGen, 2000)

1.1 Objectives of the study

- To identify the rocks penetrated by wells OW-901, OW-902 and OW-903 and thereby gain knowledge of the stratigraphy and the structures of Olkaria Domes geothermal field.
- To identify the hydrothermal alteration minerals found in Olkaria Domes and to obtain a better understanding of the water rock interaction processes occurring in this active hydrothermal system.
- To identify the textural relationships of these minerals to provide clues about the past and present conditions of Olkaria Domes reservoir.
- To determine the general location of the wells with respect to the upflow, outflow and the marginal zones of the system.
- To determine the appropriate casing depths in the field.

2.0 GEOLOGY

2.1 Regional geology

The evolution of the East African rift system was structurally controlled with the rift faults exploiting the weak collisional zone at the contact between the Archean Tanzania craton and Proterozoic orogenic belts (Smith and Mosley, 1993). The development of the rifting within Kenya started during the late Oligocene (30 Ma) in the area known as the Turkana rift (Baker et al., 1971, 1972; Kampunzu and Mohr, 1991; Smith, 1994). Volcanism associated with rifting started during the Miocene. The magmatic activity was accompanied by domal uplift of about 300 m on the crest of which erupted phonolites (Baker and Wohlenberg, 1971, Williams, 1972, Lippard, 1973, Hay and Wendlandt, 1995, Hay et al., 1995a, b). Because this volcanism preceded the major rift faulting events, the rifting process has been modeled as active with the driving force being provided by convecting asthenospheric mantle (Baker et al., 1971, 1972; Baker and Wohlenberg, 1971). The total volume of eruptive rocks associated with rifting is estimated to be more than 220,000 km^3 (Williams, 1972; Baker, 1987).

The Miocene volcanics were subsequently faulted and then followed by massive and extensive Pliocene eruption of trachytic ignimbrites in the central area to form the Mau and Kinangop Tuffs. A second faulting episode, which followed the ignimbrite eruptions, resulted in the formation of the graben structure, as it is known today. In the developing graben, fissure eruptions of trachytes, basalts, basaltic trachyandesites, and trachyandesites occurred. The plateau rocks that filled the developing graben were then block faulted to create high angle normal faults within the rift floor. The fractures apparently served as conduits for the Quaternary volcanic activity of mafic to felsic composition. The most intense volcanic activity occurred within the central sector of the rift where the volcanic succession is thought to be of the order of 5 km thick. This thickness is estimated from seismic data (Henry et al., 1990, Simiyu et al., 1995, Simiyu et al., 1997), stratigraphic correlation (e.g. Baker et al., 1972), and information from geothermal wells drilled in Olkaria area.

2.2 Geology of the Greater Olkaria volcanic complex

The Greater Olkaria volcanic complex is characterized by numerous volcanic centres of Quaternary age and is the only area within the Kenya rift with occurrences of comendite on the surface. Other Quaternary volcanic centres adjacent to Olkaria include Longonot volcano to the southeast, Suswa caldera to the south, and the Eburru volcanic complex to the north (Figure 1). Whereas the other volcanoes are associated with calderas of varying sizes, Olkaria volcanic complex does not have a clear caldera association. The presence of a ring of volcanic domes in the east and south, and southwest has been used to invoke the presence of a buried caldera (Figure 2 and 4; Naylor, 1972, Virkir, 1980, Clarke et al., 1990, Mungania, 1992). Seismic wave attenuation studies for the whole of the Olkaria area also indicate an anomaly in an area coinciding with the proposed caldera (Simiyu et al., 1998). Other studies on Olkaria have not identified the existence of the caldera e.g., resistivity studies do not map a clear discontinuity at the margin of the proposed caldera (Onacha, 1993). Ignimbrite flows that could have been associated with the caldera collapse have not been positively identified in Olkaria (Omenda, 1998a). Also, petrochemistry of lavas within the Olkaria area shows that they were produced from discrete magma chambers. Another explanation to the caldera hypothesis would be that the ring structure was produced by magmatic stresses in the Olkaria "magma chamber" with the line of weakness being loci for volcanism (Omenda 2000).

Magmatic activity associated with Olkaria volcanic complex commenced during the late Pleistocene and continues to Recent as indicated by Ololbutot comendite, which, has been dated at 180±50 yrs B.P using ^{14}C from carbonized wood obtained from a pumice flow associated with the lava (Clarke et al., 1990).
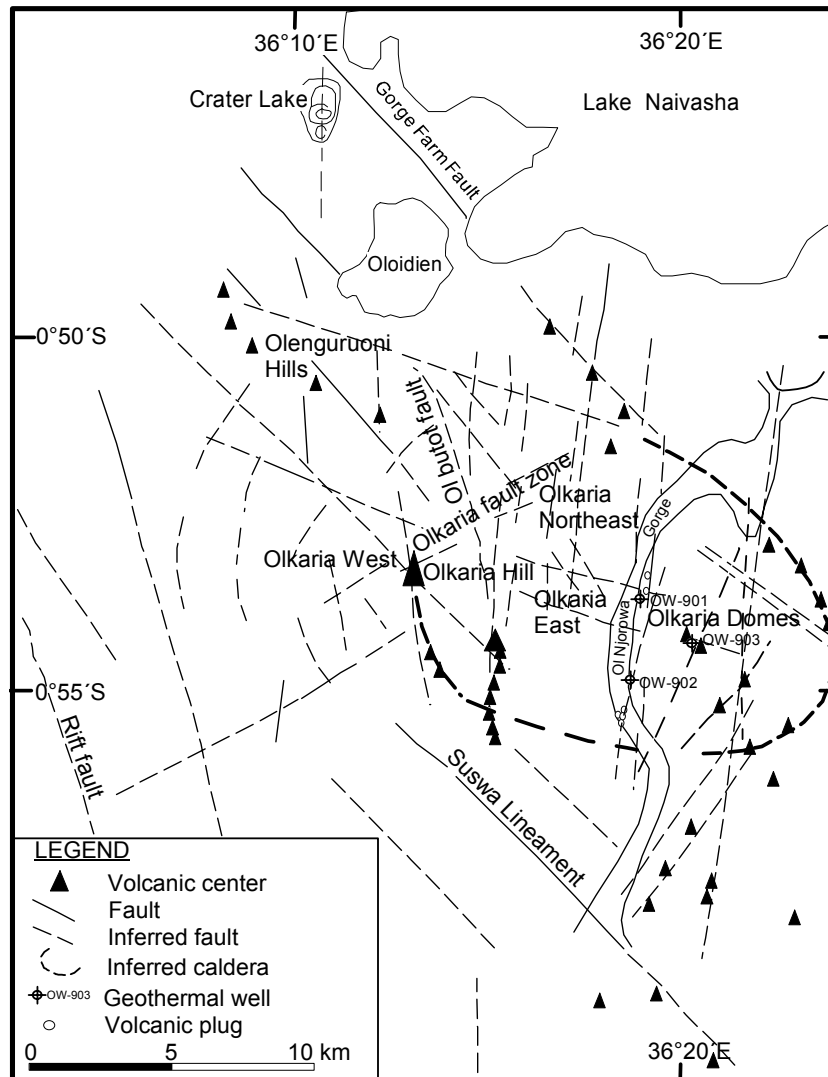
FIGURE 4: Structural map of Greater Olkaria geothermal area
based on SPOT satellite image and aerial photographs.
Modified from Muchemi (1992) and Mungania (1992)

2.3 Subsurface geology of the Greater Olkaria volcanic complex

The litho-stratigraphy of the Olkaria geothermal area as revealed by data from geothermal wells and regional geology can be divided into six main groups; namely Proterozoic "basement" formations, Pre-Mau volcanics, Mau tuffs, plateau trachytes, Olkaria basalt and Upper Olkaria volcanics (Omenda, 2000). The formations are hereby briefly discussed below in a chrono-stratigraphic order from the oldest to the youngest.

The "basement" rock in the area is considered to be the Proterozoic amphibolite grade gneisses and schists and the associated marble and quartzites of the Mozambiquan group (Shackleton, 1986, Mosley, 1993, Smith and Mosley, 1993). The rocks outcrop on the far flanks of the rift, more so, toward Magadi area in the south. In the south-central sector of the Kenya rift, the rocks are largely composed of gneisses and schists. Reflection seismic, gravity and geological correlation indicate that the depth to the "basement" is about 5-6 km in central Kenya rift (Simiyu et al., 1995, Simiyu and Keller, 1997). Seismic and gravity studies indicate the presence of a high-density magmatic intrusion into the metamorphic ''basement'' rocks (Baker and Wohlenberg, 1971, Baker et al., 1971, Simiyu, 1996).

6

The Pre-Mau formation is not exposed in the area but outcrops on the rift scarps in the parts of the southern Kenya rift. The rocks are composed of trachytes, basalts and ignimbrites and are of unknown thickness. These rocks are directly overlain by the Mau tuffs that are Pleistocene in age. Mau tuffs are the oldest rocks that crop out in the Olkaria area. These rocks are common in the area west of Olkaria Hill, but are absent in the east due to an east dipping high angle normal fault that passes through Olkaria Hill (Omenda 1994, 1998a). The rocks vary in texture from consolidated to ignimbritic and are the main geothermal reservoir rocks in the Olkaria west field as observed from drill chippings from the geothermal boreholes in the area.

Plateau trachytes encountered in the boreholes in the Olkaria area are part of the Kenya rift floor fissure flows that are well exposed in the south and north of Olkaria area. The formation is of Pleistocene age and occurs from about 1000 m to more than 2600 m in depth (Ogoso-Odongo, 1986; Omenda, 1994, 1998a). Trachytes are the main rock of the formation but minor basalts, tuffs, and rhyolites occur. The Plateau trachytes occur in the area to the east of Olkaria Hill where a graben existed prior to their eruptions (Omenda, 1994, 1998a). These rocks are the host for the geothermal reservoir for the eastern Olkaria geothermal fields.

The Olkaria basalt underlies the Upper Olkaria volcanics in the area to the east of Olkaria Hill while the formation is absent to the west. The formation consists of basalt flows and minor pyroclastics and trachytes. The formation varies in thickness from 100 m to 500 m and is considered to act as cap-rock for the Olkaria geothermal system (Haukwa, 1984, Ambusso and Ouma, 1991, Omenda, 1998a).

The Upper Olkaria formation consists of comendite lavas and their pyroclastic equivalents, ashes from Suswa and Longonot volcanoes and minor trachytes and basalts (Thompson et al., 1963, Clarke et al., 1990, Omenda, 1998a). These rocks occur from the surface down to about 500 m depth. Comendite is the dominant rock in this formation. The youngest of the lavas is the Ololbutot comendite, which, has been dated at 180±50 yrs (Clarke et al., 1990). The vents for these young lavas and pyroclastics were structurally controlled with most of the centres occurring along N-S faults/fractures and a ring structure (Figure 3 and 4).

2.4 Structures in the Greater Olkaria volcanic complex

Structures in the Greater Olkaria volcanic complex include; the ring structure, the Ol'Njorowa gorge, the ENE-WSW Olkaria fault and N-S, NNE-SSW, NW-SE and WNW-ESE trending faults (Figure 4). The faults are more prominent in the East, Northeast and West Olkaria fields but are scarce in the Olkaria Domes area, possibly due to the thick pyroclastics cover. The NW-SE and WNW-ESE faults are thought to be the oldest and are associated with the development of the rift. The most prominent of these faults is the Gorge Farm fault, which bounds the geothermal fields in the northeastern part and extends to the Olkaria Domes area. The most recent structures are the N-S and the NNE-SSW faults. Hydroclastic craters located on the northern edge of the Olkaria Domes area mark magmatic explosions, which occurred in submerged country (Mungania, 1999). These craters form a row along where the extrapolated caldera rim trace passes. Dike swarms exposed in the Ol'Njorowa gorge trend in a NNE direction further attesting to the recent reactivation of faults with that trend. The development of the Ol'Njorowa gorge was initiated by faulting along the trend of the gorge but the feature as it is known today was mainly due to catastrophic outflow of Lake Naivasha during its high stands (Clarke et al., 1990). Volcanic plugs (necks) and felsic dikes occurring along the gorge further attests to the fault control in the development of this feature (Plate 1).

Subsurface faults have been encountered in most Olkaria wells as reported in geological well reports (Ryder, 1986; Mungania, 1991; Lagat, 1998 and KenGen, 2000). The wells encountered drilling problems when these faults were dissected due to cave-ins and loss of drilling fluids and cement. Materials collected when the circulation of the drilling fluid was normalized were mainly fault breccia.

PLATE 1: Volcanic necks created due to the cutting of deep drainage channels
caused by catastrophic flooding of Lake Naivasha

2.5 Geophysics

Geophysical studies have been carried out in Olkaria geothermal area since early sixties but most of
the detailed work which included resistivity, gravity, seismology and magnetic were conducted in the
1980's and continues to the present date. Resistivity studies have been carried out by many workers
(Mwangi, 1986; Furgerson, 1972; Dimitrios, 1989; Onacha, 1989; Onacha, 1990 and Onacha, 1993).
The analysis is based on transient electromagnetic (TEM), DC Schlumberger and magnetotelluric
(MT) soundings. The results from these measurements indicate that the low resistivity anomalies are
controlled by structural trends and that the geothermal resource is defined by a low resistivity of 15
Ωm (Figure 5) at 1000 masl.

FIGURE 5: Integrated TEM and DC Schlumberger resistivity (Ωm) at
1000 masl (KenGen, 2000). The gray/yellow stars represent the ring fracture

Interpretation of gravity data within the Greater Olkaria area shows that a dense body occurs at the southern part of Olkaria between the Ol'Njorowa gorge and the Suswa lineament (Figure 6). The Olkaria West, Olkaria East and Olkaria northeast fields occur within gravity lows. The gravity survey of the shallow crust beneath Olkaria (Ndombi, 1981) indicated a volcanic zone of three layers that is down-faulted in the Olkaria West area. Dense dike material of rhyolitic composition occurs along the Ololbutot fault separating the western and eastern sectors of Greater Olkaria geothermal area. This system of dikes is thought to be a significant hydrogeological barrier between Olkaria West and Olkaria East and Olkaria Northeast fields.
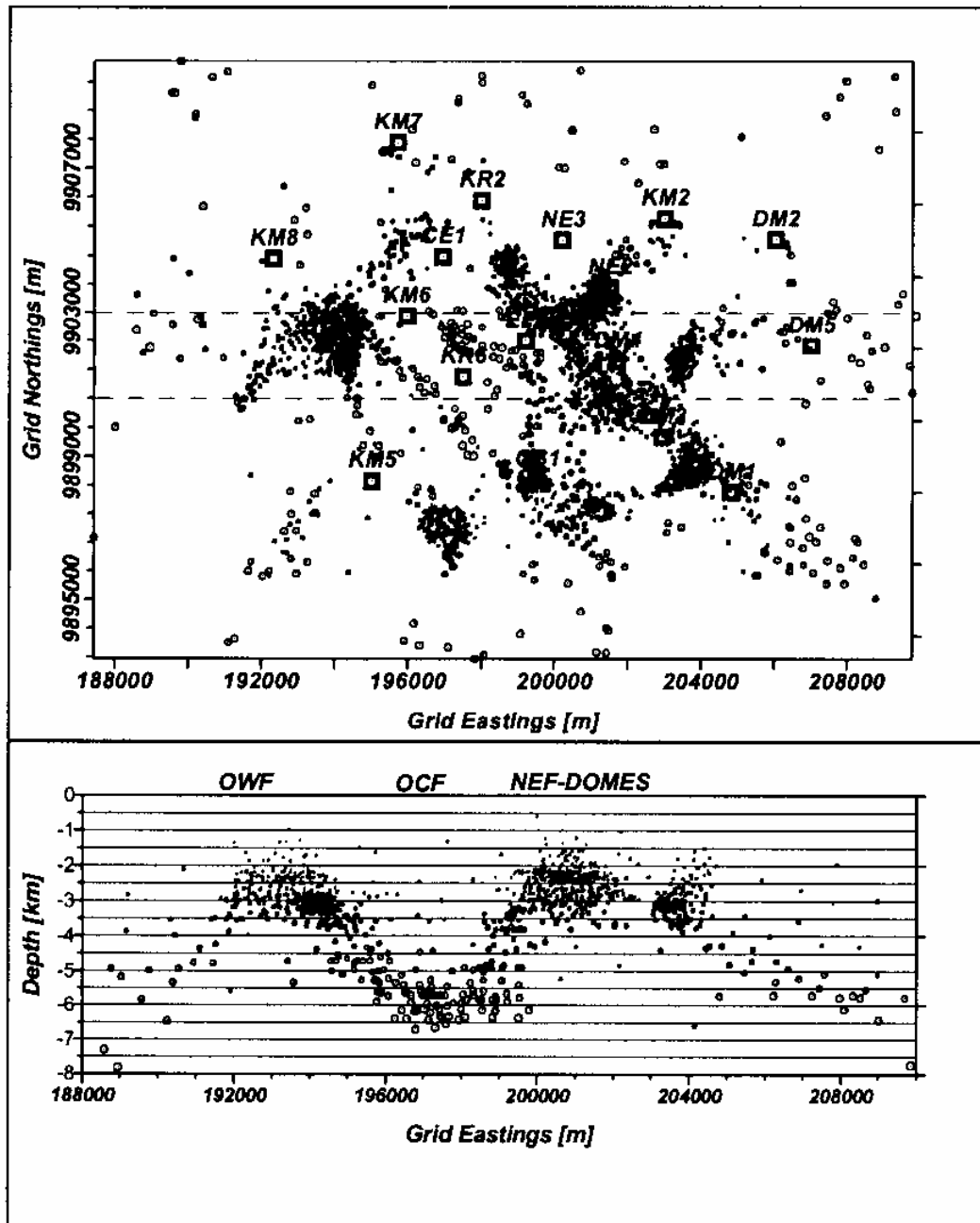
FIGURE 6: Location of micro-earthquakes in the Greater Olkaria geothermal system
(Simiyu, et al., 2000)

Seismic monitoring of micro-earthquakes indicates that the Greater Olkaria geothermal area is characterized by a relatively high level of micro-earthquake activity (Simiyu et al., 1997, Simiyu et al., 2000). The analysis of focal depth, event location and classification shows that the high frequency events and deep low frequency events occur at the intersection of structures in the area. These shallow

events are associated with fluid movements along the structures. The Olkaria Central field show seismicity characterized by deep larger magnitude events. This implies that the area is active but with a deeper brittle-ductile zone. This has been interpreted to mean that the area is not close to a strong heat source and there is cooling by a cold inflow. Seismicity shows the Olkaria Domes area to be a continuation of the Olkaria Northeast field along a major NW-SE linear structure. This area is characterized by both shallow and deep events that have been interpreted as volcano-tectonic and tectonic events (Simiyu et al., 1997). The area along the proposed southern ring fracture and the Ol Njorowa gorge are characterized by high frequency shallow events which are interpreted to be related to shallow lateral fluid movement and may therefore not have high geothermal potential.

Residual aeromagnetic data acquired within the Rift Valley shows that Olkaria area has a positive anomaly that has a NW-SE trend. The negative anomalies correspond to normally magnetized rocks whereas the positive anomaly occurs in a demagnetized zone corresponding to the heat source that is of silicic origin. This provides some evidence for heat source at a temperature above the Curie point of magnetite (above 575°C) close to the surface (Onacha, 1990). The occurrence of magnetic and gravity anomalies at the intersections of NE and NW rift faults, is an indication of distinct near surface heat sources controlling the reservoir characteristics of the geothermal systems.

2.6 Fluid chemistry of Olkaria fields

The fluid chemistry of Olkaria fields have been reported by earlier workers; Olkaria West (Kenya Power Company (KPC) 1984, 1990, Muna 1990, Wambugu 1995) Olkaria Northeast (KPC 1988, Wambugu 1996), Olkaria East (KPC 1984, 1988, Karingithi 1992, 1993, 1996, Karingithi et al, 1997), Olkaria Domes (Karingithi, 1999). The fluid in Olkaria West field contrasts sharply with that in the Olkaria East field and Olkaria Northeast field. In the Olkaria West field, the discharge is typically rich in bicarbonates (10,000 ppm) but the Cl^- content is very low (50-200 ppm). Comparatively, the bicarbonates-carbonate and Cl^- content of the Olkaria Northeast field wells are <1000 ppm and 400-600 ppm respectively. The Olkaria East fluid discharges have similar bicarbonates-carbonate concentration of <200 ppm as those in the Olkaria Northeast and relatively low deep reservoir Cl^- concentrations of 200-350 ppm as compared to Olkaria Northeast concentrations. Olkaria Central wells give deep reservoir Cl^- concentrations of 200-300 ppm except for well OW-201, which gives higher values in the order of 700 ppm. These wells produce waters with relatively high reservoir CO_2 concentrations similar to those of Olkaria West field wells. Olkaria Domes wells discharge mixed sodium bicarbonate-chloride-sulphate type with low mean chloride concentrations of 181.5-269.9 ppm.

Reservoir temperatures have been calculated using chemical geothermometers and the results indicate the K/Na ratio function by Arnorsson et al (1983) give aquifer temperature values for the Olkaria East ranging from 199-275°C with an average value of 230-260°C. In the Olkaria Northeast, the temperatures range is from 215-302°C and on average the temperatures range from 260-290°C. For the Olkaria West field, temperatures indicate minimum values of 180-264°C with an average value of 230-260°C, which is similar to those, recorded for the Olkaria East wells. Reservoir temperatures calculated using the quartz geothermometry function by Fournier et al (1982) show Olkaria East wells give aquifer temperatures ranging from 172-272°C with an average value of 230-260°C. The Olkaria Northeast wells have values ranging from 195-304°C with an average value of 265-270°C whereas Olkaria Central field give values ranging from 186-259°C. In Olkaria Domes field, the highest mean solute equilibrium temperatures of 242°C was shown in well OW-903 while wells OW-901 and OW-902 showed slightly lower mean equilibrium temperatures of 238°C and 232°C respectively. From the calculated aquifer temperatures, high peak at some wells indicate that high temperature values are associated with hot geothermal fluid up-flow and these wells are considered to be located within this up-flow, which is mainly within the Olkaria fault zone. On the other hand, some wells like OW-305 and OW-301 give comparable temperature values from the two geothermometers and they are taken to indicate proximity to a hot up-flowing region. Reduction in geothermometric temperatures is quite significant towards the edge of the fields around wells OW-304D and OW-307 in Olkaria West field and towards wells OW-708, OW-704 and OW-724 in Olkaria Northeast field. These wells could be

considered to mark the margins of the geothermal system, which could as well be recharge zones of the system.

2.7 Olkaria Domes wells

The three 2200 m deep geothermal exploration wells in Olkaria Domes encountered a high temperature system and discharged on test. During the drilling of well OW-901, a steam cap was encountered at around 700 m but was cased off as the production casing was set at 759 m. The well sustained discharge on test, but the wellhead pressures were less than 5 bars, which is the pressure required to run the conventional turbines like the ones in the Olkaria I and Olkaria II power stations. The steam cap encountered in well OW-901 was thought it would increase the productivity of the well and more so improve the wellhead pressure to over 5 bars had it not been cased off. This prompted the drilling program to be slightly altered in Olkaria Domes and the other two wells (OW-902 and OW-903) had their production casings set at 648 m and 697 m respectively. The wells did not encounter the steam cap found in well OW-901 and the wellhead pressures of the wells (OW-902 and OW-903) were still less than 5 bars and well OW-903 is cyclic. Table 1 below summarizes the parameters of the Olkaria Domes exploration wells.

TABLE 1: Olkaria Domes field exploration wells parameters

Well	Lip pipe (")	WHP (bar-a)	Mass output (kgs^{-1})	Enthalpy (kJkg^{-1})	Max temp. (°C)
OW-901	8	3.8-4.2	17-21	1300	342
	5	4.4-5.2	10-15	1200	
	4	4.5-5.5	5-10	1700	
OW-902	8	4.2-4.6	31-35	940-970	248
	6	3.8-5.0	21-28	1040	
	5	4.6	9.7	1100	
OW-903	4	4.2	9.5	1030	341
	5	4.6	18	950	
	6	4.95	27.8	930	
	8	4.6	34.5	920	

3.0 SAMPLING AND ANALYTICAL METHODS

3.1 Sampling

Cuttings samples from Olkaria Domes wells were taken at every 2 m interval, but in cases where the sample was too little and unrepresentative, up to 4 m depth interval was sampled. Preliminary analysis was done at the rig site by use of a binocular microscope and specimen samples which were representative of all the rock units penetrated in the three wells were selected for detailed laboratory analysis of hydrothermal alteration minerals and fluid inclusion studies. Very few cores were cut in Olkaria Domes field and therefore nearly all the descriptions and interpretations are based on cuttings samples.

The problem with cuttings generally, as encountered in Olkaria Domes, is that the rock chippings in some of the samples are fine, usually smaller than the crystals hence bringing about difficulty in identifying some lithologic units conclusively. Also when the soft parts of the hydrothermally altered rock is ground during drilling, only the harder components reach the surface, hence less representative of the rock unit penetrated. Another problem is when cutting chips derived from a specific depth may have fallen from a shallow level due to cave-ins resulting to mixing of cuttings. Geosweeps were, however, carried out where mixing of cuttings was suspected. Time delays in sample cuttings to reach the ground result in depth difference between the true and the indicated depth and are usually greater for deeper samples. This anomaly was corrected by reconciling with the drill logs and calculating for the error.

3.2 Analytical methods

3.2.1 Stereo microscope analysis

Binocular analysis of the cuttings samples was done using the Wild Heerbrugg binocular microscope. A sample is scooped from the sample bag into a petri dish and washed with clean water to remove impurities and dust. Wetting the cuttings is necessary to enhance visibility of samples and obscure features such as finely disseminated sulphides e.g. pyrite. The sample is then placed on a mounting stage of the binocular microscope and among the essential features noted are the colour(s) of the cuttings, rock type(s), grain size, rock fabrics, original mineralogy, alteration mineralogy and intensity.

3.2.2 Petrographic microscope analysis

Representative samples from all the lithologic units encountered in the three wells were selected and thin sections were prepared for petrographic studies. The thin sections were analyzed using the Leitz Wetzler petrographic microscope. The petrographic microscope is used to confirm the rock type(s) and the alteration minerals, additional alteration minerals not observed by the binocular microscope, and to study the mineralogical evolution of the alteration minerals.

3.2.3 X-ray diffractometer analysis

The X-ray diffractometer is used to identify individual minerals especially clays and zeolites. Samples were selected from all the lithologic units and analysed for clays. The <4 microns fractions were prepared for x-ray diffraction by use of a mechanical shaker to separate the phyllosilicates from the rock matrix. A Phillips PW 1800 diffractometer was used, with CuKα radiation (at 40 kV and 50 mA), automatic divergence slit, fine receiving slit, and graphite monochromator. Count data were collected from 2°-14° at intervals of 0.02°, 2θ for a time of 1 second. Zeolites, calcite, fluorite and sulphides were picked from the rock cuttings and ground by using a motor and a pestle. Count data were collected from 4°-56° at intervals of 0.04°, 2θ for a time of 1 second. The procedure of preparing clay and zeolite samples for XRD analysis is shown in Appendix I and the clay results are tabulated in Appendices II, III and IV.

3.2.4 Fluid inclusion analysis

Double-polished thick sections (approximately 70 microns) of cuttings from Olkaria Domes wells, which contained abundant quartz and calcite in veins, were prepared for fluid inclusion analysis. Fluid inclusions are small portions of fluid, which are trapped in a solid crystal as it grew or recrystallized. The fluids are thus samples of the original brine from which the crystal grew or a later fluid which bathed the crystal during crystallization. Primary fluid inclusions (Roedder, 1984) are concentrated along the first-order growth discontinuities or occur as isolated inclusions distributed within the crystals. Secondary fluid inclusions are trapped along healed cracks. If the crystal cools, the liquid will contract at a faster rate than the solid and a vapour bubble will form. At ambient temperatures, all types of inclusions contain a liquid aqueous solution and a gas bubble. This bubble forming process could be reversed to determine the temperature of mineral formation or temperature of homogenization (T_h). The inclusion is heated until the fluid homogenizes in a single phase (i.e. bubble disappears) and the T_h is measured.

3.2.5 Electron microprobe analysis

Electron microprobes permit the non-destructive, major and trace element analysis of small areas (~4μm diameter) of solid materials in situ. Selected thin sections from Olkaria Domes, which were prepared and analysed by Karingithi (2002) using the electron microprobe have been made use for the present study. The analysis of minerals was carried out using an updated ARL-SEMQ (Scanning Electron Microprobe Quantometer). The analysis was done at 15 kV with sample current of 15 nA and a beam diameter of 2-3 micrometres.

3.2.5 X-ray fluorescence analysis

XRF analysis of major elements of cuttings from Olkaria Domes was carried out at Activation Laboratories Ltd, Canada. The samples were run for major oxides and selected trace elements on a combination simultaneous/sequential Thermo Jarrell-Ash ENVIRO II ICP. Calibration was performed using 7 prepared USGS and Canmet certified reference materials. One of the 7 standards was used during the analysis for every group of ten samples.

4.0 RESULTS

4.1 Lithology

Wells OW-901, OW-902 and OW-903 whose altitudes are 1890 masl (m above sea level), 1957 masl and 2043 masl were drilled to depths of -309 meters above sea level (masl), -243 masl and -159 masl respectively. The preliminary geological results of these exploration drill wells are found in Omenda (1998b), Mungania (1999) and Lagat (1999). The drilled lithological column is composed of unconsolidated pyroclastics that are dominant in the shallow levels overlying a volcanic sequence whose lithological composition is dominated by comenditic rhyolite, trachyte, basalt, tuff and some doleritic and syenitic dykes. The descriptions of all the lithologic units encountered in the three wells are outlined in appendices V, VI and VII and are plotted in Figures 9, 10, 11, 12, 24, 25 and 26. Below is a summarized description of each of the lithologic units encountered by the drilled wells.

4.1.1 Pyroclastics

The pyroclastics are yellowish to brown and form the upper 216 m in well OW-901, 274 m in well OW-902 and the top less than 50 m in well OW-903. The rock unit is unindurated and consists of lithic fragments of rhyolite, trachyte and syenite. The matrix is dominated by ash size particles, crystals of glass, quartz, feldspars, amphiboles, obsidian and pumice.

4.1.2 Tuffs

Occur as intercalations below 1176 masl in well OW-901, below 1297 masl in well OW-902 and below 1315 masl in well OW-903 with a range in thickness from less than 10 m to 90 m. The tuff is brownish grey, grey to white in colour and occur in two types; the glassy and the fragmental tuff. The glassy (vitric) tuff is wholly glassy whereas the fragmental tuff is made up of lithics of lava fragments as well as subhedral to anhedral crystal lithics of quartz and feldspars.

4.1.3 Rhyolites

Rhyolites are of two types; (i) the granular non-porphyritic to quartz and sanidine porphyritic with abundant riebeckite and occasional hornblende and (ii) the spherulitic rhyolites with bands of volcanic glass enriched with quartz and feldspar crystals. The first type is light grey to brownish grey in colour, mainly comenditic and occurs from the surface to 1545 masl in OW-901, to 1449 masl in OW-902 and to 1381 masl in well OW-903. Comendites are highly siliceous (>72% SiO_2), peralkaline and relatively potassic (K_2O>Na_2O). Some of the comenditic lavas are glassy and approach obsidian in appearance. Petrographically, comendites contain phenocrysts of quartz and sanidine in a matrix dominated by fine-grained quartz, arfvedsonite-riebeckite, sanidine microlites, and rare fayalite, aenigmatite, aegirine, hornblende, zircon and opaque oxides (Omenda, 2000). The second type of rhyolite occur at 1090-1032 masl in well OW-901, at 1145-1113 masl and 517-437 masl in well OW-902 and 1079-1009 masl in well OW-903. This type is mainly spherulitic and consists of sanidine and quartz phenocrysts, microphenocrysts of aegerine, pyroxene, K-feldspar laths, riebeckite and magnetite.

4.1.4 Trachytes

Trachyte occurs alternating with tuff, basalt and rhyolite below 1522 masl in well OW-901, below 1225 masl in well OW-902 and below 1381 masl in well OW-903. It is the dominant rock type, with minor tuff intercalation at greater depths. The rock is grey to brownish grey, fine grained and is composed of phenocrysts of sanidine, arfvedsonite-riebeckite, and aegirine. The matrix consists of flow oriented feldspar microlites in a fine grained to glassy groundmass. Sanidine crystals are the most common phenocryst and occur in crystals measuring up to 5 mm.

4.1.5 Basalts

Basalt occurs below 1425 masl to 214 masl in well OW-901, below 1265 masl to 283 masl in well OW-902 and below 1285 masl to 371 masl in well OW-903 alternating with other rock types. The rock is light greenish grey to black, with holocrystalline groundmass composed of plagioclase laths and anhedral clinopyroxene and magnetite. It is porphyritic with plagioclase phenocrysts, some of which are zoned, clinopyroxene and glomeroporphyritic clots of pyroxene. Olivine occurs in unaltered basalts, but at depth the mineral has undergone metasomatism and its presence is revealed by the crystal outline of the alteration products.

4.1.6 Basaltic intrusives

Basaltic intrusives were encountered at 1009-989 masl in well OW-902 and 1203-1127 masl in well OW-903. The intrusive is fine grained, sometimes with glassy margins, porphyritic with plagioclase feldspars and has moderately to completely altered olivine microphenocrysts in the groundmass. The typical greyish metallic lustre at the contact between the intrusion and the adjacent rocks is due to contact metamorphism (Franzson, pers. comm.).

4.1.7 Microsyenites

Microsyenite occurs at 802-800 masl, 608-600 masl and 320-314 masl in well OW-901, at -25 to -33 masl and -211 to -213 masl in well OW-902 and at 229-203 masl, -53 to -61 masl in well OW-903. The rock is greyish green in colour, feldspar porphyritic and is medium grained with microcrystalline bulk showing good segregation of arfvedsonite and aegerine-augite. The alkali feldspars phenocrysts are large (> 5 mm) in length.

4.1.8 Dolerites

Doleritic intrusive rock occurs only at 87-59 masl in well OW-902. The rock is dark grey in colour, medium grained, plagioclase porphyritic, exhibits ophitic texture and has moderate to completely altered olivine in the groundmass. The adjacent rocks exhibit metallic lustre typical of contact metamorphism.

4.2 Petrochemistry of Olkaria Domes rocks

Many published chemical analysis of surface and subsurface rock samples from the flanks and within Greater Olkaria geothermal area show that the volcano complex is composed of rocks ranging in composition from basalt to rhyolite (Browne, 1981, 1984; Clarke et al, 1990; MacDonalds et al, 1987; Omenda, 2000). To determine the exact rock type, compositional variation with analysed rocks, marker units and to establish the extent of lava flows and structural controls in Olkaria Domes, selected samples were analyzed for major element chemistry. Some of the selected rocks could not be conclusively determined from binocular and thin section analysis because they were very fine grained or had a glassy or partially glassy groundmass that the individual constituents and in particular their relative abundance could not be determined with any precision. Here purely mineralogical chemical analysis would place the rock in the right classification. The selected samples were homogeneous, showed very little or no alteration at all and were from the same formation as those analyzed from Olkaria East and Olkaria Northeast fields.

Superimposed on the total alkalis versus silica (TAS) diagram in Figure 7 are results of the chemical analysis of the rocks from Olkaria East, Olkaria Northeast and Olkaria Domes fields and surface samples from Broad Acres. The sampling depths for well samples and sampling locations for the surface samples are contained in Tables 2 and 3 respectively. This plot shows that the rocks from Olkaria East, Olkaria Northeast and Broad Acres have composition similar to those of Olkaria Domes generally with somewhat alkaline compositions plotting mainly in the basaltic, trachytic and rhyolitic portions of the TAS diagram.
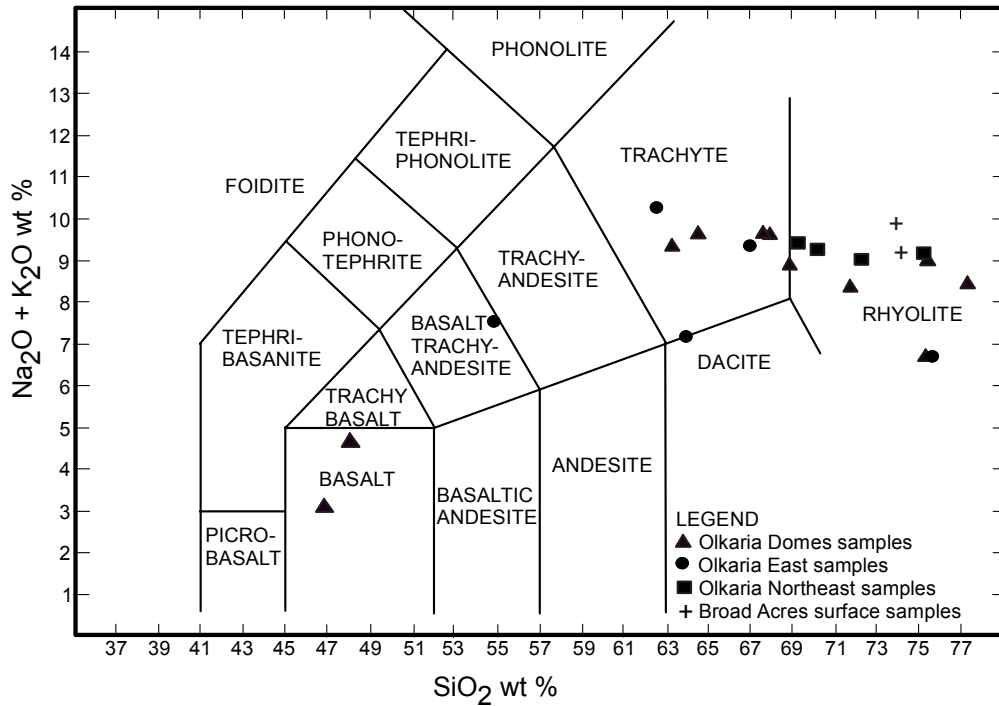
FIGURE 7: Total alkalis silica (TAS) diagram for classification of volcanic rocks using chemical analysis (Les Bas et al., 1989). Data from Olkaria Domes is from the present study, Olkaria East data is from Browne (1984), Olkaria Northeast data are from Omenda (2000), MacDonald et al., (1987) and Black et al (1997), Broad Acres data is from McDonald et al (1987)

The rhyolites are comenditic following the classification scheme of Macdonald (1974) shown in Figure 8. This classification separates them from the pantellerite, which have higher Al_2O_3, Fe_2O_3 (t), CaO, and Na_2O. The basalts have high TiO (1.73-2.11%), Al_2O_3 (15.01-16.90%), CaO (9.5-10.70%), and low MgO (4.24-6.28%), Na_2O (2.24-3.18%) and K_2O (0.84-1.45%). The comendites have high SiO_2 (71.8-77.3%) and are strongly depleted in TiO_2 (0.13-0.42%), MgO (0-0.16%), CaO (0.08-0.41%), and P_2O_5 (0.01-0.02%). The fact that the subsurface rocks showed slight alteration does not seem to have affected their major element chemistries.
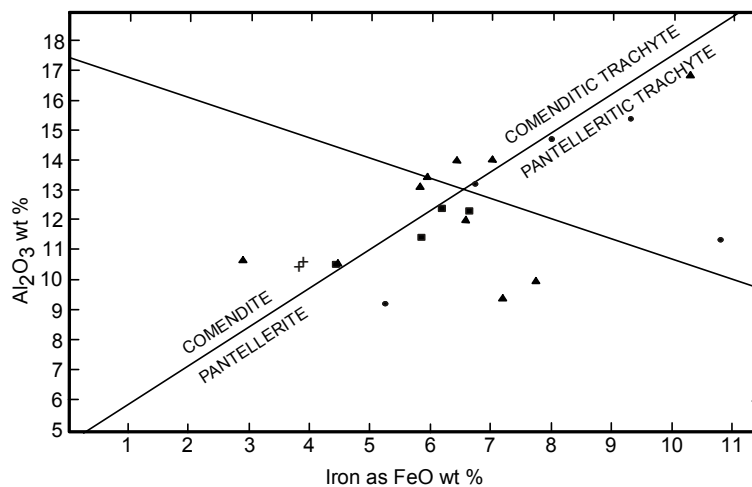
FIGURE 8: Classification in terms of Al_2O_3-total iron as FeO diagram (MacDonald, 1974). Data from Olkaria Domes is from the present study, Olkaria East data is from Browne (1984), Olkaria Northeast data are from Omenda (2000), MacDonald et al (1987) and Black et al (1997) and Broad Acres data is from McDonald et al (1987). Legend as in Figure 7 above

TABLE 2: Major and trace element analyses of Olkaria Domes wells samples (oxides in % and elements in ppm)

Rock	Trachyte	Basalt	Rhyolite	Trachyte	Rhyolite	Rhyolite	Rhyolite	Rhyolite	Trachyte	Basalt	Syenite
Well No.	901	901	901	901	902	902	903	903	903	903	903
Depth (masl)	1496-94	1418-18	1048-46	880-878	1603-10	1459-57	1755-53	1537-35	1221-19	1141-39	209-207
SiO_2	67.68	48.09	75.31	68.01	71.82	68.96	75.45	77.32	63.48	46.91	64.59
TiO_2	0.46	1.73	0.35	0.47	0.42	0.47	0.14	0.13	0.46	2.11	0.81
Al_2O_3	13.54	16.90	9.46	13.17	10.01	12.06	10.61	10.75	14.08	15.01	14.02
Fe_2O_3 (t)	5.93	10.31	7.20	5.83	7.79	6.57	4.47	2.90	6.43	12.30	7.01
MnO	0.22	0.18	0.12	0.18	0.11	0.20	0.06	0.04	0.19	0.20	0.24
MgO	0.08	4.24	0.16	0.18	0.04	0.06	0.00	0.00	0.63	6.28	0.47
CaO	1.04	9.51	0.41	0.81	0.25	0.81	0.08	0.14	3.16	10.70	1.57
Na_2O	4.65	3.18	2.55	4.42	3.30	4.07	4.56	3.18	3.81	2.24	4.65
K_2O	4.98	1.45	4.13	5.17	5.04	4.82	4.44	5.22	5.53	0.84	4.96
P_2O_5	0.03	0.28	0.02	0.04	0.02	0.03	0.01	0.01	0.05	0.21	0.10
LOI	0.95	2.97	0.32	0.73	0.54	1.01	0.33	0.29	2.35	3.42	0.87
Total	99.56	98.84	100.03	99.02	99.34	99.05	100.16	99.99	100.16	100.22	99.29
Sr	5.00	441.00	8.00	9.00	2.00	6.00	2.00	2.00	29.00	424.00	41.00
Y	94.00	30.00	178.00	96.00	152.00	102.00	269.00	126.00	79.00	23.00	89.00
Zr	876.00	219.00	1681.00	849.00	1447.00	945.00	1998.00	1019.00	690.00	103.00	983.00
Ba	47.00	376.00	12.00	119.00	9.00	50.00	0.00	3.00	45.00	254.00	176.00
V	0.00	232.00	0.00	0.00	0.00	0.00	0.00	0.00	7.00	290.00	13.00
Sc	2.00	26.00	0.00	4.00	0.00	2.00	0.00	0.00	2.00	31.00	5.00
Be	5.00	4.00	8.00	7.00	11.00	7.00	19.00	8.00	6.00	2.00	8.00

TABLE 3: Major element concentrations of Olkaria subsurface and surface rocks (oxides in % and elements in ppm). Data from MacDonald et al (1987), Black et al (1997) and Omenda (2000)

Rock	Comendite	Comendite	Trachyte	Trachyte	Rhyolite	Trachyte	Trachyte	Basalt	Trachyte	Rhyolite	Rhyolite
Well No.	707	706	M3	714	16	16	17	17	17	Broad Acres	Broad Acres
Depth (masl)	1737	1834	1499	1494	1193	751	1698	1386	702	Surface	Surface
SiO_2	72.37	75.3	70.26	69.33	75.73	67.10	62.70	54.95	64.04	74.19	73.98
TiO_2	0.34	0.17	0.48	0.48	0.33	0.72	0.62	0.42	0.80	0.19	0.19
Al_2O_3	11.49	10.58	12.47	12.41	9.26	13.26	14.76	15.44	11.41	10.52	10.67
Fe_2O_3 (t)	5.84	4.43	6.19	6.64	5.25	6.74	8.00	9.33	10.82	3.80	3.87
MnO	0.13	0,07	0.18	0.02	0.16	0.23	0.31	0.21	0.40	0.06	0.06
MgO	0.02	0	0.09	0.06	0.10	0.19	0.13	2.07	0.57	0.07	0.07
CaO	0.33	0.1	0.4	0.37	0.11	0.76	0.85	4.77	0.52	0.26	0.18
Na_2O	4.11	4.64	3.65	4.43	1.03	3.88	4.55	4.49	3.39	4.67	5.50
K_2O	4.9	4.53	5.57	4.94	5.64	5.45	5.65	3.05	3.76	4.51	4.39
P_2O_5	0	0	0.02	0.02	0.02	0.07	0.06	0.34	0.09	0.09	0.02
LOI	0.40	0.22	0.66	0.55	1.86	1.01	2.13	3.37	3.14	0.83	0.52
Total	99.53	99.75	99.97	99.25	99.49	99.41	99.76	98.44	98.94	99.19	99.45

4.3 Stratigraphic correlation

Geologic cross-section across wells OW-08, OW-09, OW-15, OW-19 and OW-22 in Olkaria East field and wells OW-901, OW-903 and 902 in Olkaria Domes along A-B-C-D (Figure 3) shown in Figure 9 has revealed to some extent the geological structural system between the two fields. The structures in the area are composed of faults, intrusions and extrusion of rhyolitic domes whose effects has resulted to minor unconformities in the correlation between the wells.
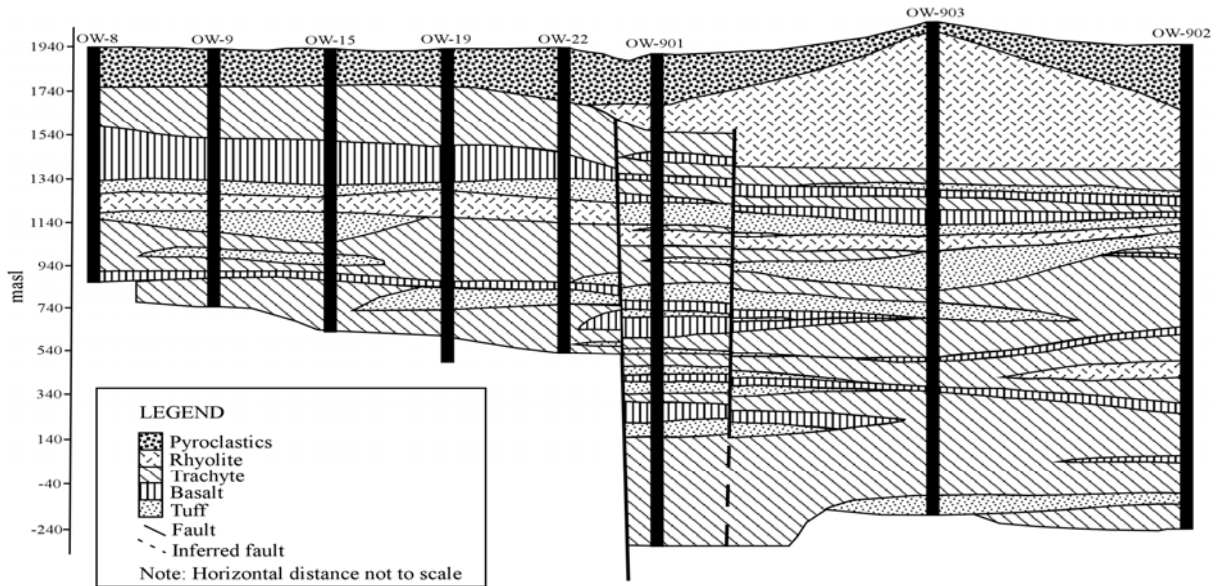
FIGURE 9: Geological cross-section along A-B-C-D (see Figure 3) between Olkaria East
and Olkaria Domes fields. Correlation through wells OW-8, OW-9, OW-19
and OW-901 modified from Omenda (1999)

The stratigraphy of Olkaria Domes field shows some similarity to that of Olkaria East field, with the top 200 m being made up of mainly unconsolidated pyroclastics. The pyroclastic unit thins towards well OW-903 due to erosion because the area is topographically high but thickens towards well OW-902. The upper trachytes and upper basalts are thick in Olkaria East field but thin towards Olkaria Domes. The basaltic rock unit which occurs around 1500-1300 masl and act as a marker horizon in Olkaria East is thin and downthrown in Olkaria Domes. Rhyolites, trachytes and basalts with occasional tuff intercalations occur in both the fields to the bottom of the wells with mainly trachyte and occasional tuff intercalations dominating at greater depths. The faults occurring between well OW-22 in Olkaria East and well OW-901 in Olkaria Domes and wells OW-901 and OW-903 both in Olkaria Domes have a resultant downthrow of about 300 m. The faults displace the rocks below the pyroclastics indicating that these faults are older than the recent volcanism in the area. There is no fault structure noted between wells OW-903 and well OW-902. The two main faults can be identified as those inferred from the SPOT satellite images and aerial photographs (Figure 4).

4.4 Hydrothermal alteration

In the Olkaria Domes geothermal field, hydrothermal alteration minerals appear both as replacement of the primary minerals, as well as fillings in vesicles, vugs and fractures. The distribution and abundance of the hydrothermal minerals were obtained from the petrographic studies of drill cuttings samples taken after every 2 m from the three exploration wells drilled in the area. Although hydrothermal alteration has changed the primary minerals in different ways and magnitude, often the original textures and minerals are still recognizable.

Factors that influence the distribution and kind of mineral assemblages present in hydrothermal systems include permeability, rock and water composition, temperature, pressure and duration of hydrothermal alteration (Browne and Ellis, 1970). These factors are largely independent, but the effects of one or more of the factors can exert a dominant influence in the location and extent of hydrothermal alteration. Permeability of the rocks controls the access of thermal fluids, which cause hydrothermal alteration of the rocks and precipitation of secondary minerals in open spaces. Rocks which have very restricted permeability or are completely impervious to fluid will be only slightly altered as observed in dense lavas in the Olkaria Domes field. Crystallinity of the host rock is of importance because glass is more easily altered than crystalline rock. The chemical composition of the host rock determines the availability of components to form alteration minerals as well as possible fugitive components from the presumed magmatic heat source. Temperature is the most significant factor in hydrothermal alteration because most of the chemical reactions require elevated temperatures and also minerals are thermodynamically stable at high temperatures. Pressures at the depths penetrated by Olkaria Domes drill holes, like in other geothermal fields elsewhere in the world are not sufficient to greatly affect hydrothermal alteration minerals transformation (Browne and Ellis, 1970). Duration of the hydrothermal alteration at Olkaria Domes is not precisely known, but hydrothermal alteration is undoubtedly occurring at the present time and likely extends back through Quaternary period, which is the onset of volcanic activity in Olkaria area.

The main hydrothermal minerals in Olkaria Domes field are albite, amphibole (actinolite), biotite, calcite, chlorite, chalcedony, epidote, fluorite, garnet, illite, K-feldspar (adularia), mordenite, secondary Fe-Ti oxides, sulfides (pyrite), titanite (sphene) and quartz. In addition, minor amounts of wairakite and prehnite are present. Mineral associations in vesicles are common and consist of two or more of the following minerals; chlorite, quartz, calcite, epidote and pyrite with the paragenetic sequence varying with depth and from one well to another. Table 4 below shows the primary minerals observed in Olkaria Domes geothermal field and their alteration products.

TABLE 4: Primary minerals, order of replacement and alteration products of
Olkaria Domes volcanics (modified from Browne, 1984a)

Primary phases	Alteration products
Volcanic glass	Zeolites, clays, quartz, calcite
Olivine	Chlorite, actinolite, hematite, clay minerals
Pyroxenes, amphiboles	Chlorite, illite, quartz, pyrite, calcite
Ca-plagioclase	Calcite, albite, adularia, quartz, illite, epidote sphene
Sanidine, orthoclase, microcline	Adularia
Magnetite	Pyrite, sphene, haematite

4.4.1 Description and distribution of hydrothermal alteration minerals

The distribution of hydrothermal minerals in wells OW-901, OW-902 and OW-903 are shown in Figures 10, 11 and 12 respectively. Below is a description of the hydrothermal alteration minerals encountered in the Olkaria Domes wells.

Adularia occurs below 1238 masl in well OW-901; below 1197 masl in well OW-902 and below 1315 masl in well OW-903. The mineral forms minute anhedral to euhedral crystals that are pseudo-orthorhombic and are usually diamond shaped. It occurs as replacement of plagioclase or primary K-feldspars and is occasionally deposited in veins as well as forming incrustations in fissured rocks. Where it occurs as a replacement of plagioclase or K-feldspars, there is nearly an isochemical transformation to an optically and structurally different phase –adularia. In pseudomorphs after plagioclase phenocrysts, it produces a streaky extinction suggesting that the pseudomorphs are made up of numerous overlapping crystals of rhombic section. The mineral becomes rare until it disappears at 404 masl in well OW-901, 79 masl in well OW-902 and 441 masl in well OW-903.

Well OW-901
Lithology and Drilling Data

Location: **Olkaria Domes, Kenya** *Rig:* **N370** *Circulation fluid:* **Mud and aerated water**

Well no.: **OW-903** *Depth range:* **0-2200 m** *Logger (-s):* **G. Muchemi, P. Omenda, J. Mungania and J. Lagat**
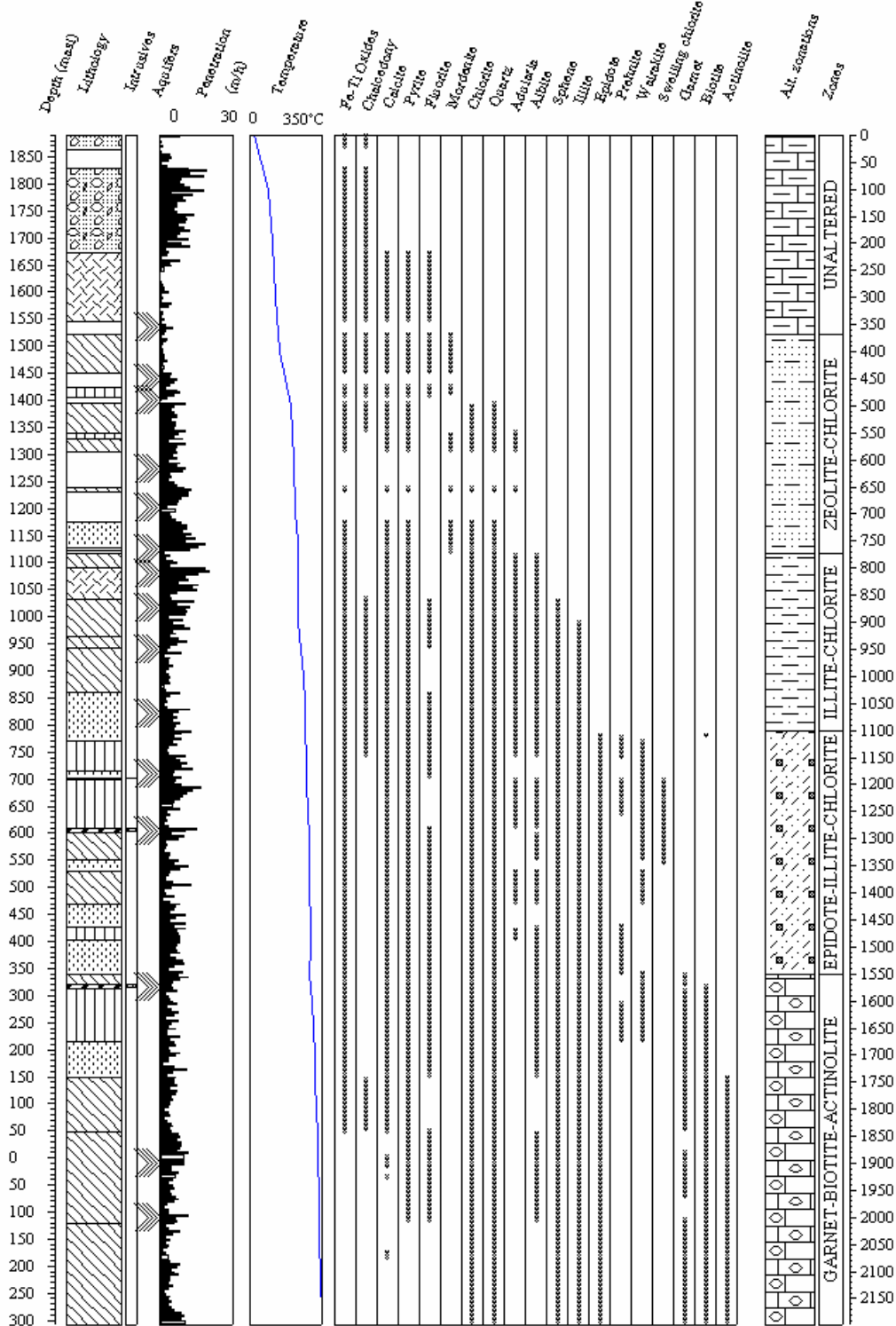
FIGURE 10: Lithology, distribution of hydrothermal alteration minerals and zonations
in well OW-901. Legend on lithology is as in Figure 9

21

Well OW-902
Lithology and Drilling Data

Location: **Olkaria Domes, Kenya** Rig: **N 370** Circulation fluid: **Mud and aerated water**
Well no.: **OW-902** Depth range: **0-2199 m** Logger (-s): **G. Muchemi, P. Omenda, J. Mungania and J. Lagat**
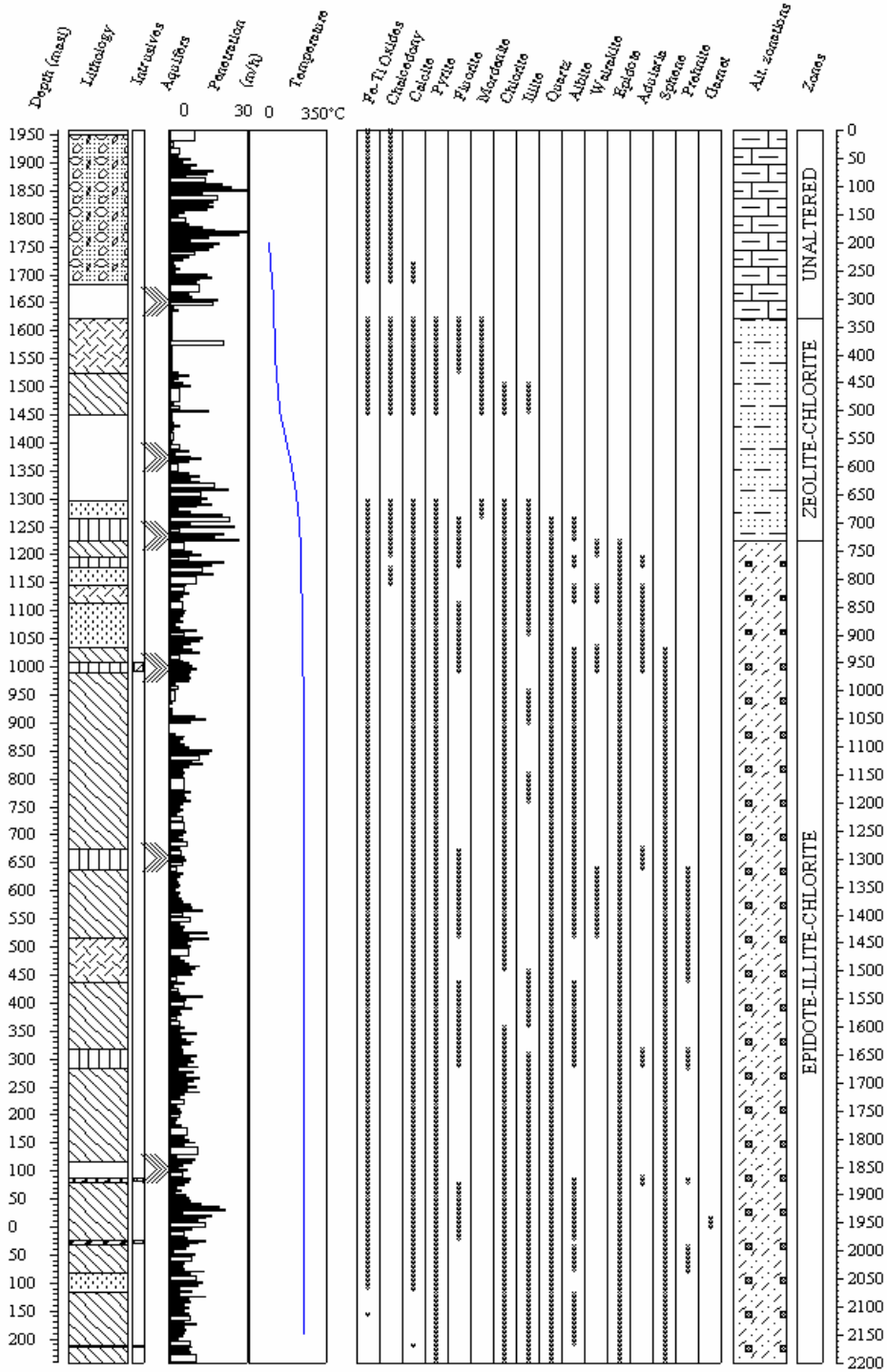
FIGURE 11: Lithology, distribution of hydrothermal alteration minerals and zonations
in well OW-902. Legend on lithology is as in Figure 9.

22

FIGURE 12: Lithology, distribution of hydrothermal alteration minerals and zonations in well OW-903. Legend on lithology is as in Figure 9

Actinolite is green to greyish green in colour, forms radiating fibers or acicular crystals and also massive to granular aggregates in the groundmass and has a moderate birefringence. The mineral is formed as a replacement of ferromagnesian minerals in association with epidote and chlorite. Actinolite appeared in the deeper hotter parts of wells OW-901 and OW-903 (below 150 masl in well OW-901 and below 143 masl in well OW-903) but was conspicuously absent in well OW-902.

Albite. The term albitization here is referred to replacement of primary K-feldspar and plagioclase phenocrysts by hydrothermal albite. Albitization occurs below 1116 masl in well OW-901, below 1265 masl in well OW-902 and below 1203 masl in well OW-903. Albatized K-feldspar has a low refractive index and shows no zoning but typical chessboard like twinning is common.

Biotite. Authigenic biotite is occasionally present in several geothermal systems (e.g. Salton Sea, McDowell and Elders, 1980; Cerro Prieto, Schiffman et al., 1984; Philippines, Reyes, 1990; Ngawha, Cox and Browne, 1998 and Aluto-Langano, Teklemariam et al., 1996). Biotite at Olkaria Domes occurs sparingly at around 860 masl and continuously below 312 masl in well OW-901 and continuously below 517 masl in well OW-903. The mineral was, however, not encountered in well OW-902. Biotite forms weakly pleochroic, pale-green to brown-green crystals, which range from patchy aggregates of grains to sheet-like forms with sometimes radial fan-shaped arrays. In association with garnet and actinolite, biotite is commonly used as an indicator of high temperatures of over 280°C (Bird et al 1984).

Calcite is a widely distributed alteration mineral occurring in all the three Olkaria Domes wells. Vesicles, fractures and veins contain white massive or colourless crystalline calcite deposits. Calcite replaces plagioclase phenocrysts, pyroxenes and volcanic glass. Crystal morphology of calcite is variable and ranges from individual thin-bladed crystals to equant or needle like crystals. Calcite crystals deposited in veins at 1578-1576 masl in well OW-901 were analysed qualitatively by X-ray diffraction (XRD) and the most intense peak ranged from about 3.02 to 3.05 Å, however, some of the calcite samples had their most intense X-ray reflection between 2.99 and 3.01 Å which indicate that the mineral contains significant manganese (Bargar and Beeson, 1984). A typical calcite diffractogram is shown in Figure 13.

Calcite (Well OW-901, 1578-1576 masl)

36147/2D   D5MEAS - Program:MIN-B.DQL D5MEAS - Program:MIN-B.DQL - File: 36147.raw - Type: 2Th/Th locked - Start: 4.000 ° - End: 56.000 ° - Step: 0.040 ° - Step tir
Operations: Smooth 0.150 | Import
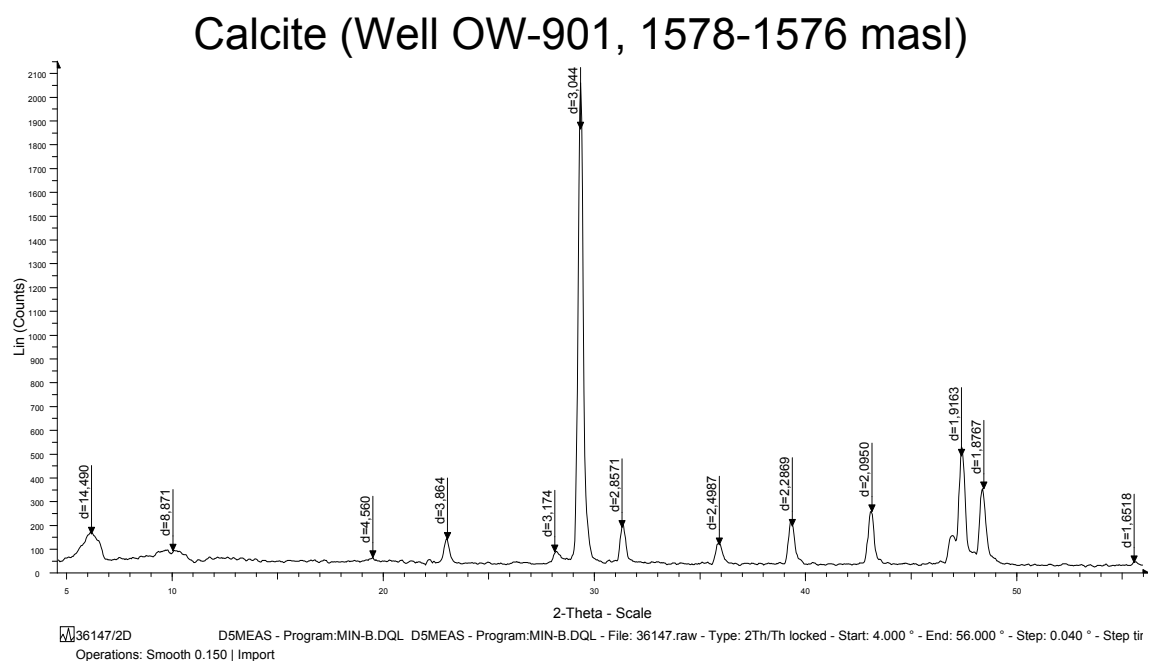
FIGURE 13: Diffractogram of calcite showing a strong peak at 3.044 Å

Chalcedony. In well OW-901 chalcedony occurs from the surface (1890 masl) to 1340 masl, at 1032-740 masl and at the deeper parts of the well at 150-48 masl where it is seen to be partly transformed

24

into quartz. In well OW-902, it occurs from the surface (1957 masl) to 1145 masl except for basaltic formation at 1197-1177 masl where it was absent. In well OW-903, it occurs from the surface of the well (2043 masl) to 1539 masl, at 1203-1127 masl and from 1009-737 masl. Colourless, white, or bluish-grey cryptocrystalline chalcedony lines vesicles and coat fractures and veins. The open space cryptocrystalline silica deposits generally have massive, banded, or botryoidal texture. At greater depths where temperatures are high, chalcedony in vesicles is seen transforming or is completely transformed into quartz but the chalcedonic outline is still preserved.

Chlorite occurs below 1390 masl in well OW-901, below 1507 masl in well OW-902 and below 1234 masl in well OW-903 down to the bottom of the three wells. Chlorite shows a wide distribution and a big variability in colours, forms and textures. It varies in colour from light-to-dark green, has low birefringence and occasionally shows anomalously blue, brown or purple interference colours and presents two different forms. In the upper levels of the volcanic sequences, chlorite appears in small intergranular patches whereas at the deepest levels, chlorite is idiomorphic, forming radial aggregates in veinlets and vugs in association with quartz, calcite, epidote, amphibole and pyrite. Within veins, chlorite occurs as microspherules enclosed within epidote, but it may also replace primary pyroxene, and the matrix. XRD analyses of chlorite show conspicuous peaks at 7.0-7.2 Å and 14.0-14.5 Å in the untreated, glycolated and oven heated samples. A typical XRD characteristic of chlorite with some illite is shown in Figure 14.
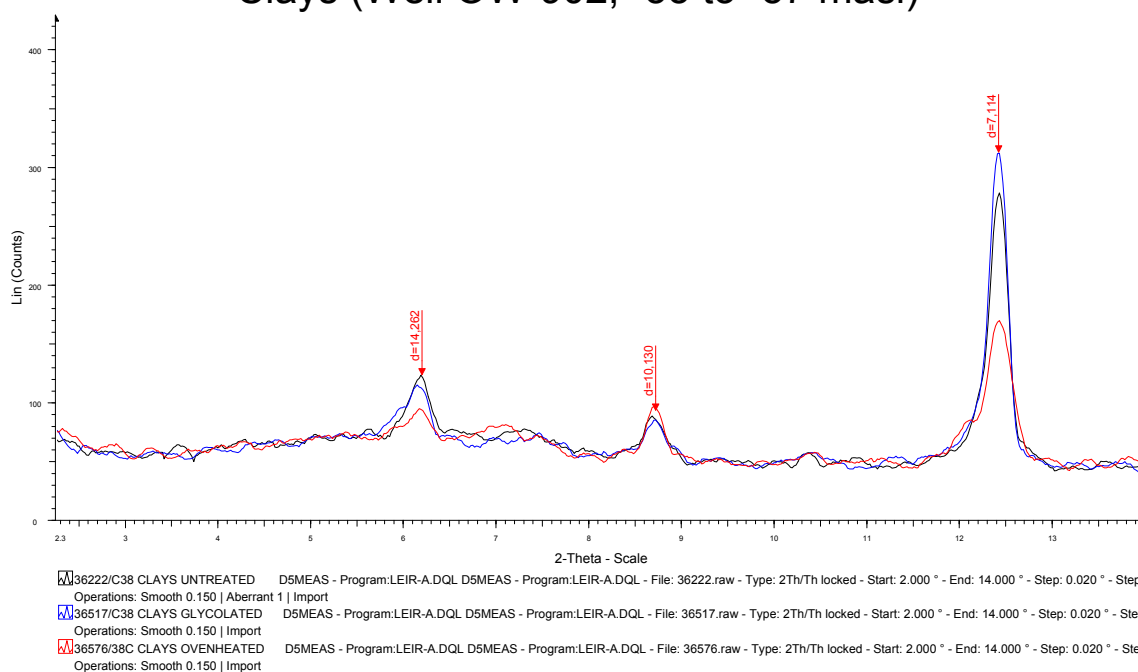
FIGURE 14: Diffractograms of clays showing unchanged peaks at 7.11 Å and 14.26 Å for chlorite and 10.13 Å for illite in the untreated, glycolated and the oven heated runs

Epidote. The first appearance of epidote is from 780 masl in well OW-901, from 1225 masl in well OW-902 and from 955 masl in well OW-903 to the bottom of all the three wells. Epidote shows a systematic textural development with increasing depth. First crystals are anhedral and form fine grained aggregates and in deeper zones they are idiomorphic, tabular, radiated or fibrous. Epidote is found filling fractures, vesicles, and replacing primary plagioclase and pyroxene and in most cases forms mineral associations with mainly quartz, chlorite and sometimes calcite, wairakite and pyrite. Microprobe analyses of epidote from well OW-901 at 288 masl (Karingithi, 2002) shown in Table 5 indicate that the mineral is a solid solution between epidote and clinozoisite.

TABLE 5: Epidote solid solution chemical formulae and mole fraction (data from Karingithi 2002)

Well	Chemical formulae	Ca	Fe	Al	Si	X_{epi}	X_{czo}
OW-05	$Ca_{1.94}Fe_{1.07}Al_{1.93}Si_{3.01}O_{12}(OH)$	1.94	1.07	1.93	3.01	0.36	0.64
OW-19	$Ca_{1.99}Fe_{1.11}Al_{1.92}Si_{2.98}O_{12}(OH)$	1.99	1.11	1.92	2.98	0.37	0.63
OW-28	$Ca_{2.01}Fe_{0.79}Al_{2.34}Si_{2.90}O_{12}(OH)$	2.01	0.79	2.34	2.90	0.25	0.75
OW-33	$Ca_{1.96}Fe_{0.92}Al_{2.16}Si_{2.95}O_{12}(OH)$	1.96	0.92	2.16	2.95	0.30	0.70
OW-34	$Ca_{1.92}Fe_{0.81}Al_{2.26}Si_{2.94}O_{12}(OH)$	1.92	0.81	2.26	2.94	0.26	0.74
OW-901	$Ca_{2.05}Fe_{0.88}Al_{2.09}Si_{2.97}O_{12}(OH)$	2.05	0.88	2.09	2.97	0.30	0.70
Average		1.98	0.93	2.12	2.96	0.31	0.69

Fluorite. In all the three wells fluorite occurs intermittently, to the bottom of the wells from 1675 masl, 1621 masl and 1663 masl in wells OW-901, OW-902 and OW-903 respectively. Fluorite is dark brown, pink to reddish orange in colour and occurs in veins in association with calcite and quartz. It forms a typical cubic and to a lesser extent the octahedron as well as combinations of these two and other rarer isometric habits. A vein filling analyzed for mineral identification qualitatively using the XRD in well OW-901 at 1578-1576 masl consisted of both calcite and fluorite. Fluorite crystals picked in well OW-903 at 1221-1219 masl were analyzed qualitatively using the XRD and the diffractogram showed strong peaks at 3.16 Å and 1.93 Å (Figure 15).
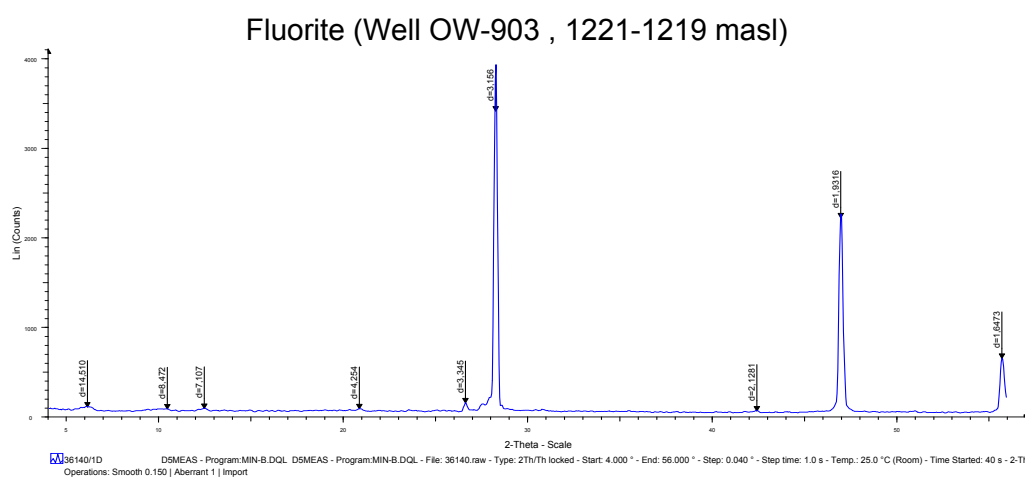
FIGURE 15: Diffractogram of fluorite showing a strong peak at 3.156 Å

Garnet occurs as clusters of anhedral to subhedral crystals in association with epidote, biotite, amphibole and chlorite in veins in rocks below 1550 masl in well OW-901 and below 405 masl in well OW-903. Microscopic studies failed to identify garnet in OW-902, but it was detected by the electron microprobe at 9-3 masl. The exact depth of its first occurrence and distribution is not therefore certain. Garnet has a moderately high relief, exhibits no cleavage and is isotropic. Table 6 shows the electron microprobe analyses of garnet from 288-286 masl in well OW-901, 9-3 masl in well OW-902 and 27-25 masl in well OW-903 by Karingithi (2002). The results indicate garnet to be a solid solution between andradite and grossular. Presence of garnet normally indicates temperatures of over 300°C (Bird et al 1984).

Illite is detected below 990 masl in well OW-901, below 1557 masl in well OW-902 and below 1243 masl in well OW-903. The mineral is light green to white in colour, replaces K-feldspar and occurs as a vein and vesicle filling mineral. XRD analyses of illite show no change at the 10 Å XRD in the untreated, glycolated and oven heated samples (Grim, 1968). A typical illite XRD patterns is shown in Figure 16.

TABLE 6: Garnet solid solution chemical formulae and mole fraction (data from Karingithi 2002)

Well	Chemical formulae	Ca	Fe	Al	Si	X_{and}	X_{gro}
OW-05	$Ca_{2.95}Fe_{1.29}Al_{0.73}Si_{2.94}O_{12}$	2.95	1.29	0.73	2.94	0.64	0.36
OW-19	$Ca_{2.97}Fe_{1.16}Al_{0.82}Si_{2.99}O_{12}$	2.97	1.16	0.82	2.99	0.58	0.42
OW-28	$Ca_{3.09}Fe_{1.25}Al_{0.79}Si_{2.88}O_{12}$	3.09	1.25	0.79	2.88	0.61	0.39
OW-33	$Ca_{3.03}Fe_{1.01}Al_{1.06}Si_{2.89}O_{12}$	3.03	1.01	1.06	2.89	0.49	0.51
OW-34	$Ca_{2.96}Fe_{1.13}Al_{0.97}Si_{2.89}O_{12}$	2.96	1.13	0.97	2.89	0.54	0.46
OW-901	$Ca_{2.98}Fe_{1.20}Al_{0.84}Si_{2.91}O_{12}$	2.98	1.20	0.84	2.91	0.59	0.41
OW-902	$Ca_{3.01}Fe_{1.20}Al_{1.07}Si_{2.84}O_{12}$	3.01	1.20	1.07	2.84	0.53	0.47
OW-903	$Ca_{2.88}Fe_{1.30}Al_{0.88}Si_{2.66}O_{12}$	2.88	1.30	0.88	2.66	0.60	0.40
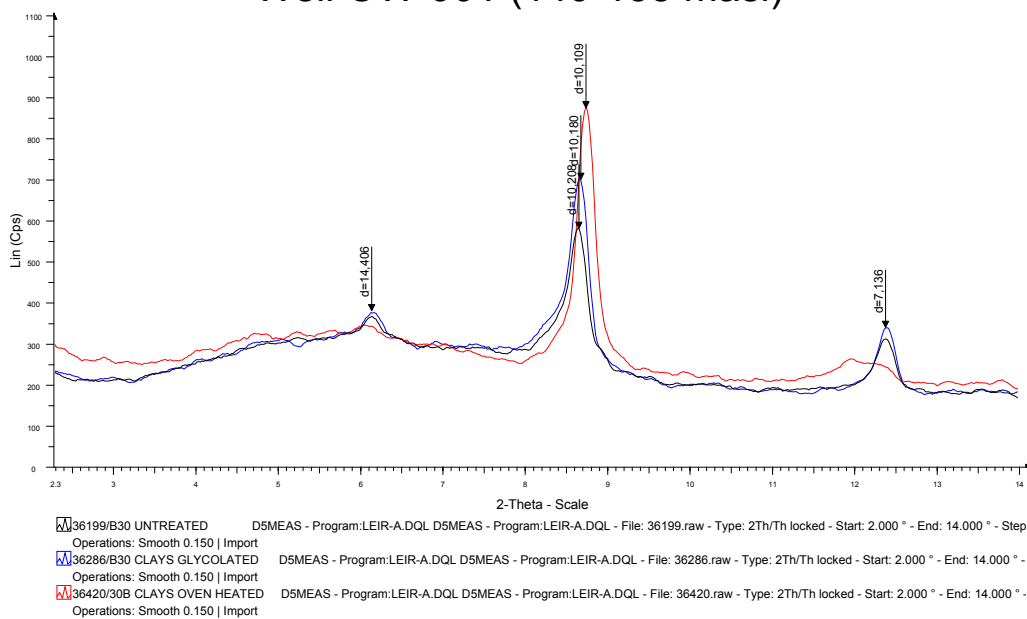
FIGURE 16: Diffractograms of clays showing strong illite peaks at around 10 Å and minor chlorite component with peaks at 7.14 Å and at 14.41 Å in the untreated, glycolated and the oven heated runs

Mordenite. White fibrous radiating hemispherical crystals of acicular mordenite are deposited in vesicles of lavas, open spaces between breccia fragments and perlitic cracks of partly altered glass in the upper few hundred meters of the three wells. Qualitative XRD analysis of the mineral showed strong peaks at 9.08 Å and 3.35 Å. In Icelandic geothermal systems, mordenite forms over a temperature range of about 75°C to around 230°C (Kristmannsdóttir and Tómasson, 1978). The measured temperature range at the depths where mordenite occurs in Olkaria Domes is in the range 100-220°C which is comparable to that of Icelandic systems. Typical XRD mordenite diffractogram is shown in Figure 17.

Oxides. Oxidation is simply the formation of any type of oxide mineral. The most common ones to form are mainly iron oxides, but many different types can form, depending on the metal cations present. Sulfide minerals often weather easily because they are susceptible to oxidation and replacement by iron oxides. Oxides form readily in the surface or near surface environment, where oxygen from the atmosphere is more readily available and at the baked contact between the cold and the hot rock. Oxidation was noted in all the three wells from the surface to near the bottom of the wells where it becomes rare to none at all.

Mordenite (Well OW-901, 1500-1498 masl)

36628/D12 MINERAL ID (ZEOLITE) D5MEAS - Program:MIN-B.DQL D5MEAS - Program:MIN-B.DQL - File: 36628.raw - Type: 2Th/Th locked - Start: 4.000 ° - End: 56.00
Operations: Smooth 0.150 | Import
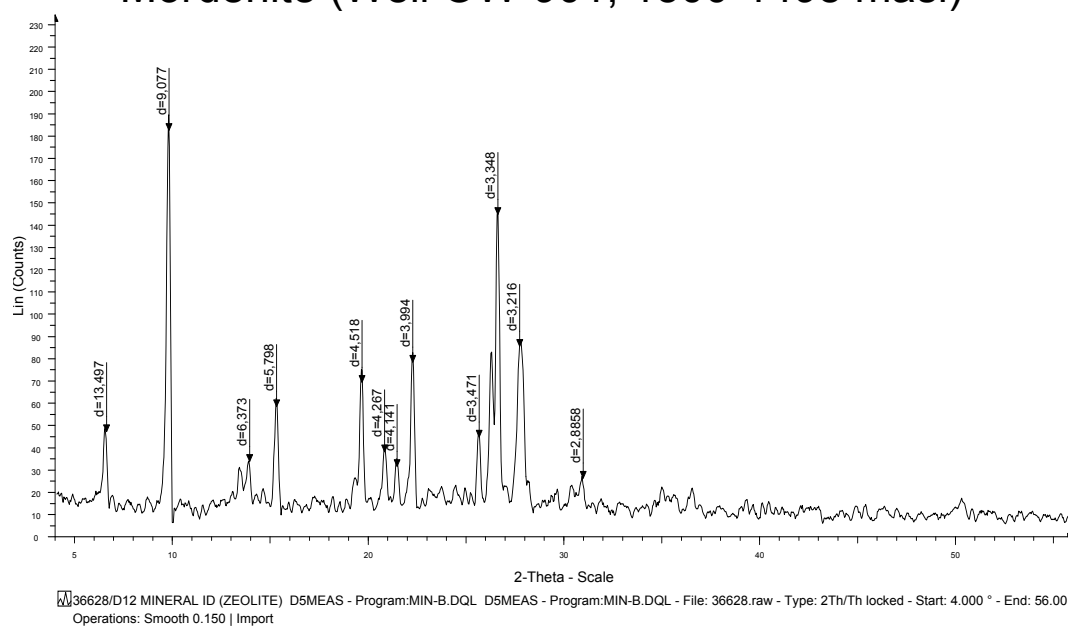
FIGURE 17: Diffractogram of mordenite showing strong peaks at 9.077 Å and 3.348 Å

Prehnite is a rare mineral in Olkaria Domes wells and occurs intermittently below 770 masl in well OW-901, below 639 masl in well OW-902 and below 701 masl in well OW-903. The mineral becomes rare disappearing completely below 214 masl in well OW-901, below -81 masl in well OW-902 and below 95 masl in well OW-903. It occurs as a vein filling mineral mainly in association with albite, epidote, chlorite, calcite and quartz. It is recognized in thin section by its sheaf like 'bow-tie' structure, good cleavage in one direction and strong birefringence. Three analyses of prehnite in well OW-901 at 288-286 masl indicate an average composition of $Ca_{2.4}Fe_{0.8}Al_{1.2}Si_{3.3}O_{10}(OH)_2$ (Karingithi, 2002). The few analyses may not be representative, but they may indicate substantial concentration of iron (Fe) in the prehnite.

Pyrite crystals are present in well OW-901 from 1675 masl, becoming rare until it disappears below -120. In well OW-902 it occurs from 1621 masl to the bottom of the well and in well OW-903 it occurs from 1991 masl to the bottom of the well. It occurs as euhedral cubic crystals with brassy yellow luster in reflected light. Tiny cubic pyrite crystals were deposited in fractures, vesicles and veins and as disseminations in the groundmass. XRD analysis of pyrite indicate strong peaks at 3.13 Å, 2.71 Å, 2.42 Å, 2.21 Å and 1.91 Å as shown in the typical XRD diffractogram in Figure 18.

Quartz is colourless to white in colour and occurs in euhedral to subhedral crystals. It is identified both as open space (vesicle) fillings and vein filling mineral. In well OW-901, quartz occurs from 1395 masl to the bottom of the well, in well OW-902, it occurs from 1265 masl to the bottom of the well and in well OW-903 it occurs from 1663 masl to the bottom of the well. Euhedral open space quartz crystals up to 2 mm long were deposited later than chalcedony in basaltic formation at 1203-1127 masl in well OW-903. Most of these quartz deposits consist of tiny euhedral to subhedral crystals that formed on top of botryoidal chalcedony in vesicles, veins and fractures. The same rock unit also consists of thin veins of quartz or tiny colourless crystals that formed in open spaces without earlier chalcedony deposits.

Sphene. In well OW-901, sphene was encountered from 1032 masl to the bottom of the well, in well OW-902, it occurs from 1035 masl to the bottom of the well and in well OW-903, it occurs sporadically from 1079 masl to the bottom of the well. Sphene occurs mainly as irregular grains and rarely as clear euhedral crystals having acute rhombic sections. The mineral occurs mainly as a result of alteration of ferromagnesian minerals in association with chlorite, quartz and calcite.

28

Pyrite Well OW-901 (1420-1418 masl)
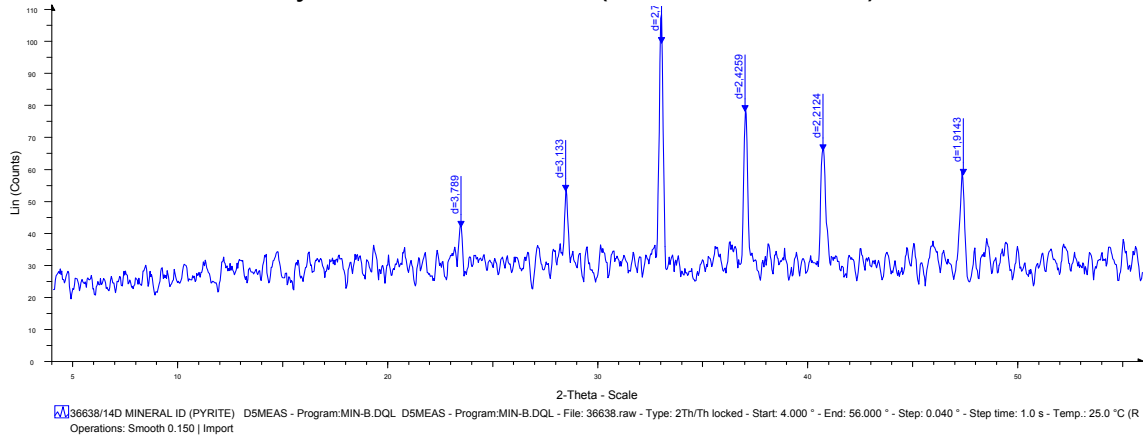
FIGURE 18: Diffractogram of pyrite showing strong peaks at
3.13 Å, 2.71 Å, 2.42 Å, 2.21 Å and 1.91 Å

Swelling chlorite and corrensite. Swelling chlorite was encountered in a basaltic formation at 686-588 masl in well OW-901.   XRD analysis of the clay showed peaks for the untreated run at 14.28 Å, the glycolated run swells to 16.74 Å and the oven heated run collapses to 14.16 Å. Corrensite was also identified in a basaltic formation in well OW-903 at 1143-1137 masl.   The untreated sample peak is at 29.30 Å, the glycolated peak swell to 31.30 Å and the oven heated run collapses completely. Typical XRD diffractograms of swelling chlorite and corrensite are shown in Figures 19 and 20, respectively.

Clays (Well OW-901 688-686 masl)
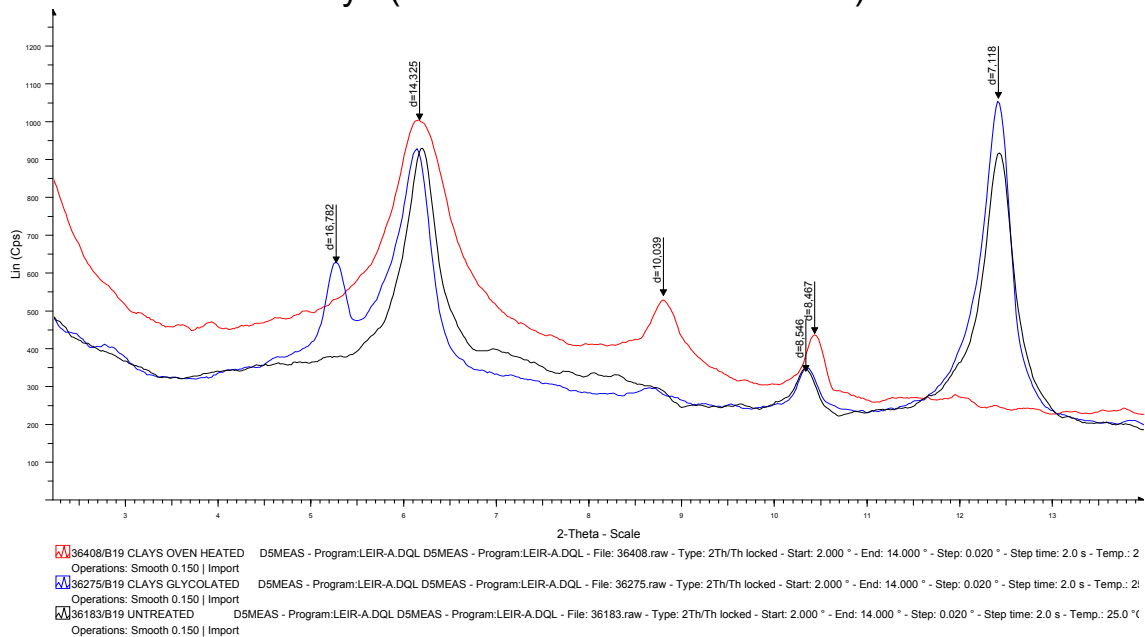
FIGURE 19: Diffractograms of clays showing swelling chlorite peaks at 14.28 Å for the
untreated run, the glycolated run swells to 16.78 Å and the oven heated run collapses
to 14.33 Å. Illite and chlorite are also present in the analysed sample

Wairakite occurs rarely and intermittently below 770 masl in well OW-901, below 1225 masl in well OW-902 and below 103 masl in well OW-903, disappearing at depth in all the three wells. The mineral is found as open space filling in association with quartz and calcite. XRD analysis indicated strong peaks at 3.39 Å and 5.56 Å as shown in the typical wairakite diffractogram in Figure 21.
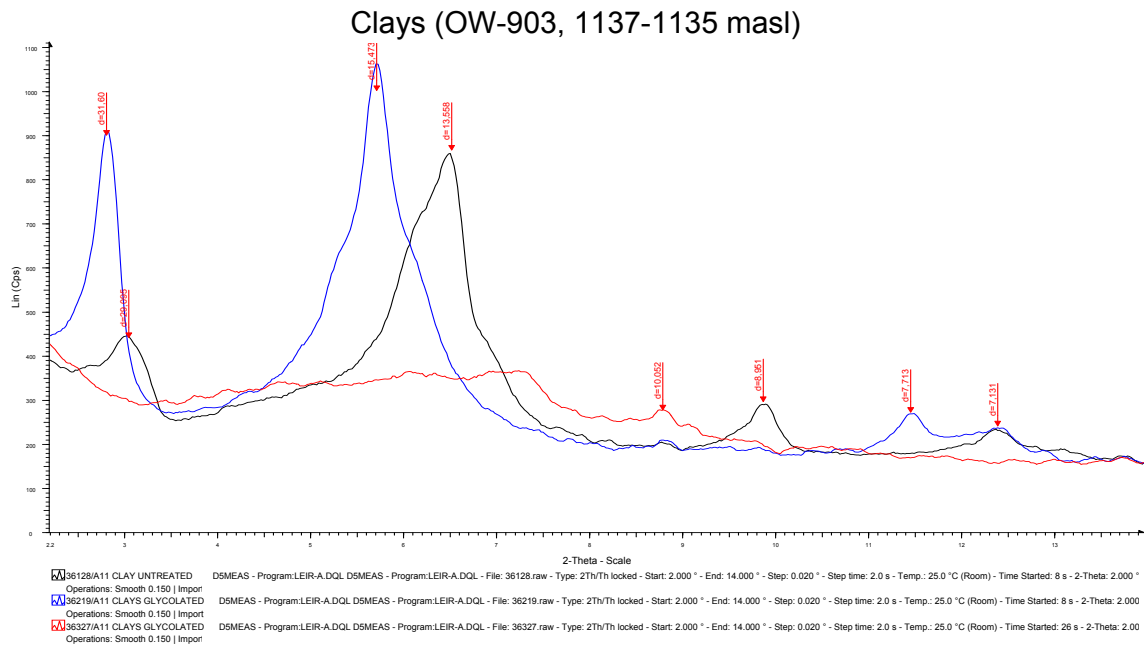
FIGURE 20: Diffractograms of clays showing strong corrensite 001 peak at 29.10 Å for the
untreated run, the glycolated run swell to 31.60 Å and the oven heated run collapses
completely, the 002 peaks are at 13.56 Å and 15.47 Å for the untreated
and the glycolated runs while the oven heated collapses completely
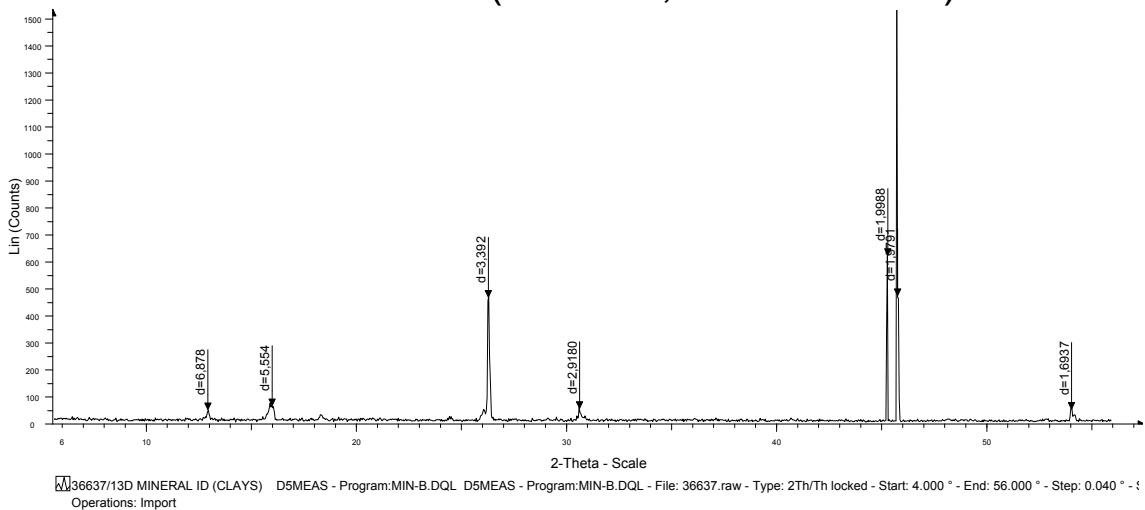
FIGURE 21: Diffractogram of wairakite showing strong peaks at 3.92 Å and at approximately 2.00 Å

4.5 Hydrothermal mineral zonations

Based on hydrothermal alteration minerals assemblages in Olkaria Domes geothermal field, four
alteration zonations can be recognized with a possibility of one or two sub-zones (Figure 10, 11, 12
and 22). The zones are:

1) The zeolite-chlorite zone;
2) The illite-chlorite zone;
3) The epidote-illite-chlorite zone; and
4) The garnet-biotite-actinolite zone.
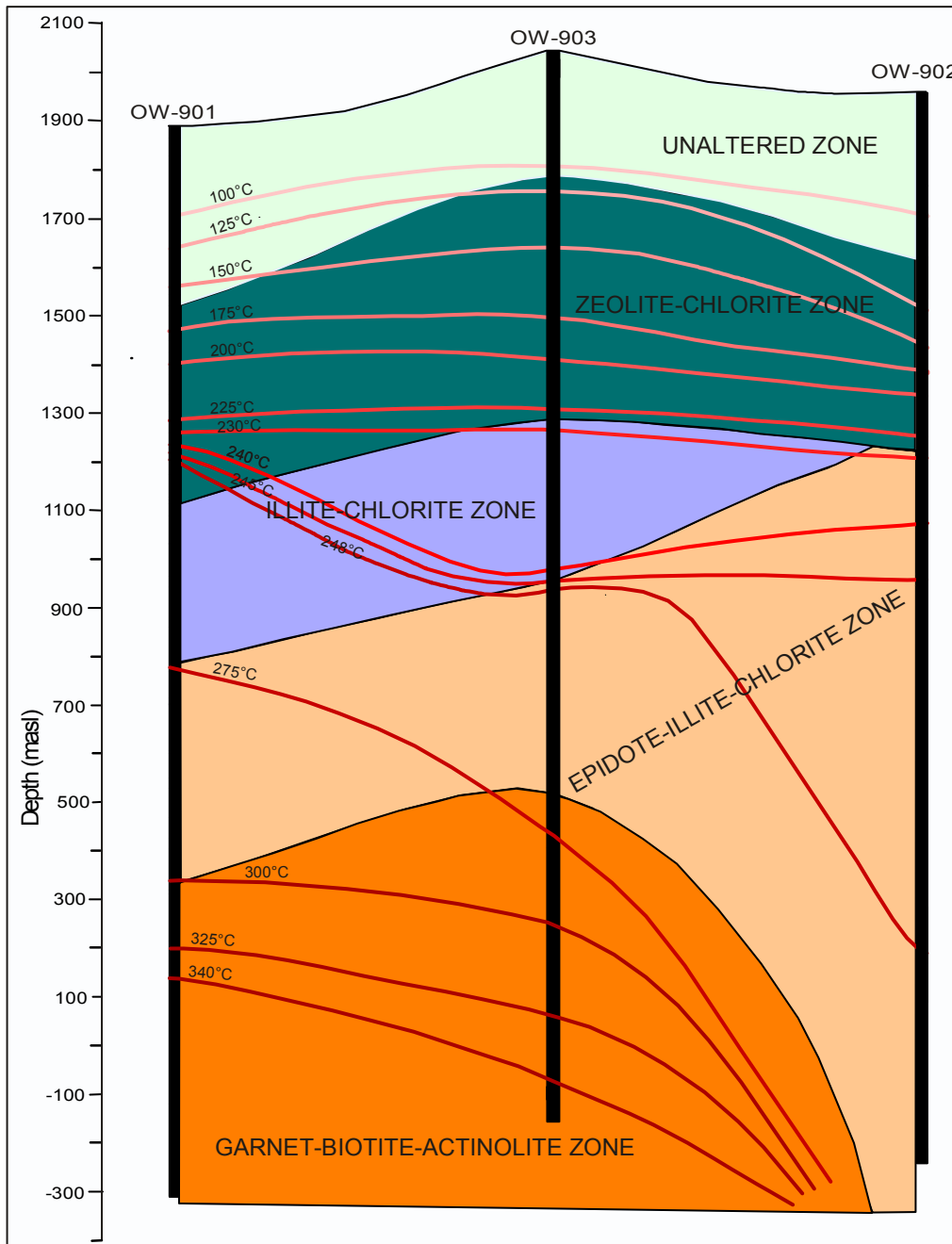
FIGURE 22: Distribution of zonations and measured formation temperature isotherms
with depth across wells OW-901, OW-903 and OW-902 in Olkaria Dome field

The upper few hundred meters of each well is unaltered. The zeolite-chlorite zone, which occurs immediately below the unaltered zone, is about 400 m in wells OW-901 and OW-902 and 500 m thick in well OW-903. Other minerals characterized by this zone include chalcedony, pyrite and to a lesser extent calcite. The illite-chlorite zone is not present in well OW-902 and is about 330 m thick in wells OW-901 and OW-903. The chlorite-illite-epidote zone is 450 m in both wells OW-901 and OW-903 and in well OW-902 the zone occurs to the bottom of the well. The garnet-biotite-actinolite zone is over 650 m in both wells OW-901 and OW-903 but is absent in well OW-902. The mineral assemblages (biotite and actinolite) representing the zone were not observed in well OW-902 and although petrographic analysis did not detect garnet, electron microprobe analysis was able to detect it at 9-3 masl. Other minerals present in this zone include chlorite, pyrite, epidote, prehnite and wairakite.

4.6 Mineralogical evolution

The paragenetic sequences in hydrothermal systems are identified from cross-cutting veins and amygdale infilling sequences. Due to exclusive use of rotary bits and very few and unrepresentative cores having been cut at Olkaria Domes field, most of the macroscopic vein fillings and amygdales textures providing information on the time relationships were lost. Table 7 shows the depositional sequences of hydrothermal alteration minerals in cuttings from various depths in Olkaria Domes wells as deduced from textural relationships. The reconstruction of the paragenetic sequences is difficult from the microscopic veins and vesicles since the sequences are highly variable and depict local conditions.   Most likely all the high temperature veins or vesicle filling minerals have been forming over a period of time and all forming at more or less the same time with their deposition being governed by the kinetics of mineral dissolution and their precipitation.

TABLE 7: Depositional sequences of hydrothermal alteration minerals
at various depths in Olkaria Domes geothermal field

Well	Depth (masl)	Depositional sequence (early»late)	Filling type
OW-901	1578-1576	chalcedony»pyrite»calcite	vein
OW-901	1324-1322	chlorite»calcite	vein
OW-901	980-978	chlorite»chalcedony	vesicle
OW-901	972-970	pyrite»quartz	vein
OW-901	780-778	quartz»epidote	vein
OW-901	754-752	quartz»calcite	vein
OW-901	288-286	epidote»quartz	vein
OW-901	132-130	quartz»epidote	vesicle
OW-901	-4 to -6	quartz»epidote	vein
OW-902	1297-1295	chlorite»calcite	vesicle
OW-902	671-669	epidote»calcite	vein
OW-902	113-111	calcite»epidote	vein
OW-903	1282-1283	quartz»calcite	vesicle
OW-903	1257-1255	calcite»chlorite»calcite	vesicle
OW-903	1251-1249	chlorite»calcite»chlorite	vesicle
OW-903	1207-1205	quartz»chlorite	vesicle
OW-903	1198-1187	oxide»quartz»chlorite»quartz	vesicle
OW-903	1183-1181	chalcedony»quartz	vesicle
OW-903	425-423	epidote»quartz	vein
OW-903	401-399	calcite »epidote	vein

4.7 Fluid inclusion geothermometry

The homogenization temperatures (T_h) of fluid inclusions in Olkaria Domes samples were measured and the results are presented in Table 8. These inclusions are all hosted by calcite and quartz, which occurs widely in the geothermal system. The T_h values at 240 masl in well OW-901 ranged from 238-272°C in quartz veins and from 280-320°C in calcite veins. The formation temperature at this depth is 314°C.

The lowest T_h value (238°C) in quartz veins from this well is 76°C below the measured formation temperature and the highest value (272°C) is 42°C below to the measured formation temperature (314°C). The average value for the inclusions in quartz veins is 256°C and is 58°C below the measured formation temperature. In the calcite veins the lowest T_h value of 280°C is 34°C below the measured formation temperature and the highest T_h value (320°C) is 6°C above the measured formation temperatures (314°C). The average value for the inclusions in the calcite vein is 301°C and is 13°C below the measured formation temperature. These measurements indicate the inclusions in calcite vein represent close to the current formation temperatures whereas the quartz veins indicate

past cooler conditions. If this interpretation is valid, it implies that the silica in quartz precipitated from hotter fluids is mostly derived from the primary feldspars of the rock and not of the earlier quartz precipitated under cooler conditions. A fluid inclusion hosted by a calcite vein from well OW-901 at 240 masl is shown in Plate 2 below.

TABLE 8: Fluid inclusion homogenization temperatures (T_h) of Olkaria Domes wells.
Measured temp. indicates measured formation temperature at that depth.

Well OW-901 (240 masl)		Well OW-902 (671 masl)		Well OW-903 (517 masl)	
Measured temp. 314°C		Measured temp. 247°C		Measured temp. 256°C	
Vein	**T_h (°C)**	**Vein**	**T_h (°C)**	**Vein**	**T_h (°C)**
Quartz	258	Quartz	246	Quartz	187
Quartz	258	Quartz	253	Quartz	216
Quartz	238	Quartz	221	Quartz	220
Quartz	240	Quartz	248	Quartz	242
Quartz	260	Quartz	256	Quartz	222
Quartz	238	Quartz	240	Quartz	220
Quartz	269	Quartz	238	Quartz	240
Quartz	271	Quartz	217	Quartz	240
Quartz	271	Quartz	215	Quartz	195
Quartz	247	Quartz	220	Quartz	185
Quartz	260	Quartz	252	Quartz	200
Quartz	272	Quartz	235	Quartz	240
Quartz	258			Quartz	224
Quartz	247			Quartz	178
Calcite	320			Quartz	204
Calcite	304			Quartz	191
Calcite	280			Quartz	275
Calcite	298			Quartz	228
				Quartz	196
				Quartz	234
				Quartz	240
				Quartz	242
Average	**301*** **256†**	**Average**	**237**	**Average**	**219**

*Average for calcite;   †Average for quartz
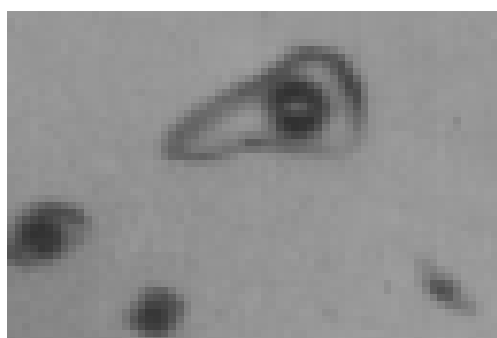
PLATE 2: Fluid inclusion in hydro-thermal calcite with a homogenization temperature of 320°C at 240 masl in well OW-901

In well OW-902 at 689 masl T_h values in inclusions hosted in quartz veins ranged from 210-256°C with an average of 237°C, whereas the formation temperature at this depth is 247°C. In well OW-902, the highest value from the T_h value (256°C) is equivalent to the boiling point curve value (256°C) and 8°C above the measured formation temperature of 247°C. The lowest T_h value (210°C) is 37°C lower than the maximum measured formation temperature. The average T_h value of 237°C in this well corresponds fairly well with the present day conditions.

The T_h values of inclusions in quartz veins at 517 masl in well OW-903 varied widely between 178-275°C with an average of 219°C whereas the formation temperature at this depth is 265°C. The lowest T_h value of 178°C is 87°C lower than the measured formation temperature suggesting that the fluids were trapped when temperatures were lower than the present day values. The highest T_h measurement of 275°C is 10°C

higher that the measured formation temperature indicating that the fluids in these inclusions were trapped at nearly the same temperatures as current measured formation temperatures.

4.8 Measured, hydrothermal alteration and fluid inclusion temperatures

In any geothermal system, there is always some uncertainty whether observed minerals distribution and zonations reflect current formation temperatures or are related to some previous thermal events or regimes. In the Greater Olkaria geothermal area as in other geothermal fields throughout the world, hydrothermal alteration minerals are important indicators of subsurface thermal changes. A correlation between measured, hydrothermal alteration and fluid inclusion temperatures indicate how a particular geothermal system has evolved with time. Common hydrothermal alteration minerals used as geothermometers in Olkaria and their stability temperature ranges as estimated from measured formation temperatures are shown in Figure 23.
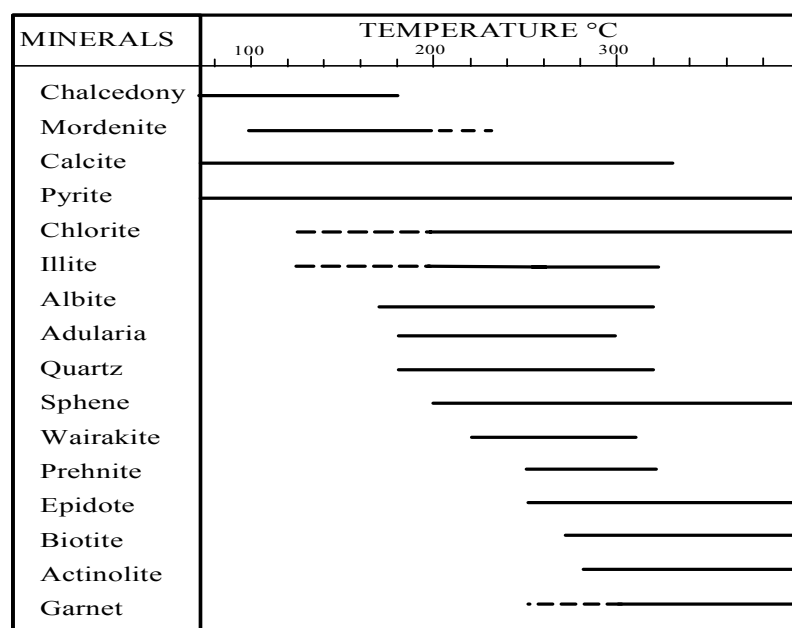
FIGURE 23: Common hydrothermal alteration minerals used as geothermometers and their temperature stability ranges. Dotted sections indicate mineral outside their usual stability ranges (modified from Reyes, 1990)

Figure 24 shows the correlation between measured, interpreted hydrothermal alteration and fluid inclusion temperatures in well OW-901. Geothermometry of alteration minerals and fluid inclusions in well OW-901 indicate that there has been some heating. The occurrence of chalcedony (stable below 180°C) and presence fluid inclusions from quartz veins (with homogenization temperatures averaging 256°C) at higher current formation temperatures reflect progressive heating through time. However, calcite veins with homogenization temperatures averaging 301°C closely reflect current conditions in the reservoir. High temperature hydrothermal alteration minerals e.g. epidote, biotite, actinolite and garnet seem to be in equilibrium with the present geothermal system in well OW-901, with all the minerals occurring within their temperature stability ranges.

The correlation between measured, interpreted hydrothermal alteration and fluid inclusion temperatures in well OW-902 shown in Figure 25 indicate probable cooling with hydrothermal minerals occurring below their stability temperature ranges. Here garnet occurs where the measured formation temperature is below its temperature stability range indicating it is relict. Fluid inclusion temperatures, however, seem to reflect current conditions with the average homogenization temperature of 237°C being close to the measured formation temperatures of 247°C.

Well OW-903 (Figure 26) had average fluid inclusion temperatures in quartz veins way below the measured formation temperatures with an average of 219°C while the measured formation temperature at that depth is 265°C. This indicates that there has been heating in the system since the inclusions were trapped. The interpreted hydrothermal alteration temperatures indicate that the alteration minerals are in equilibrium with the geothermal system with illite, epidote, biotite, garnet and actinolite all occurring within their temperature stability ranges.
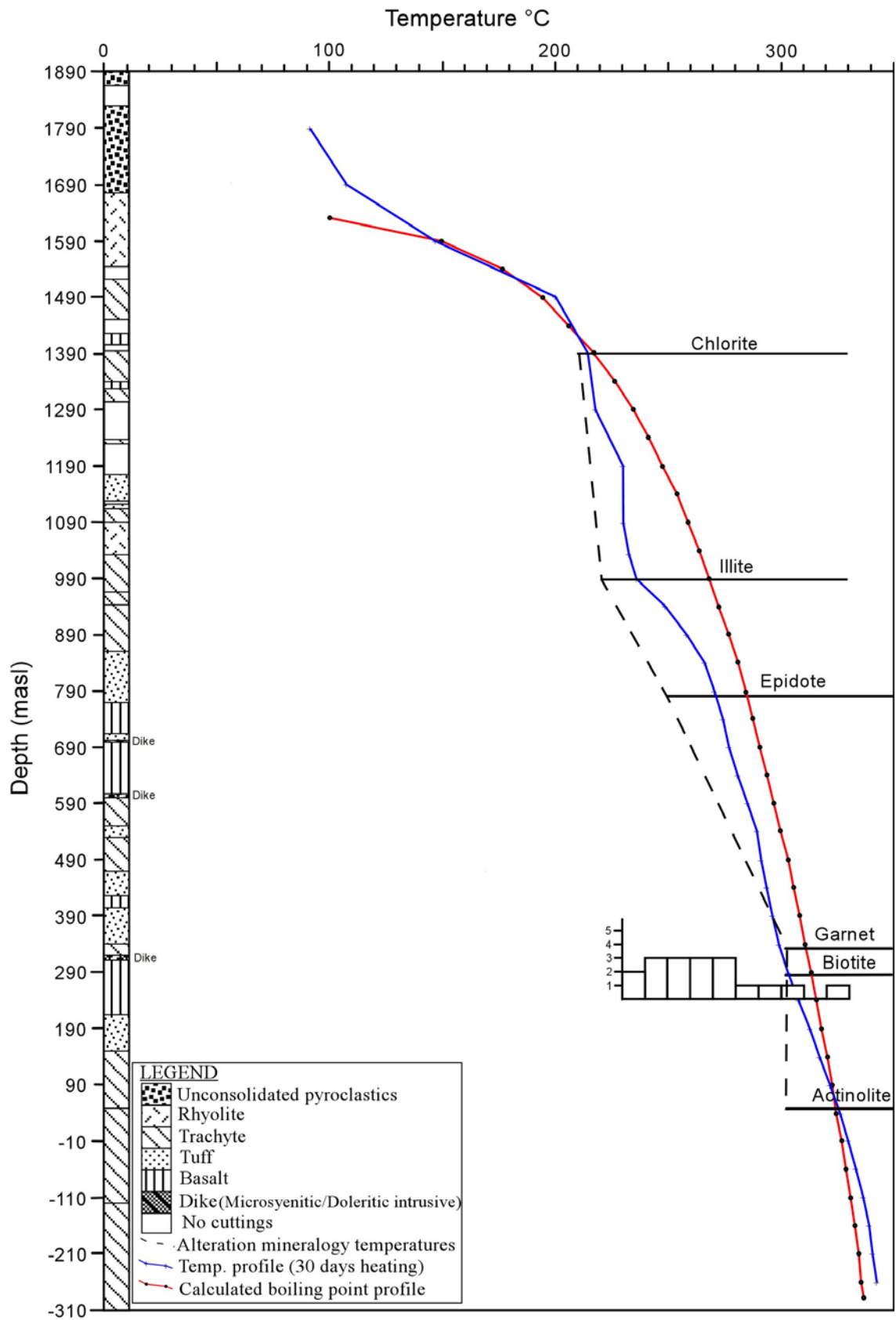
FIGURE 24: Plot of lithology and correlation between measured, interpreted hydrothermal alteration minerals and fluid inclusion temperatures with depth of well OW-901
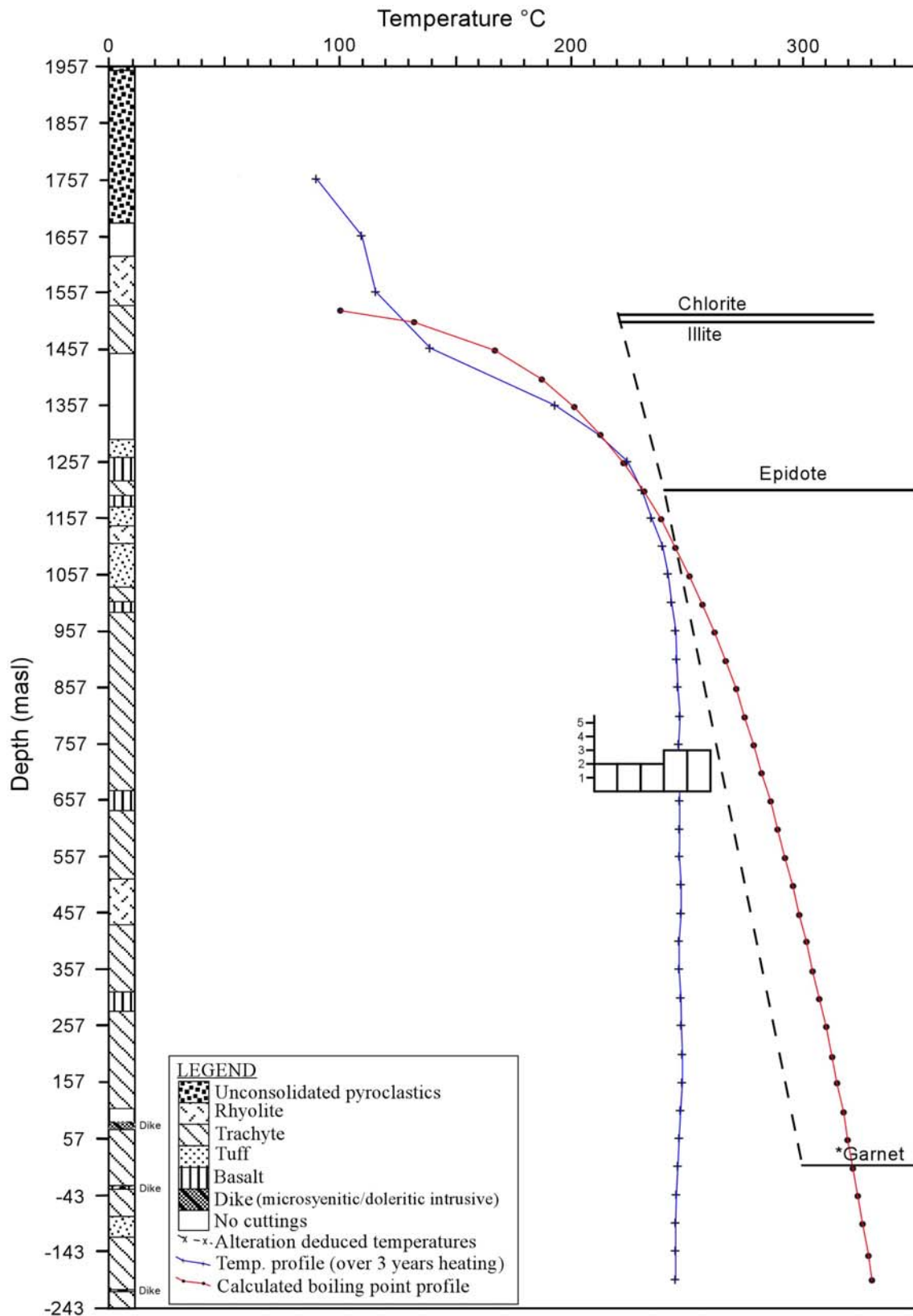
FIGURE 25: Plot of lithology and correlation between measured, interpreted hydrothermal
alteration minerals and fluid inclusion temperatures with depth of well OW-902.
*Based on electron microprobe analysis Karingithi (2002)
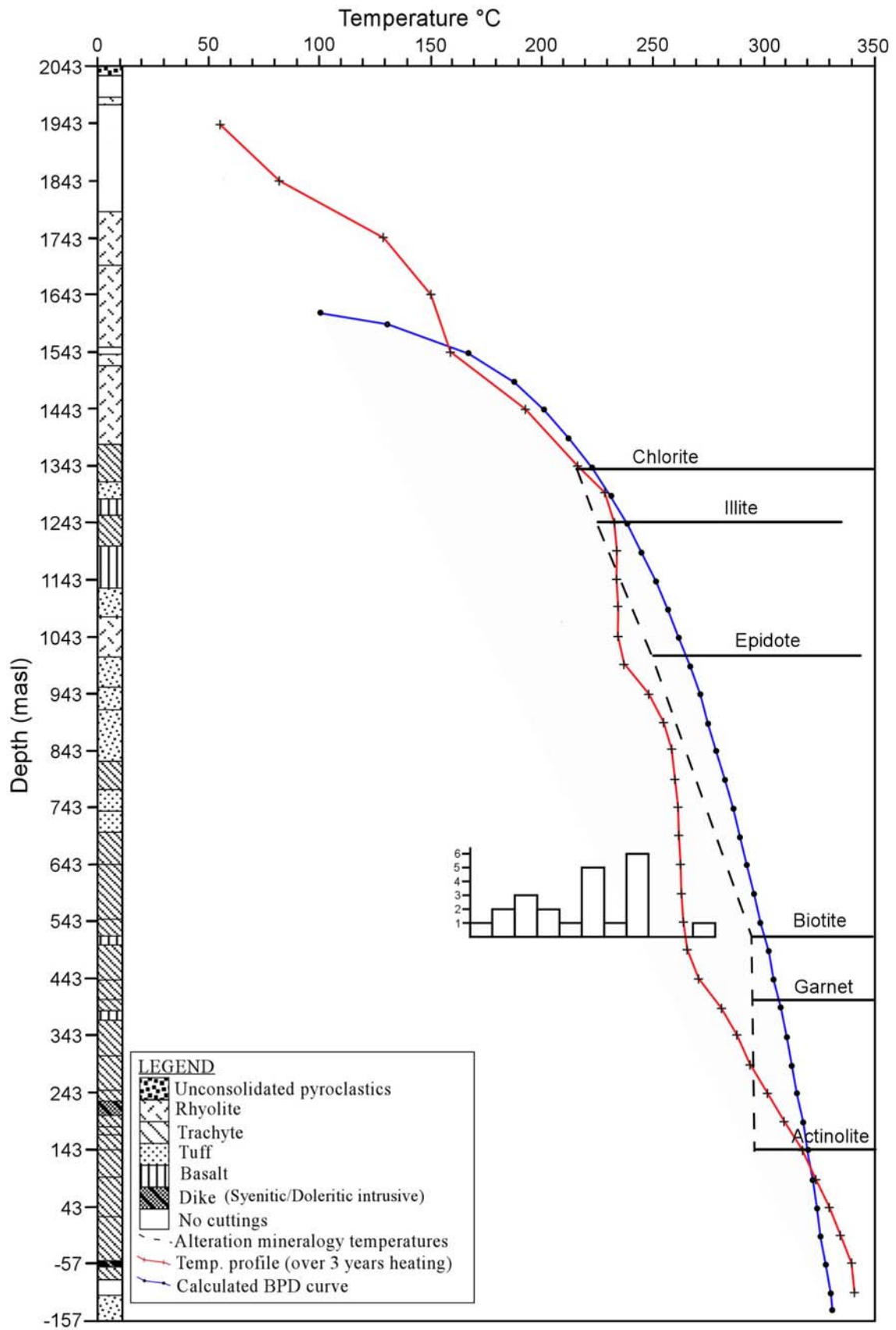
FIGURE 26: Plot of lithology and correlation between measured, interpreted hydrothermal alteration minerals and fluid inclusion temperatures with depth of well OW-903

37

Index minerals used to construct isograds across wells OW-901, OW-903 and OW-903 in Olkaria Domes field include actinolite, chlorite, epidote, garnet and illite. Isograds give a general picture of the temperature distribution in a geothermal system. Strictly speaking, however, a definite isograd (e.g. the epidote isograd) does not necessarily represent a definite temperature. The distribution of hydrothermal minerals isograds is not distinctly parallel to the isothermal contours (Figure 27) indicating that hydrothermal alteration is not a function of subsurface temperature only but the rock composition also influences the kinetics of the hydrothermal alteration minerals formation. The isograds clearly indicate high and shallow temperatures towards well OW-901 and low temperatures towards well OW-902. In well OW-902, below 1000 masl, the temperature becomes more or less isothermal, with very little or no change with depth. Biotite and actinolite were not encountered in the well, but garnet was encountered at temperatures well below its stability temperature range.
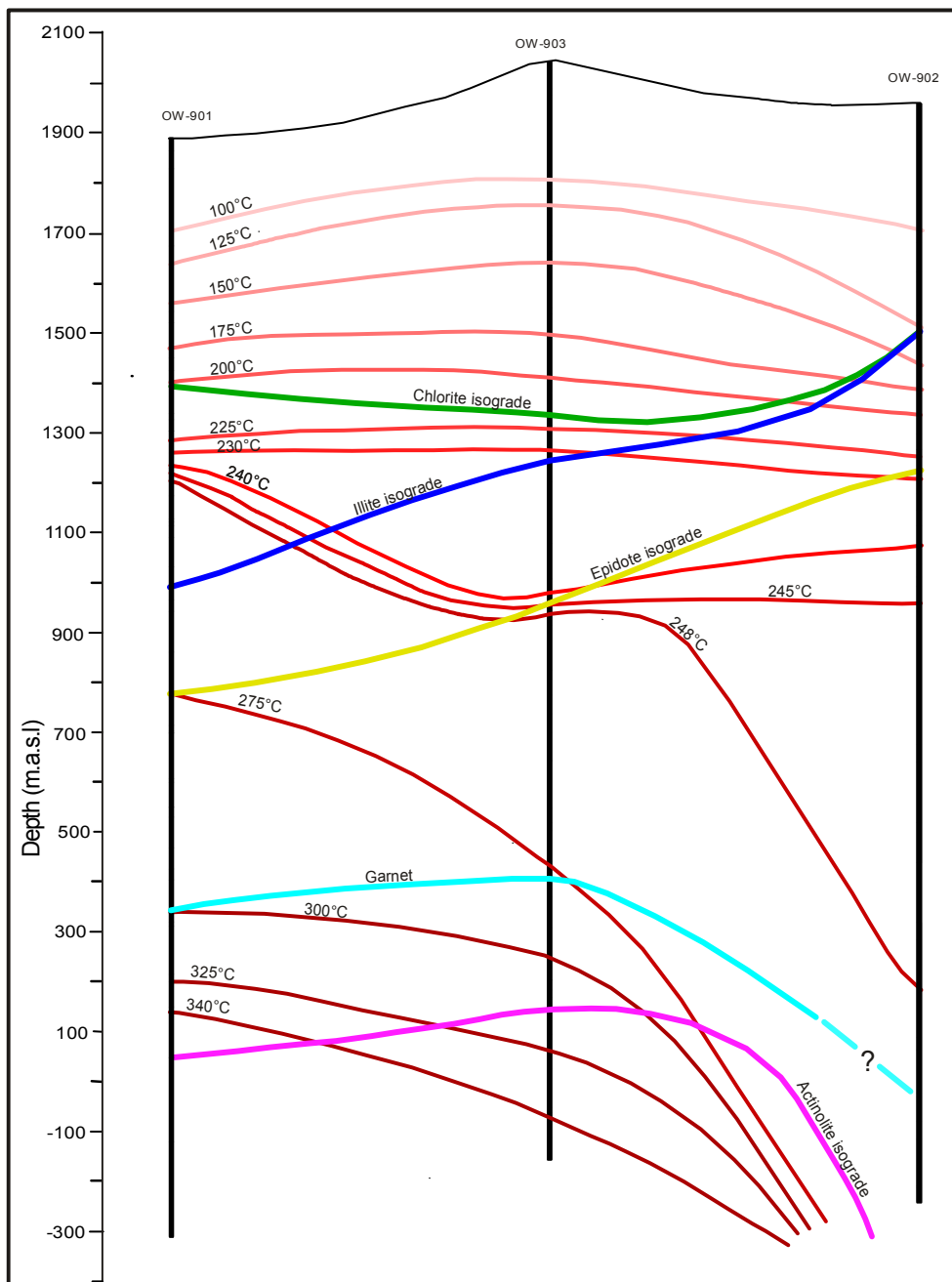
FIGURE 27: Plot of epidote, illite, chlorite, actinolite and garnet isograds and measured temperature isotherms across wells OW-901, OW-903 and OW-902

4.9 Aquifers

Sources of permeability in Olkaria Domes geothermal field include fractures and joints due to intrusions and along edges of plugs and domes, lithological contacts, joints, clast-matrix or fragment contacts in some breccias. Permeable zones in the field were interpreted by loss or gain of circulation fluid, hydrothermal alteration mineralogy patterns, and temperature recovery tests. Indicators of high permeability in Olkaria Domes geothermal system apart from high alteration intensity and sheared rocks include presence of abundant pyrite and calcite. These minerals are commonly found in or adjacent to aquifers penetrated by the wells and occur as alteration of the rock as well as in veins often as coarse grains. Browne (1984) indicated some relationship between the alteration of feldspars and deduced permeability in Olkaria East field whereby no alteration indicate little or no permeability and where feldspars are highly altered with adularia occurring throughout the rock matrix indicate high permeability. Alteration intensity applies to Olkaria Domes, but there was no clear relationship observed between occurrences of abundant adularia and permeable zones. Low permeability on the other hand apart from absence of the above minerals is indicated by low alteration and presence of tight veins.
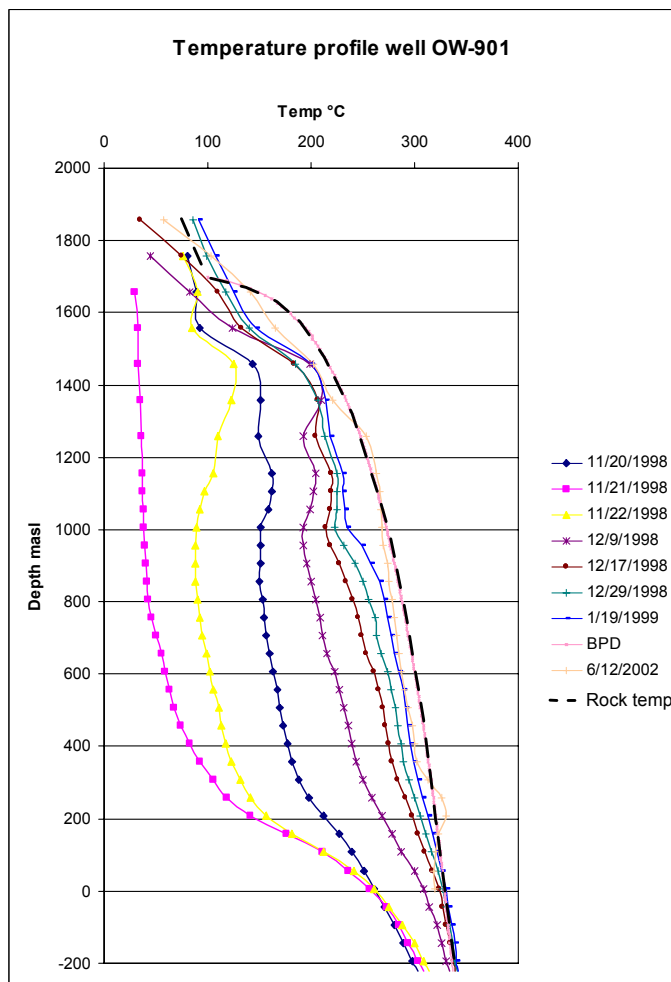
FIGURE 28: Temperature profiles of well OW-901

Circulation losses recorded at shallow depths above the groundwater table are due to blocky comenditic lavas but most of these zones including the unwanted cold aquifers were cased off. From completion tests (Figure 28), feed zones in well OW-901 at occur around 1090 masl, 930 masl, 690 masl and 390 masl (Ofwona 1998). Well OW-902 from completion tests (Figure 29) had feed zones located at around 1057 masl, 757 masl and 357 masl (Odeny et al, 1999). In well OW-903 (Figure 30), completion tests recorded feed zones at around 1193 masl, 889 masl, 419 masl and 43 masl (Ofwona 1999). The aquifers from the temperature recovery tests correspond to the aquifers from geological observations. Other feeder zones were mainly confined to lithologic contacts between the rocks formations. Minor loss or gain in circulation could not be established because the volume of circulation fluid coming out of the bore hole was not being measured and therefore small aquifers could not be identified.

Completion test carried out in Olkaria Domes wells indicated that OW-903 is more permeable than the two other exploration wells OW-901 and OW-902 (Ofwona 1999). This agrees with the higher fracture permeability encountered in well OW-903 compared to wells OW-901 and OW-902. Table 9 above shows the location of major feed zones interpreted from geological observations together with drilling observations and temperature recovery tests.
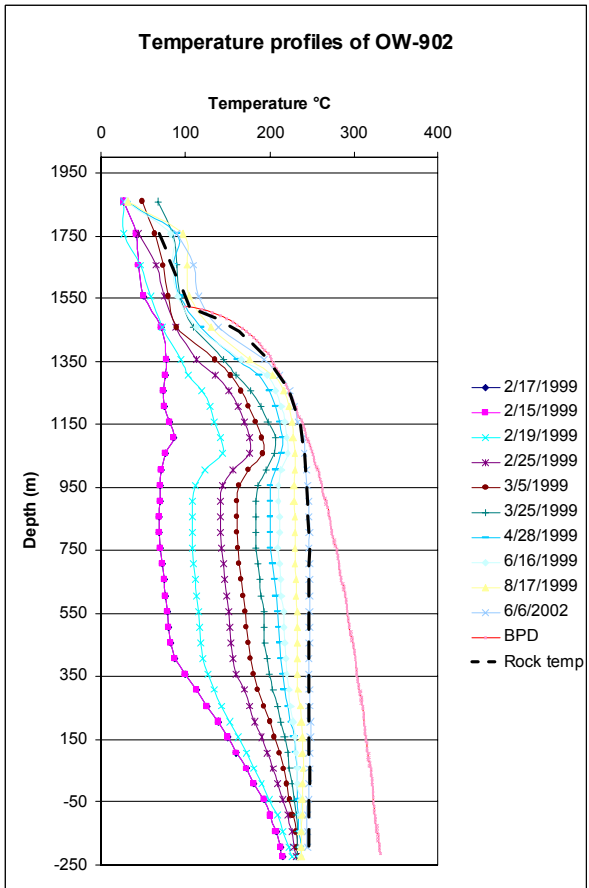
FIGURE 29: Temperature profiles of
well OW-902
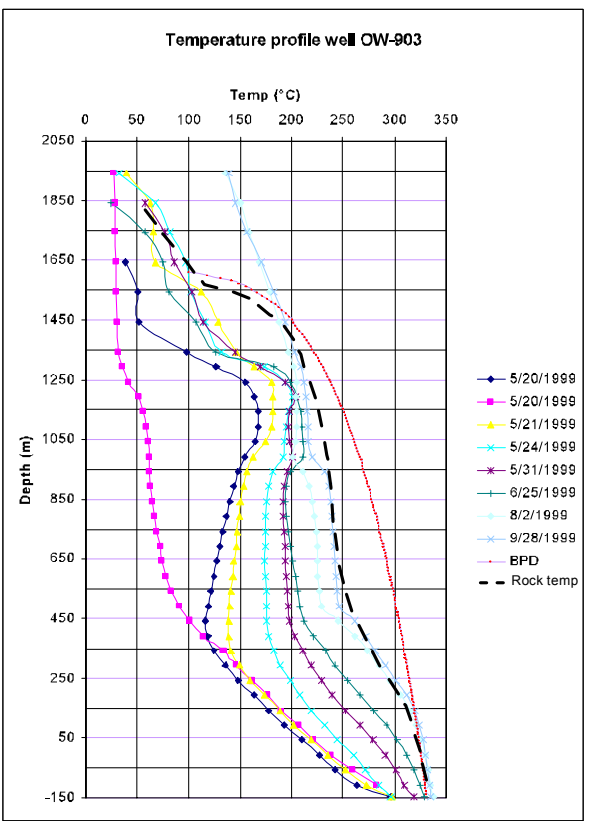
FIGURE 30: Temperature profiles of
well OW-903

TABLE 9: Interpreted permeable zones based on geological observations and
temperature recovery tests in wells OW-901, OW-902 and OW-903

Well	Depth (masl)	Evidence from geological observations, drilling observations and temperature recovery profiles
OW-901	1544-1522	Circulation loss and presence of abundant calcite
	1450-1424	Circulation loss
	1405-1395	Circulation loss
	1306-1238	Circulation loss and presence of abundant pyrite
	1230-1176	Circulation loss
	1090-1066	Contact between trachyte and rhyolite and abundant pyrite in veins. Quick temperature recovery also noted.
	1030-1000	Fracture permeability in trachyte
	950-940	Contact between two trachytic formations
	825-820	Associated with primary permeability in tuff
	708-698	Fracture permeability
	614-590	Tuff/basalt contact
	540-530	Fractured formation and contact between tuff and trachyte
	308-304	Fractured basalt
	16 to -12	Fractured trachyte
OW-902	1683-1620	Loss of circulation
	1449-1298	Loss of circulation
	1285-1183	Vesicular basaltic flow
	1009-989	Fracture along an intrusive
	675-639	Highly altered basaltic lava flow
	117-87	Loss of circulation
OW-903	2027-1787	Loss of circulation
	1599-1585	Fractured zone
	1551-1539	Loss of circulation
	1473-1469	Fractured zone
	1415-1411	Fractured zone
	1389-1381	Contact between two rhyolitic formations
	1101-1097	Abundant calcite and pyrite
	1013-1009	Contact between tuff and rhyolite
	861-855	Fractured zone
	783-775	Contact between tuff and trachyte
	717-709	Contact between tuff and trachyte
	645-641	Contact between trachyte and trachyte
	593-591	Contact between trachyte and trachyte
	443-439	Contact between trachyte and tuff and fast temperature recovery
	-85 to -111	Loss of circulation

5.0 CONCEPTUALIZED GEOLOGICAL MODEL OF THE GREATER OLKARIA GEOTHERMAL AREA

The development of a conceptualized model of the Greater Olkaria geothermal area was first proposed by Sweco and Virkir (1976) and since then the model has been reviewed from time to time as new data from newly drilled wells and reservoir simulation studies have become available. The reviewed models, which covered mainly Olkaria East, Olkaria Northeast and Olkaria West, have refined the original models. The main concepts remain, however, more or less the same (KenGen 2000). The inflows, outflow and upflow zones as well as fluid movement along faults and fractures and steam losses at the reservoir top mainly along the Ololbutot fault between wells OW-201 and well OW-01 as indicated by strong surface manifestations in those areas are some of the features outlined.

For a hydrothermal system to exist, the following conditions must be present; (i) a heat source, (ii) recharge fluid (iii) permeable formations and/or structures to allow water to percolate though and (iv) time for heat transfer from the hot intrusive to the water which is the media. Seismic studies in Olkaria indicate that the brittle-ductile transition occur from 6 km (Simiyu et al., 1998). The presence of a semi molten magma bodies, whose depths to their roots is not known have been determined by shear wave attenuation below the 6 km depth. A magma chamber under Olkaria volcanic complex exists between 7-10 km as observed from both geological and geophysical studies (Omenda, 2000). Occurrences of acid (comenditic) lavas on the surface and at shallow depths and trachytic lavas at deeper levels indicate that the magma chamber is highly differentiated. Extrusions and intrusions of magma occur along the N-S structures and the ring structure has resulted in an emplacement of a shallow heat source. Dikes have been formed by intrusion of magma along linear structures and therefore a strong lateral control of permeability in an east-west direction exists and is supported by different fluid chemistries between Olkaria East and Olkaria West fields (KenGen, 2000). The geothermal system at Olkaria is still active and this can be attributed to tectonics leading to increased activity in the area as evident by the recent Ololbutot eruption, which has been dated at 180±50 yrs B.P (Clarke et al., 1990). Isotopic studies (Ojiambo et al, 1993) indicate sources of the hydrothermal fluids in the Olkaria geothermal field to be from surface groundwater (meteoric) from the rift flanks and Lake Naivasha, which is a large fresh water body north of the area. Another possible source is from the magmatic rocks themselves, which exsolve juvenile water during the final stages of cooling. Sources of permeability in the Olkaria Domes geothermal field are both primary and secondary and include tectonic fractures, the thermally induced joints, lithologic contacts and clast-matrix or fragment contacts in breccias.

Apart from the faults, which have a total downthrow of about 300 m to the east, there is no major structural divide between Olkaria East and Olkaria Domes and therefore there could be a possibility that the two fields could be interconnected hydrologically. With only three wells drilled in Olkaria Domes field it is apparently difficult to tell whether there is for sure different upflows between the Olkaria East and Olkaria Domes field (Ofwona, 2002). The hottest region in Olkaria Domes is located around OW-901 as defined by measured temperatures and the distribution of mineral geothermometers. Stable measured formation temperature isotherms and geothermometer isograds confirm that the hottest part of the field occurs around OW-901 sector, where maximum formation temperatures of approximately 342°C were recorded close to the well bottom. The lowest temperatures are definitely towards well OW-902 with a maximum measured temperature of 247°C at well bottom. A NNW-SSE temperature cross section (Figure 31) clearly shows temperature isotherms indicating lower temperatures towards well OW-902.

The proposed conceptualized geological model, which is an update of the earlier model (KenGen 2000) and includes Olkaria Domes field indicate an inflow along the N-S striking fault west of the drill holes, an upflow around well OW-901 and the outflow to the south and east towards well OW-902 and OW-903. The pressure pivot point in well OW-901 is at 790 masl and the average pressure at that depth is 65.4 bars. In well OW-902 the pressure pivot point is located at 1057 masl and the pressure at the point averages 40.6 bars and in well OW-903 the pressure pivot point is located at 1143 masl and the averages pressure at the point averages 39.6 bars. From the pressure differences between the wells, it is clear that there is a pressure drop from well OW-901 towards wells OW-902 and OW-

903 indicating that these wells are located in the outflow zones. The upflow zone is located in area around well OW-901. The updated model is shown in Figure 32.
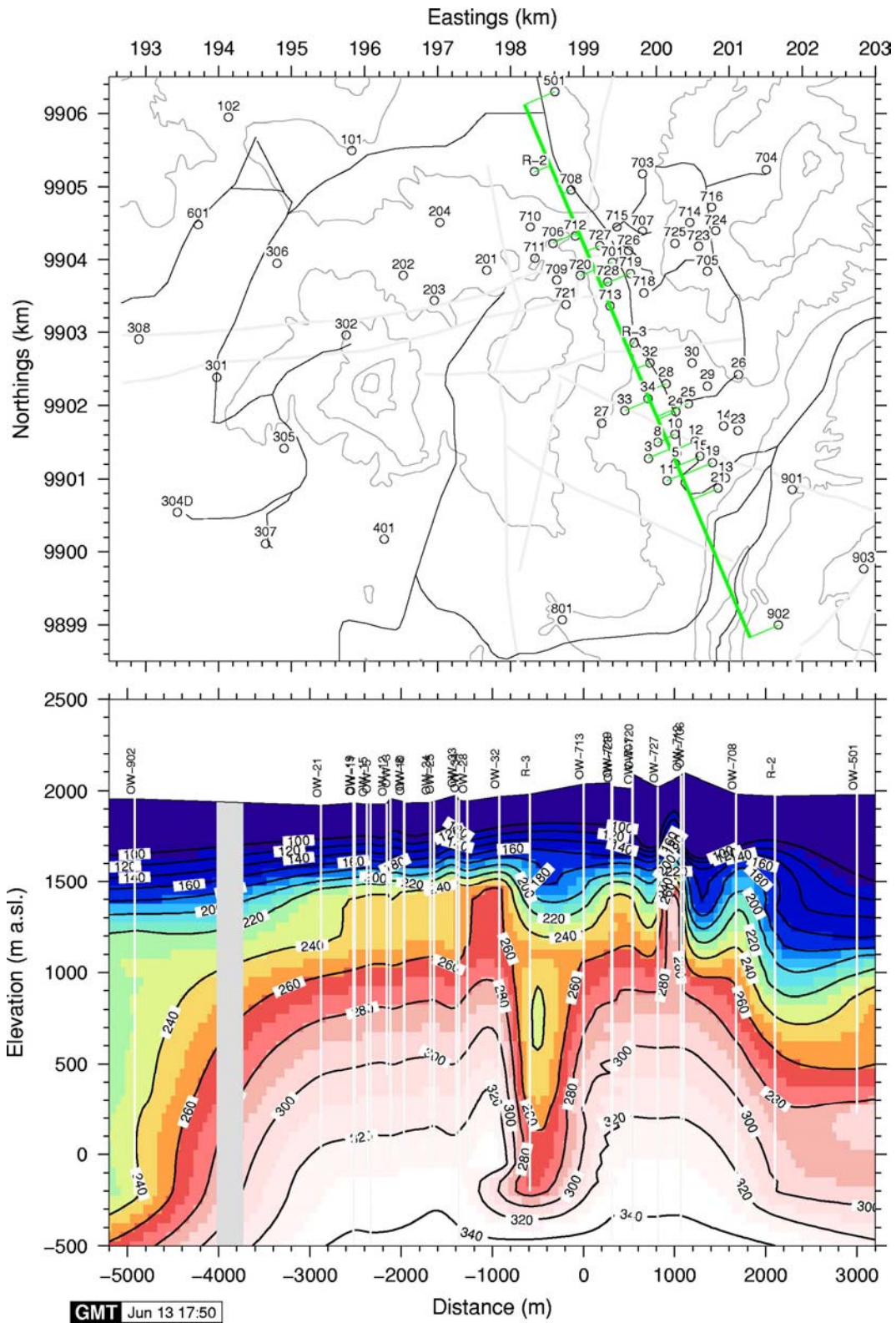
FIGURE 31: A temperature cross-section across Olkaria Northeast, Olkaria East and
Olkaria Domes fields in a NNW-SSE direction (Ofwona, 2002)
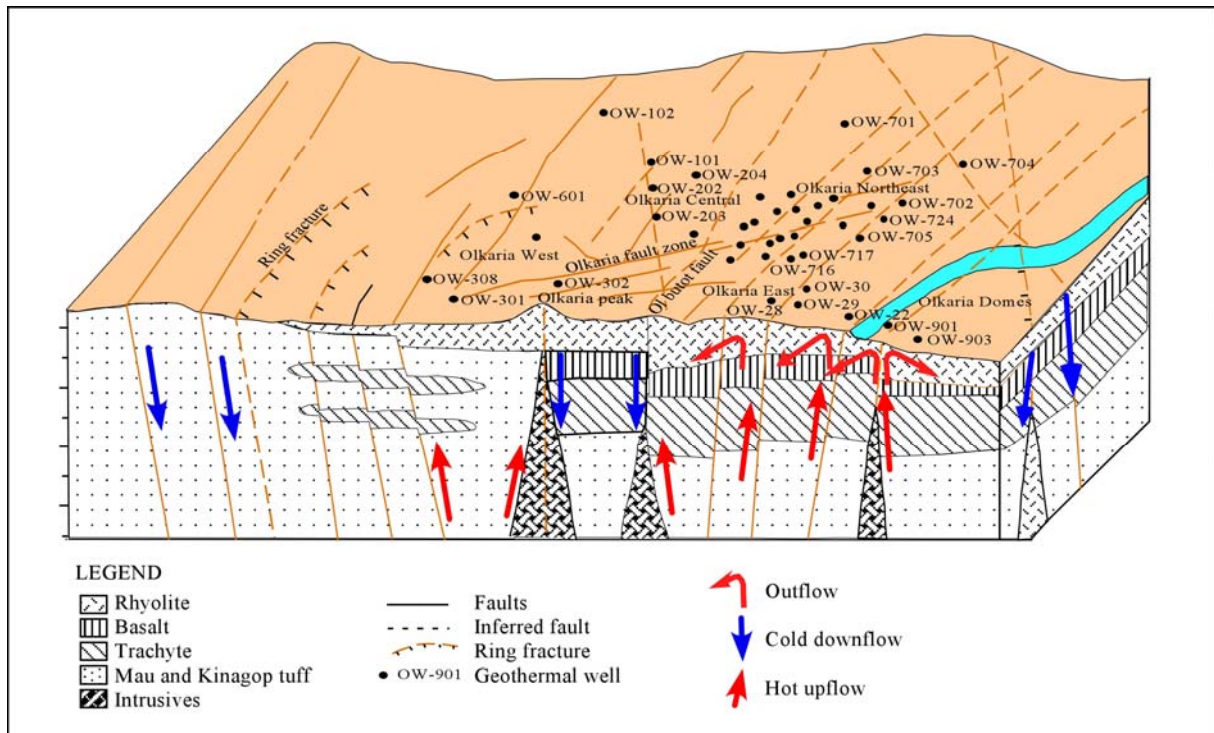
FIGURE 32: An update of the conceptualized geological model of the Greater Olkaria
geothermal area showing generalized geology and the locations of the fields
with respect to downflow, upflow and the outflow zones

6.0 DISCUSSION

The geology of the Greater Olkaria geothermal area is dominated by Pleistocene to Holocene comenditic rhyolite flows on the surface and tuffs, basalts, trachytes and minor dolerite and microsyenite intrusives in the subsurface. Major elements analyses of rocks from Olkaria Domes indicate their composition to range from basalt through trachyte to rhyolite. Their compositions plot in the same field as those of analysed samples from Olkaria East, Olkaria Northeast and the unaltered surface rocks. A geological cross section across wells from Olkaria East field and Olkaria Domes indicate no major structural divide between the two fields and the same formations occur in both fields.

Understanding subsurface geological structures of a geothermal area is essential in determining the factors that control the ascent of the geothermal fluid. It is also necessary to determine whether all faults in the existing fault pattern are equally important as channelways, or whether some faults are more permeable than others. A rock formation which has a well-developed fracture system may serve as an excellent host rock. Veins form where the fluids flow through larger, open space fractures and precipitate mineralization along the walls of the fracture, eventually filling it completely. The form of mineralization and alteration associated with faults is highly variable, and may include massive to fine-grained, networks of veinlets, and occasionally vuggy textures in some breccias as observed in Olkaria Domes wells.

On the surface at Olkaria Domes area, the distribution of geothermal manifestations is strongly associated with structural features. Fumarolic activities are concentrated along the ring structure on the eastern side of the field and along the N-S trending fault (Mungania, 1992; Clarke et al 1990). The manifestations indicate these structures are deep seated and extend into the geothermal system. Drilling of the three exploration wells in the Olkaria Domes field has revealed to some extent the structural patterns of the area. The area is crossed by faults and fractures as revealed by fault breccias, sheared zones and circulation losses experienced during drilling. Only certain buried faults provide efficient conduits for the ascent of geothermal fluid. . Main feeders of geothermal fluids in the area seem to be fissured zones associated with subsurface faults, fractures and contact zones between the formations. Such feeders were intercepted by all the three wells and are identified by loss zones, quick recovery in temperature profiles, sheared rocks and abundant calcite and pyrite in veins.

Hydrothermal minerals are mainly present in veinlets, vugs and as replacements of primary minerals in the volcanic rocks. Their distribution in this geothermal system is similar to the prograde variations observed in other geothermal fields. Due to their ubiquity and reactivity as a function of the physico-chemical environment of crystallization, clay minerals have been used as markers of paleoconditions in both fossil and active geothermal systems. They have proved to be useful in particular temperature estimations, which were based either on modification of crystal structure or modification of crystal chemistry of the crystallites. The regular change with depth seen in Olkaria Domes is from chlorite at shallower levels, followed by both illite and chlorite virtually to the bottom of the wells. Swelling chlorite and corrensite were restricted to basaltic formations at medium depths. On the basis of hydrothermal alteration minerals and their variation with depth, four hydrothermal mineral zonations can be recognized in the order of increasing temperature and depth. They are; (1) the zeolite-chlorite zone, (2) the illite-chlorite zone, (3) the epidote-illite-chlorite zone and (4) the garnet-biotite-actinolite zone. The upper few hundred meter of each well is unaltered. The illite-chlorite zone is absent in well OW-902 due to the presence of epidote at shallow levels, hence illite-chlorite-epidote occurring at a shallower depth. The garnet-biotite-actinolite is also absent in well OW-902 due to the absence of the index minerals representing the zone.

The homogenization temperatures (T_h) of fluid inclusions in quartz and calcite are particularly reliable predictors of past to present subsurface temperatures. The fluid inclusion temperatures in Olkaria Domes wells generally ranged from 178 to 320°C. The T_h values at 240 masl in well OW-901 ranged from 238-272°C in quartz veins and from 280-320°C in calcite veins. The formation temperature at the depth is 314°C. In well OW-902 at 689 masl, the T_h values in inclusions hosted in quartz veins ranged from 210-256°C with an average of 237°C. The formation temperature at the depth is 247°C.

The T_h values at 517 masl in well OW-903 varied widely between 178-275°C with an average of 219°C. The formation temperature at the depth is 265°C. Under ideal conditions the quartz in veins is supposed to dissolve and precipitate if the geothermal fluid is undersaturated with respect to silica and new inclusions are formed. In this case the source of silica could be from the feldspars hence the geothermal fluid is saturated with respect to silica and the quartz veins hosting past fluid inclusions are preserved. The fluid inclusions in calcite veins have T_h values close to the measured formation temperatures and therefore it must have been deposited in the present conditions of the reservoir, hence represent the current state of the reservoir. The inclusions therefore indicate that wells OW-901 and OW-903 have undergone some heating while well OW-902 has undergone some cooling.

Temporal changes in Olkaria Domes field must have occurred in the past. The age of the geothermal system at Olkaria system is not exactly known but there is evidence that during its lifetime, the thermal activity has changed both in location and character. The occurrence of quartz and other hydrothermal alteration minerals, which line joints in dykes, exposed within Ol'Njorowa gorge show that at some time in the past these dikes clearly served as fluid channels. Intuitively one would expect that the intrusion of Holocene lavas such as Ololbutot would induce profound changes in the Olkaria subsurface thermal regime (Browne 1984). There are no data available on the alteration ages, however, textures and fluid inclusion temperatures show the existence of at least two thermal episodes in the past. The presence of high-temperature minerals at shallow depths is associated with an early stage of hydrothermal activity. Petrographic studies show that some high temperature minerals, such as garnet are present at depths whose formation temperatures are low. A sample analysed using electrode microprobe in well OW-902 at 9-3 masl had garnet and the measured temperatures at that depth is 246°C. This phase now exist where the present temperature is much lower than what would be expected from the thermal stability range of garnet, which is above 300°C (Bird et al., 1984). Homogenization temperatures indicate there has been some heating in the portion of the field around wells OW-901 and OW-903. The portion of the field around well OW-902 indicates cooling must have occurred. It can be concluded that some part of the active geothermal system at Olkaria Domes field as undergone some heating while some parts have undergone some cooling. The heating could be attributed to tectonics leading to increased activity in the area as evident by the recent Ololbutot eruption, which has been dated at 180±50 yrs B.P (Clarke et al., 1990).

Subsurface temperature distribution in the Olkaria Domes geothermal field was estimated from temperature recovery tests, shut-in temperature profiles, hydrothermal alteration mineralogy and fluid inclusion measurements. Temperature profiles (Figures 28, 29 and 30) of these wells show, in downward progression; (1) a steadily increasing conductive profile in well OW-901; (2) a steadily-increasing, conductive profile which becomes more isothermal in its deeper reaches as the temperature approaching 250°C in well OW-902 and (3) a steadily increasing conductive profile to near-isothermal interval and then an increasing conductive profile in well OW-903. Well OW-901 in its undisturbed state, the formation temperature profile is close to the boiling point curve. The thermal pattern indicates clearly that the maximum temperatures in the Olkaria Domes geothermal field occur around well OW-901. The temperature in well OW-901 is over 342°C close to the bottom at a depth of -260 masl. The thermal gradient at depth decreases slightly to the southeast towards well OW-903 and sharply to the southwest towards well OW-902, suggesting that the area towards well OW-902 is cold and probably in the marginal parts of the field. The observation from the temperature and pressure profiles indicate both pressure and temperature drop from well OW-901 to wells OW-902 and OW-903 indicating that the latter two wells are located in the outflow zones.

7.0 CONCLUSIONS

1. The lithology of Olkaria Domes is composed of pyroclastics, tuffs, rhyolites, trachytes and basalts with minor dolerite and microsyenite intrusives. Chemical analyses of major elements from Olkaria Domes show similarity with those of surface and other Olkaria field's subsurface rocks.

2. Apart from major faults occurring between Olkaria Domes and Olkaria East field, there is no major structural divide between the two fields.

3. Sources of permeability in Olkaria Domes geothermal field are both primary and secondary and include; fractures and thermally induced joints, lithologic contacts, clast-matrix or fragment contacts in breccias.

4. Indicators of high permeability in Olkaria Domes geothermal area are; high alteration intensity and sheared rocks, large veins and occurrence of abundant pyrite and calcite. Low permeability on the other hand is indicated by low alteration and tight veins and absence or trace occurrence of the above minerals.

5. Hydrothermal alteration mineral assemblages in Olkaria Domes are mainly controlled by temperature, rock type and permeability.

6. Hydrothermal alteration mineralogy indicate equilibrium conditions in the sector around wells OW-901 and OW-903. However in the sector around well OW-902, hydrothermal alteration mineralogy indicate possible reservoir cooling.

7. Four hydrothermal zonations are recognized in Olkaria Domes. They are the zeolite-chlorite zone, the illite-chlorite zone, the epidote-illite-chlorite zone and the garnet-biotite-actinolite zone.

8. Temporal changes have occurred in Olkaria Domes with heating of up to 60°C recorded. This could be attributed tectonics in the area resulting to intrusion and extrusion of lavas such as Ololbutot, which would induce profound changes in the subsurface thermal regime resulting to heating.

9. The observation from alteration minerals isograds, pressure and temperature profiles indicate that well OW-901 is drilled close to the upflow zone whereas well OW-903 is in the outflow zone and OW-902 is in the outflow and the marginal zone of the field.

10. Olkaria Domes having the same lithology like other Olkaria fields and no influx of cold water is noted at depth, the production casing should be set at similar depths like other Olkaria wells.

REFERENCES

Ambusso, W.J. and Ouma, P.A., 1991: Thermodynamic and permeability structure of Olkaria northeast field: Olkaria fault. *Geothermal Resource Council Transactions,* 15, 237-242.

Arnorsson, S., Gunnlaugsson, E., and Svarvarson, H., 1983: The chemistry of geothermal waters in Iceland III. Chemical geothermometry in geothermal investigations. *Geochim. Cosmochim. Acta*, 46, 1513-1532.

Baker, B.H., Williams, L.A.J., Miller, J.A., and Fitch, F.J., 1971: Sequence and geochronology of the Kenya Rift volcanics. *Tectonophysics,* 11, 191-215.

Baker, B.H. and Wohlenberg, J., 1971: Structural evolution of the Kenya Rift Valley. *Nature*, 229, 538-542.

Baker, B.H., Mohr, P.A., and Williams, L.A.J., 1972: Geology of the Eastern Rift System of Africa. *Geological Society of America*. Special Paper 136, 1-67.

Baker, B.H., 1987: Outline of the petrology of the Kenya rift alkaline province. In Fitton, J.G., and Upton, B.G.J., (eds.), *Alkaline igneous rocks*. Geol. Soc. Spec. Publ. 30, 293-311.

Bargar, K.E., and Beeson, M.H., 1984: Hydrothermal alteration in research drill hole Y-2 Lower Geyser Basin, Yellowstone National Park, Wyoming, USA. *Geological Survey Professional paper* 1054-B, 24 pp.

Bird, D.K., Schiffman, P., Elders, W.A., Williams, A.E., and McDowell, S.D., (1984): Calc-silicate mineralization in active geothermal systems. *Economic geology*, 79, 671-695.

Black, S., Macdonald, R. and Kelly, M.R., 1997: Crustal origin for the peralkaline rhyolites from Kenya: evidence from U-series disequilibria and Th-isotopes. *Journal of Petrology*, 38, 277-297.

Browne, P.R.L., Ellis, A.J., 1970: The Ohaki-Broadlands hydrothermal area, New Zealand: Mineralogy and related chemistry. *American Journal. of Science* 269, 97-133.

Browne, P.R.L., 1978: Hydrothermal alteration in active geothermal fields. *Annual Review Earth and Planetary Sciences* 6, 229–250.

Browne, P.R.L., 1981: *Petrographic study of cuttings from drilled wells at the Olkaria Geothermal field, Kenya*. Kenya Power Company internal report.

Browne, P.R.L., 1984: Subsurface stratigraphy and hydrothermal alteration of Eastern section of the Olkaria geothermal field, Kenya. *Proceedings of the 6th New Zealand Geothermal Workshop,* Geothermal Institute, Auckland, 33-41.

Browne, P.R.L., 1984: *Lectures in geothermal geology and petrology*. UNU-GTP, Iceland, report 2, 92 pp.

Cox, M.E., and Browne, P.R.L., 1998: Hydrothermal alteration mineralogy as an indicator of hydrology at the Ngawha geothermal field, New Zealand. *Geothermics*, 27, 259-270.

Clarke, M.C.G., Woodhall, D.G., Allen, D., and Darling, G., 1990: *Geological, volcanological and hydogeological controls of the occurrence of geothermal activity in the area surrounding Lake Naivasha, Kenya*. Ministry of Energy report.

Dimitrios, G., 1989: *Magnetotelluric studies in geothermal areas in Greece and Kenya.* Ph.D. Thesis, University of Edinburgh.

Fournier, R.O and Potter, R.W.II, 1982: A revised and expanded silica (quartz) geothermometer. *Geothermal Resource Council Bulletin*, 11-10, 3-13.

Furgerson R.B., 1972: *Electrical Resistivity Survey of the Olkaria project, Kenya.* East African Power & Lighting Co. Ltd. Geothermal Exploration Project report.

Grim, R.E., 1968: *Clay mineralogy.* McGraw-Hill Book Co., San Francisco, 596 pp.

Haukwa, C.B., 1984: *Recent measurements within Olkaria East and west fields.* Kenya Power Company internal report, 13 pp.

Hay, D.E., and Wendlandt, R.F., 1995: The origin of Kenya rift plateau type phonolites: Results of high pressure and high temperature experiments in the systems, phonolite-H_2O and phonolite-H_2O-CO_2. *Journal of Geophysics Research*, 100, 401 - 410.

Hay, D.E., Wendlandt, R.F and, Wendlandt, E.D., 1995a: The origin of Kenya rift plateau type flood phonolites: evidence from geochemical studies for fusion of lower crust modified by alkali basaltic magmatism. *Journal of Geophysics Research,* 100, 411-422.

Hay, D.E., Wendlandt, R.F., and Keller, G.R., 1995b: Origin of Kenya Plateau type flood phonolites: integrated petrologic and geophysical constraints on the evolution of the crust and upper mantle beneath the Kenya rift. *Journal of Geophysics Research*, 100, 10549-10557.

Henry, W.J., Mechie, J., Maguire, P.K.H., Khan, M.A., Prodehl, C., Keller, G.R., and Patel, J., 1990: A seismic investigation of the Kenya rift valley. *Geophys. J. Int.*, 100, 107-130.

Kampunzu, A.B., and Mohr, P., 1991: Magmatic evolution and petrogenesis in the East African Rift System. In Kampunzu, A.B., and Lubala, R.T. (eds.), *Magmatism in extensional structural settings: The Phanerozoic African plate.* Springer-Verlag, 85-136.

Karingithi, C.W., 1992: *Olkaria East Production Field geochemical report.* Kenya Power Company report.

Karingithi, C.W., 1993: *Olkaria East Production Field geochemical report.* Kenya Power Company internal report.

Karingithi, C.W., 1996: *Olkaria East Production Field geochemical report.* Kenya Power Company internal report.

Karingithi, C.W., and Wambugu, J.M., 1997: *Olkaria Geochemical Model.* Kenya Power Company internal report.

Karingithi, C.W., 1999: *Olkaria Domes geothermal field Kenya: Geochemical model.* KenGen internal report.

Karingithi, C.W., 2002: *Hydrothermal mineral buffers controlling reactive gases concentration in the Greater Olkaria geothermal system, Kenya.* University of Iceland, MSc thesis, UNU-GTP, Iceland, report 2, 61 pp.

KenGen, 2000: *Conceptualized model of Olkaria geothermal field.* Compiled by Muchemi, G.G. The Kenya Electricity Generating Company Ltd internal report, 13 pp.

Kenya Power Company, 1984: *Background report for Scientific and Technical Review Meeting.* Kenya Power Company report prepared by KRTA.

Kenya Power Company, 1988: *Report on Olkaria and Eburru Geothermal development.* Working papers of the North East Olkaria, *STRM*.

Kenya Power Company, 1990**:** *Olkaria West Field information report.* STRM.

Kristmannsdóttir, H and Tómasson, J., 1978: Zeolite zones in geothermal areas of Iceland; natural zeolite occurrences in geothermal areas, properties, uses. *Pergamon, Oxford,* 277-288.

Lagat, J.K., 1998: *Borehole geology of well OW-801, Olkaria Southeast field.* KenGen internal report.

Lagat, J.K., 1999: *Borehole geology of well OW-903, Olkaria Domes area.* KenGen internal report.

Les Bas, M.J., 1987: A chemical classification of volcanic rocks based on the total alkalis versus silica diagram. *Journal of Petrology*, 27, 745-750.

Lippard, S.J., 1973: The petrology of phonolites from the Kenya rift. *Lithos*, 6, 217-234.

McDowell, S.D., Elders, W.A., 1980: Authigenic layer silicate minerals in borehole Elmore 1, Salton Sea geothermal field, California, USA. *Contributions to Mineralogy and Petrology* 74, 293-310.

Macdonald, R., 1974: Nomenclature and petrochemistry of the peralkaline oversaturated extrusive rocks. *Bulletin of Volcanology,* 38, 498-516.

Macdonald, R., Davies, G.R., Bliss, C.M., Leat, P.T., Bailey, D.K., and Smith, R.L., (1987): Geochemistry of high silica peralkaline rhyolites, Naivasha, Kenya rift valley. *Journal of Petrology*, 28, 979-1008.

Mosley, P.N., 1993: Geological evolution of the late Proterozoic "Mozambique belt" of Kenya. *Tectonophysics*, 221, 223-250.

Muchemi, G.G., 1992: *Structural map of Olkaria geothermal field showing inferred ring structures.* Kenya Power Company internal report

Muna, Z.W., 1990: *An overview of the geochemistry of the Olkaria West geothermal field.* Kenya Power Company internal report

Mungania, J., 1992: *Preliminary field report on geology of Olkaria volcanic complex with emphasis on Domes area field investigations.* Kenya Power Company internal report.

Mungania, J., 1999: *Geological report of well OW-714.* Kenya Power Company internal report.

Mungania, J., 1999a: *Borehole geology of well OW-902.* KenGen internal report.

Mungania J., 1999b: *Summary of the updates of the geology of Olkaria Domes geothermal field.* KenGen internal report.

Mwangi, M.N., 1986: *Interpretation of additional sounding data at Olkaria, Kenya.* Kenya Power Company internal report.

Ndombi, J.M., 1981: The Structure of the shallow crust beneath the Olkaria geothermal field, Kenya, deduced from gravity studies. *Journal of Volcanology and Geothermal Research,,* 9, 237-251.

Naylor, W.I., 1972: *The geology of the Eburru and Olkaria geothermal projects.* Geothermal Resource Exploration Prospects, UNDP report. Restricted.

Ofwona, C.O., 1998: *Completion tests report for well OW-901.* KenGen internal report.

Odeny, J.N., and Ofwona, C.O., 1999: *Completion tests report for well OW-902.* KenGen internal report.

Ofwona, C.O., 1999: *Completion tests report for well OW-903.* KenGen internal report.

Ojiambo, B.S., and Lyons, W.B., 1993: Stable isotope composition of Olkaria geothermal field fluids, Kenya. *Geothermal Resource Council, Transactions* 17, 149-154.

Ogoso-Odongo, M.E., 1986: Geology of Olkaria geothermal field. *Geothermics*, 15, 741-748.

Omenda, P.A., 1994: The geological structure of the Olkaria west geothermal field, Kenya. *Stanford Geothermal Reservoir Engineering Workshop*, 19, 125-130.

Omenda, P.A., 1998a: The geology and structural controls of the Olkaria geothermal system, Kenya. *Geothermics*, 27, 55-74.

Omenda, P.A., 1998: *The geology of well OW-901.* KenGen internal report.

Omenda, P.A., 2000: Anatectic origin for Comendite in Olkaria geothermal field, Kenya Rift; Geochemical evidence for syenitic protholith. *African Journal of Science and Technology. Science and Engineering series,* 1, 39-47.

Omenda, P.A. 1990. *Update of the geology of the Olkaria West and Central fields.* Kenya Power Company internal report.

Onacha, S.A., 1989: *An Electrical Resistivity study of the area between Mt. Suswa and the Olkaria Geothermal Field, Kenya.* MSc. thesis, University of Nairobi.

Onacha, S.A., 1990: *Olkaria West Field information report.* Kenya Power Company internal report.

Onacha, S.A., 1993: *Resistivity studies of the Olkaria-Domes geothermal project.* Kenya Power Company internal report.

Reyes, A.G., 1990: Petrology of Philippine geothermal system and the application of alteration mineralogy to their assessment. *Journal of Volcanology and Geothermal Research,* 43, 279-304.

Roedder, E., 1984: Fluid Inclusions. *Rev. Mineral. 12. Mineral. Soc. Am.*, Washington, DC.

Ryder, A.J.D. 1986: *Geological Report of Well OW-701 Olkaria Geothermal Field, Kenya.* Kenya Power Company report, prepared by GENZL.

Schiffman, P., Elders, W.A., Williams, A.E., McDowell, S.D., and Bird, D.K., 1984: Active metasomatism in the Cerro Prieto geothermal system, Baja California, Mexico: a telescoped low-pressure, low-temperature metamorphic facies series: *Geology*, 12, 12-15.

Shackleton, R. M., 1986: Precambrian collision tectonics in Africa. In: Coward, M.P., and Ries, A.C. (eds.). *Collision Tectonics. Geol. Soc. Spec. Publ.* No. 19, 329-349.

Simiyu, S.M., Omenda, P.A., Keller, G.R., and Anthony, E.Y., 1995: Geophysical and geological evidence for the occurrence of shallow magmatic intrusions in the Naivasha sub-basin of the Kenya rift. *AGU Fall 1995 meeting abst.,* F657, no. V21A-12.

Simiyu, S.M., 1996: *Integrated geophysical study of the southern Kenya rift.* PhD dissertation, University of Texas at El Paso.

Simiyu, S.M., and Keller, G.R., 1997: An integrated analysis of lithospheric structure across the East African plateau based on gravity anomalies and recent seismic studies. In: Structure and dynamic processes in the lithosphere of the Afro-Arabian rift system. Fuchs, K., Altherr, R., Müller, B., and Prodehl, C. (eds.), *Tectonophysics*, 278, 291-313.

Simiyu, S.M., Malin, P.E., 2000: A "volcano seismic" approach to geothermal exploration and reservoir monitoring: Olkaria, Kenya and Casa Diablo, U.S.A. *Proceedings of the World Geothermal Congress 2000, Kyoto-Tohoku Japan*, 1759-1763.

Simiyu, S.M., Oduong, E.O., and Mboya, T.K., 1998: *Shear wave attenuation beneath the Olkaria volcanic field*. KenGen internal report.

Smith, M., and Mosley, P., 1993: Crustal heterogeneity and basement influence on the development of the Kenya rift, East Africa. *Tectonics*, 12, 591-606.

Smith, M., 1994: Stratigraphic and structural constraints on mechanisms of active rifting in the Gregory Rift, Kenya. In: Prodehl, C., Keller, G.R., and Khan, M.A., (eds.): Crustal and upper mantle structure of the Kenya rift. *Tectonophysics,* 236, 3-22.

Sweco-Virkir., 1976: *Feasibility report for the Olkaria Geothermal Project*. United Nations-Government of Kenya report.

Teklemariam, M., Battaglia, S, Gianelli, G., Ruggieri, G., 1996: Hydrothermal alteration in the Aluto-Langano geothermal field Ethiopia. *Geothermics* 25, 679-702.

Thompson, A.O., and Dodson, R.G., 1963: *Geology of the Naivasha area*. Geological Survey Kenya, report No. 55.

VIRKIR Consulting Group, 1980: *Geothermal development at Olkaria*. Report prepared for Kenya Power Company.

Wambugu, J.M., 1995: *Geochemical up-date of Olkaria West geothermal Field.* Kenya Power Company internal report.

Wambugu, J.M., 1996: *Assessment of Olkaria North East geothermal reservoir, based on well discharge chemistry*. Kenya Power Company internal report.

Williams, L.A.J., 1972: The Kenya rift volcanics: a note on volumes and chemical composition. *Tectonophysics*, 15, 83 - 96.

APPENDIX I: Preparation of samples for analysis

(a) Clay mineral analysis:

1. Into a clean test tube place approximately two spoonfuls of drill cuttings. Wash the cuttings to remove the dust with distilled water and fill the tube to approximately two-third full with distilled water. Place the tubes in a mechanical shaker for 4-6 hours depending on the intensity of alteration of the cuttings.
2. Allow the particles to settle for 1-2 hours, until those particles less than approximately 4 Å are left in suspension. Pipette a few milliliters from each tube and place approximately 10 drops on a labeled glass plate, not making the film thick. Make a duplicate of each sample and let them dry at room temperature overnight.
3. Place one sample at the desiccator containing glycol ($C_2H_6O_2$) solution and the other in a set of desiccator containing hydrated calcium chloride ($CaCl_2.H_2O$). Store it at room temperature for at least 24 hours. Thicker samples need more time at least 48 hours.
4. Run both sets of samples in the range 2-14° at intervals of 0.02°, 2θ for a time of 1 second on the XRD machine.
5. Place one set of samples (usually the glycolated one) on an asbestos plate and insert in a preheated oven. Heat the samples at 500-550°C for one hour making sure the oven temperatures do not exceed 600°C. When the samples have cooled, run them in the range 2-14° on the XRD machine.

(b) XRD qualitative mineral analysis

1. Handpick grain fillings from vein fillings or vesicles under the binocular microscope and put them in an agate bowl.
2. Crush the samples to a grain size of 5-10 Å. Acetone is usually added to prevent loss of sample while powdering.
3. Smear the sample on quartz plate and let the acetone dry.
4. Run the sample from 5°-56° at intervals of 0.04°, 2θ for a time of 1 second on the XRD machine.

APPENDIX II: X-Ray diffractometer clay results of well OW-901

Depth (masl)	Rock type	Untreated			Glycolated				Oven heated			Clay type
1880-1878	Pyroclastics											No clay
1824-1822	Pyroclastics											No clay
1784-1782	Pyroclastics											No clay
1742-1740	Pyroclastics											No clay
1690-1688	Pyroclastics											No clay
1638-1636	Rhyolite											No clay
1590-1588	Rhyolite	16.16		7.17	16.16			7.18	Collapse		Collapse	Chlorite
1550-1548	Rhyolite	15.34		7.15	15.34			7.15	15.43		Collapse	Chlorite
1490-1488	Trachyte	15.84		7.18	15.84			7.17	Collapse		Collapse	Chlorite
1452-1450	Trachyte	15.55			15.55				15.50		Collapse	Chlorite
1390-1386	Trachyte	14.30		7.12	14.30			7.12	Collapse		7.14	Chlorite
1340-1338	Basalt	14.22		7.10	14.22			7.10	14.22		Collapse	Chlorite
1308-1306	Trachyte	15.24		7.18	15.24			7.18	14.3		7.18	Chlorite
1234-1230	Trachyte	14.30		7.11	14.30			7.11	Collapse		7.58	Chlorite
1112-1110	Trachyte	16.10		7.14	16.01			7.14	16.01		Collapse	Chlorite
1084-1082	Rhyolite	14.28		7.11	14.28			7.11	14.85		7.45	Chlorite
1034-1032	Rhyolite	14.40		7.12	14.40			7.12	15.33		Collapse	Chlorite
990-988	Trachyte	14.31	10.07	7.14	14.31		10.07	7.14	16.60	10.07	Collapse	Chlorite, Illite
940-938	Trachyte	15.66	10.06	7.13	15.66		10.06	Collapse	15.66	10.07	Collapse	Chlorite, Illite
888-886	Trachyte	16.29	10.07	7.13	16.29		10.07	7.13	16.29	10.10	Collapse	Chlorite, Illite
840-838	Tuff	14.42	10.01	7.12	14.42		10.01	7.12	14.95	10.01	7.48	Chlorite, Illite
788-786	Tuff	14.28	10.01	7.10	14.28		10.01	7.10	14.90	10.01	7.42	Chlorite, Illite
740-738	Tuff	14.34	10.01	7.11	14.34		10.01	7.11	14.67	10.01	Collapse	Chlorite, Illite
688-686	Basalt	14.28	10.04	7.11	16.74	14.28	10.01	7.11	14.28	10.01	Collapse	Swelling Chlorite,
640-638	Basalt	14.26	10.04	7.10	16.74	14.26	10.04	7.10	14.71	10.04	7.48	Swelling Chlorite,
588-586	Trachyte	14.26	10.06	7.12	16.60	14.26	10.06	7.12	14.68	10.06	Collapse	Swelling Chlorite,
540-538	Tuff	14.31	10.18	7.11	14.31		10.18	7.11	14.85	10.03	Collapse	Chlorite, Illite
488-486	Trachyte	14.28	10.17	7.12	14.28		10.17	7.12	14.28	10.03	7.48	Chlorite, Illite
440-438	Tuff	14.31	10.18	7.13	14.31		10.18	7.13	14.90	10.01	7.43	Chlorite, Illite
384-382	Tuff	14.31	10.16	7.12	14.34		10.15	7.12	14.90	10.01	7.44	Chlorite, Illite
340-338	Trachyte	14.36	10.19	7.11	14.36		10.18	7.11	14.36	10.00	7.47	Chlorite, Illite
288-286	Basalt	14.26	10.11	7.12	14.26		10.16	7.12	14.28	10.04	Collapse	Chlorite, Illite

Depth (masl)	Rock type	Untreated			Glycolated			Oven heated			Clay type
248-246	Basalt	14.20	10.16	7.11		10.18	7.11	14.20	10.16	7.11	Chlorite, Illite
188-186	Tuff	14.26	10.17	7.11		10.18	7.11	14.26	10.09	7.36	Chlorite, Illite
140-138	Trachyte	14.37	10.22	7.11		10.20	7.11	14.37	10.01	7.32	Chlorite, Illite
90-88	Trachyte	14.42	10.18	7.12		10.18	7.12	14.42	10.11	7.30	Chlorite, Illite
34-32	Trachyte	14.42	10.18	7.12			Collapse	14.42	10.15	7.55	Chlorite, Illite
-12 to -14	Trachyte	14.34	10.19	7.12		10.19	7.12	14.95	10.00	7.47	Chlorite, Illite
-60 to -62	Trachyte	14.34	10.20	7.11		10.20	7.11	14.87	10.00	7.47	Chlorite, Illite
-116 to -118	Trachyte	14.37	10.15	7.11		10.15	7.11	14.67	10.00	7.38	Chlorite, Illite
-164 to -166	Trachyte	14.40	10.16	7.12		10.16	7.12	15.50	10.24	7.51	Chlorite, Illite
-212 to -214	Trachyte	14.92	10.05	7.11		10.05	7.11	14.92	10.05	7.02	Chlorite, Illite
-258 to -260	Trachyte	14.66	10.17	7.11		10.17	7.11	14.66	10.04	Collapse	Chlorite, Illite
-304 to -310	Trachyte	14.37	10.19	7.11		10.19	7.11	14.37	10.08	7.11	Chlorite, Illite

APPENDIX III: X-Ray diffractometer clay results of well OW-902

Depth (masl)	Rock type	Untreated			Glycolated			Oven heated			Clay type
1951-1949	Pyroclastics										No clay
1907-1905	Pyroclastics										No clay
1855-1853	Pyroclastics										No clay
1807-1805	Pyroclastics										No clay
1747-1745	Pyroclastics										No clay
1705-1703	Pyroclastics										No clay
1621-1619	Rhyolite			7.11			7.12			7.12	Chlorite
1555-1553	Rhyolite		10.09	7.10		10.09	7.07		10.09	Collapse	Illite, Chlorite
1501-1499	Trachyte		10.09	7.10		10.17	7.06		10.09	Collapse	Illite, Chlorite
1453-1451	Trachyte			7.13			7.14			Collapse	Chlorite
1291-1289	Tuff	14.33	10.09	7.12		10.02	7.11		10.07	Collapse	Illite, Chlorite
1255-1253	Basalt	14.25	10.08	7.10	14.21	10.01	7.10	14.42	10.10	Collapse	Illite, Chlorite
1211-1209	Trachyte	14.37	10.08	7.11	14.25	10.04	7.10	Collapse	10.15	Collapse	Illite, Chlorite
1153-1151	Tuff	14.34	10.10	7.12	14.14	10.10	7.10	14.14	10.10	Collapse	Illite, Chlorite
1105-1103	Tuff	14.31	10.10	7.12	14.31	10.10	7.12	14.31	10.10	Collapse	Illite, Chlorite
1057-1055	Tuff	14.31	10.02	7.12	15.20	10.02	7.12	14.31	10.02	Collapse	Illite, Chlorite
1009-1007	Basalt	14.23		7.11	14.23		7.11	14.23		Collapse	Chlorite

Depth (masl)	Rock type	Untreated			Glycolated			Oven heated			Clay type
975-955	Trachyte	14.35	10.11	7.11	14.35	10.11	7.11	14.35	7.11	7.56	Illite, Chlorite
907-905	Trachyte	14.06	10.14	7.13	14.06	10.14	7.13	14.06	7.11	Collapse	Illite, Chlorite
857-855	Trachyte	14.70		7.10	14.70		7.10	14.70		Collapse	Chlorite
809-807	Trachyte	15.99	10.07	7.10	15.99	10.07	7.10	16.36		Collapse	Illite, Chlorite
755-753	Trachyte	14.70		7.11	14.20		7.11	14.20		Collapse	Chlorite
707-705	Trachyte			7.10			7.10			Collapse	Chlorite
653-651	Basalt	14.36		7.12	14.36		7.12	14.36	10.10	Collapse	Chlorite
604-603	Trachyte	14.30		7.12	14.30		7.12	17.80		Collapse	Chlorite
557-555	Trachyte	14.28		7.11	14.28		7.11	14.28		7.35	Chlorite
503-501	Rhyolite	14.36		7.08	14.30		7.08	15.01	10.20	Collapse	Chlorite
455-453	Rhyolite	14.40	10.14	7.12	14.40		7.12	14.40	10.05	Collapse	Chlorite
405-403	Trachyte		10.15			10.15			10.03		Illite
353-351	Trachyte	14.29		7.11	14.19		7.11	14.92		Collapse	Chlorite
305-303	Basalt	14.26		7.12	14.25		7.12	14.73		Collapse	Illite, Chlorite
257-255	Trachyte		10.17	7.11		10.17	7.11		10.04	Collapse	Illite, Chlorite
203-201	Trachyte	14.27	10.19	7.12	14.22	10.19	7.12		10.00	Collapse	Illite, Chlorite
155-153	Trachyte	14.31	10.14	7.12	14.26	10.14	7.12	14.17	10.00	Collapse	Illite, Chlorite
79-77	Trachyte	14.32	10.17	7.12	14.32	10.15	7.12	14.39	10.04	Collapse	Illite, Chlorite
53-51	Trachyte		10.16	7.12		10.12	7.10		10.05	Collapse	Illite, Chlorite
-19 to -21	Trachyte	14.18	10.16	7.11	14.32	10.16	7.11	14.13	10.05	Collapse	Illite, Chlorite
-55 to -57	Trachyte	14.29	10.16	7.11	14.38	10.12	7.12	14.30	10.15	7.12	Illite, Chlorite
-99 to -101	Tuff	14.24	10.13	7.11	14.24	10.02	7.10	14.24	10.08	7.10	Illite, Chlorite
-145 to -147	Trachyte	14.18	10.16	7.11	14.18	10.16	7.10	14.27	10.06	7.10	Illite, Chlorite
-193 to -195	Trachyte		10.18	7.11		10.16	7.11		10.00	Collapse	Illite, Chlorite
-239 to -243	Trachyte	14.21	10.16	7.10	14.40	10.16	7.10	14.46	10.02	Collapse	Illite, Chlorite

Depth (masl)	Rock type	Untreated			Glycolated			Oven heated			Clay type
2033-2031	Pyroclastics										No clay
1981-1979	Rhyolite										No clay
1783-1781	Rhyolite										No clay
1743-1741	Rhyolite										No clay

APPENDIX IV: X-Ray diffractometer clay results of well OW-903

Depth (masl)	Rock type	Untreated				Glycolated				Oven heated			Clay type
1641-1639	Rhyolite	14.33		10.07	7.13	14.33		10.07	7.13	14.33	10.07	Collapse	Chlorite, Illite
1529-1527	Rhyolite	16.32				16.32				16.32	8.47	Collapse	No clay
1437-1435	Rhyolite	18.12			7.13	18.12			7.13	18.12	8.44	Collapse	Chlorite
1335-1333	Trachyte	15.49			7.11	15.49			7.11	15.49		7.54	Chlorite
1241-1239	Trachyte	14.30		10.14	7.12	14.30		10.14	7.12	14.30	10.14	Collapse	Chlorite, Illite
1187-1185	Basalt	14.30		10.13	7.15	14.30		10.13	7.15	14.30	10.13	Collapse	Chlorite, Illite
1137-1135	Basalt	29.30	13.60	10.04	7.12	31.30	15.44	10.04	7.12	Collapse	10.13	Collapse	Corrensite,
1089-1087	Tuff	14.29		10.22	7.11	14.29		10.22	7.11	14.29	10.22	6.52	Chlorite, Illite
1043-1041	Rhyolite	14.02		10.07	7.12	14.02		10.07	7.12	14.02	10.07	Collapse	Chlorite, Illite
989-987	Tuff	14.25		10.07	7.07	14.25		10.07	7.07	14.25	10.07		Chlorite, Illite
945-941	Tuff	14.39		10.14		14.39		10.14		14.39	10.14	7.55	Chlorite, Illite
891-889	Tuff	14.36		10.03	7.11	14.36		10.03	7.11	15.94	10.03	7.59	Chlorite, Illite
837-837	Tuff	14.27		10.04	7.09	14.27		10.04	7.11	15.13	10.04	7.55	Chlorite, Illite
787-783	Trachyte	14.25			7.09	14.25			7.09	15.09		7.58	Chlorite, Illite
741-739	Tuff	14.31		10.08	7.11	14.31		10.08	7.11	14.31	10.08	7.55	Chlorite, Illite
691-689	Trachyte	14.26		10.04	7.11	14.26		10.04	7.11	15.06	10.04	7.55	Chlorite, Illite
647-643	Trachyte	14.31		10.19	7.11	14.31		10.19	7.10	14.31	10.19	7.13	Chlorite, Illite
597-595	Trachyte	14.20			7.11	14.20			7.11	14.20	10.10	7.11	Chlorite, Illite
541-539	Trachyte	14.26		10.18	7.11	14.26		10.07	7.11	14.26		7.11	Chlorite, Illite
489-487	Trachyte	14.29			7.09	14.29		10.18	7.09	14.29		7.09	Chlorite, Illite
441-439	Trachyte	14.36			7.12	14.36		10.19	7.12	14.36		7.51	Chlorite, Illite
391-389	Trachyte	14.36			7.11	14.36		10.21	7.11	14.36		7.49	Chlorite, Illite
341-339	Trachyte	14.33			7.11	14.33		10.06	7.10	14.33		Collapse	Chlorite, Illite
301-299	Trachyte	14.25			7.11	14.25		10.04	7.11	15.18	10.04	7.55 C	Chlorite, Illite
241-239	Trachyte	14.26			7.11	14.27		10.18	7.11	14.27	10.18	7.61 C	Chlorite, Illite
193-191	Trachyte	14.30		10.06	7.11	14.30		10.06	7.11	14.90	10.06	Collapse	Chlorite, Illite
145-143	Trachyte	14.47		10.15	7.11	14.47		10.15	7.11	14.47	10.15	Collapse	Chlorite, Illite
97-95	Trachyte	14.27		10.10	7.16	14.27		10.10	7.11	14.89	10.10	Collapse	Chlorite, Illite
37-35	Trachyte	14.32		10.10	7.10	14.32		10.10	7.10	15.44	10.10	7.57	Chlorite, Illite
-7 to -9	Trachyte	14.32			7.10	14.32			7.10	14.32		7.40	Chlorite
-67 to -69	Trachyte	14.32			7.11	14.32			7.11	14.94		7.44	Chlorite
-115 to -117	Tuff	14.27		10.08	7.10	14.27		10.08	7.10	15.11	10.08	7.58	Chlorite, Illite
-155 to -157	Tuff	14.35			7.13	14.35			7.13	14.73		7.48	Chlorite

APPENDIX V: **Lithologic description and hydrothermal alteration minerals of drill cuttings of well OW-901. The list of hydrothermal alteration minerals given for each rock type is based on binocular and petrographic microscopes, X-ray diffraction and electron microprobe analyses**

1890-1864 masl (0-26 m)   **Pyroclastics**
Pyroclastics comprising of pumice, obsidian and blocks of collapsed breccia associated with the formation of Ol Njorowa gorge.
Alteration minerals: Chalcedony, oxides

1864-1832 masl (26-58 m)   **No cuttings (Loss of circulation)**

1832-1675 masl (58-215 m)   **Pyroclastics**
Pyroclastic rock unit consisting of lithic fragments of rhyolite, trachyte, syenite and pumice. The matrix is dominated by ash size particles, crystals of glass, quartz, feldspars, amphiboles, obsidian and pumice.
Alteration minerals: Chalcedony, oxides

1675-1545 masl (215-345 m)   **Rhyolite**
Light grey rock consisting of feldspar phenocrysts in a fine grained matrix. Euhedral quartz phenocrysts also occur but not abundant. Chalcedony is deposited in veins and vesicles. Paragenetic sequences observed in veins and vugs within the rock unit indicate chalcedony to be the earlier formed mineral followed by pyrite and calcite in that order.
Alteration minerals: Calcite, chalcedony, fluorite, oxides, pyrite

1544-1522 masl (346-368 m)   **No cuttings (loss of circulation)**

1522-1450 masl (368-440 m)   **Trachyte**
Grey, porphyritic lava with phenocrysts of mainly feldspars and rarely clinopyroxenes. The matrix is siliceous and consists of feldspar microlites exhibiting flow texture. The white patches present in the groundmass are due to recrystallized quartz.
Alteration minerals: Calcite, chalcedony, fluorite, mordenite, oxides, pyrite

1450-1425 masl (440-465 m)   **No cuttings (Loss of circulation)**

1425-1405 masl (465-485 m)   **Basalt**
Dark greenish to grey, fine grained rock. The groundmass is holocrystalline with plagioclase laths, clinopyroxene and magnetite. Locally zoned and partly resorbed plagioclase and clinopyroxenes form the phenocrysts. Olivine has been completely altered to chlorite. Colorless and white calcite is a late fracture and vug filling and partly replaces plagioclase crystals. Cubic pyrite crystals are abundant in the rock unit. Reddish haematite partly replaces magnetite.
Alteration minerals: Calcite, chalcedony, fluorite, chlorite, mordenite, oxides, pyrite

1405-1395 masl (485-495 m)   **No cuttings (Loss of circulation)**

1395-1340 masl (495-550 m)   **Trachyte**
Grey, fine grained porphyritic rock consisting of large plagioclase phenocrysts and rarer pale green clinopyroxenes in a fine grained matrix. The matrix shows trachytic flow texture and is moderately altered to light green clays. Chalcedony transforming into quartz observed at around 1356 masl.
Alteration minerals: Calcite, chalcedony, chlorite, oxides, pyrite, quartz

1340-1328 masl (550-562 m)   **Basalt**
Dark grey, fine grained rock consisting of plagioclase phenocrysts in a holocrystalline groundmass. The plagioclase phenocrysts show moderate alteration to calcite whereas clinopyroxenes are also extensively to completely altered to chlorite. Calcite, light green clays and crystals of tiny pyrite occur in veins and vesicles. Pyrite is also disseminated in the groundmass.
Alteration minerals: Adularia, calcite, chlorite, mordenite, oxides, pyrite, quartz

1328-1306 masl (562-584 m)   **Trachyte**

Grey, fine grained rock consisting of feldspar phenocrysts measuring about 3 mm in length in a fine grained matrix containing feldspar microlites. The microlites exhibit trachytic flow texture. The paragenetic sequence indicates chlorite to be an earlier formed mineral followed by calcite.

Alteration minerals: Adularia, calcite, chlorite, mordenite, oxides, pyrite, quartz

1306-1238 masl (584-652 m)   **No cuttings (Loss of circulation)**

1238-1230 masl (652-660 m)   **Trachyte**

Grey, fine grained feldspar porphyritic rock. The phenocrysts are made up of embayed K-feldspar. Pale green clinopyroxenes forms subhedral to anhedral crystals. The groundmass consists mainly of K-feldspar, rare quartz and iron oxides. The minerals show alteration to mainly chlorite, quartz and calcite. Pyrite cubes occur in veins and also as fine disseminations in the groundmass.

Alteration minerals: Adularia, calcite, chlorite, mordenite, oxides, pyrite, quartz

1230-1176 masl (660-714 m)   **No cuttings (loss of circulation)**

1176-1128 masl (714-762 m)   **Tuff**

Whitish coloured, fragmental rock dominated by pumice, glass, quartz and rhyolitic lithics set in a glassy to ashy matrix. The rock is highly altered to clays and consists of tiny pyrite disseminations in the matrix.

Alteration minerals: Calcite, chlorite, mordenite, oxides, pyrite, quartz

1128-1122 masl (762-768 m)   **No cuttings (loss of circulation)**

1122-1116 masl (768-774 m)   **Tuff**

Whitish coloured, fragmental rock dominated by pumice, glass, quartz, rhyolite and ash particles. The rock is highly altered to light green clays and consists of tiny pyrite disseminations in the matrix and has veins infilled with mainly quartz and calcite.

Alteration minerals: Calcite, chlorite, mordenite, oxides, pyrite, quartz

1116-1090 masl (774-800 m)   **Trachyte**

Greyish brown, fine grained feldspar and rarely quartz porphyritic rock. Phenocrysts of slightly embayed K-feldspar and anorthoclase and rare pale green clinopyroxene occur in a fine grained oxidized matrix. Plagioclase shows zoning and replacement by calcite.

Alteration minerals: Adularia, albite, calcite, chlorite, oxides, pyrite, quartz

1090-1032 masl (800-858 m)   **Rhyolite**

Brownish-grey, fine grained feldspar porphyritic weakly altered lava. The rock consists of phenocrysts of feldspars and quartz in a fine grained groundmass with feldspar microlites displaying trachytic flow texture. Magnetite shows rusty oxidation to reddish brown colour.

Alteration minerals: Adularia, albite, calcite, chlorite, oxides, pyrite, quartz

1032-942 masl (858-948 m)   **Trachyte**

Greyish, moderately altered porphyritic lava. The rock is porphyritic with euhedral phenocrysts of K-feldspar including sanidine. The rock also consists of rare quartz phenocrysts. Stumpy plagioclase crystallites exhibit trachoid texture. Pyrite cubes are embedded and also disseminated in the groundmass. Chalcedonic silica is transforming into quartz in veins and vesicles. Two paragenetic sequences occur; (i) Vesicle filling where chlorite is the earlier formed mineral followed by chalcedony and (ii) In veins where pyrite is the earlier deposited mineral followed by quartz.

Alteration minerals: Adularia, albite, calcite, chalcedony, chlorite, fluorite, illite, oxides, pyrite, quartz, sphene

942-860 masl   (948-1030 m)   Trachyte
Grey, fine grained feldspar porphyritic rock. The phenocrysts consist of embayed K-feldspar. Pale green clinopyroxenes forms subhedral to anhedral crystals. The groundmass consists mainly of microlites of feldspars and iron oxides. The rock shows alteration to green and white clays.
Alteration minerals: Adularia, albite, calcite, chalcedony, chlorite, illite, oxides, pyrite, quartz, sphene

860-770 masl (1030-1120 m)   Tuff
Whitish coloured, glassy tuffaceous rock dominated by pumice, glass, quartz, rhyolite and ash particles.   The rock is highly altered to clays and consists of tiny pyrite disseminations in the matrix. Quartz, chalcedony and calcite occur in veins but most of the chalcedony is being transformed into quartz. First occurrence of well crystalline epidote and biotite is at 790 masl. Paragenetic sequence in vein fillings, indicate quartz as an earlier formed mineral followed by epidote.
Alteration minerals: Adularia, albite, biotite (trace), calcite, chalcedony, chlorite, epidote, fluorite, illite, oxides, pyrite, quartz, sphene

770-740 masl   (1120-1150 m)   Basalt
Dark grey, fine grained porphyritic lava with ophitic texture. The groundmass contains plagioclase laths enclosed by euhedral clinopyroxene, subhedral magnetite partly altered to haematite and dark brown interstitial glass partly altered to clays.   The clinopyroxene shows alteration to clays. Paragenetic sequence in veins indicates quartz to be the earlier deposited mineral followed by calcite.
Alteration minerals: Adularia, albite, calcite, chalcedony, chlorite, epidote, fluorite, illite, oxides, prehnite, pyrite, quartz, sphene, wairakite

740-702 masl   (1150-1188 m)   Tuff
Whitish to brownish coloured, tuffaceous rock consisting of lava, quartz and feldspar fragments cemented in an ashy to glassy matrix. The rock is moderately altered to clays.
Alteration minerals: Calcite, chlorite, epidote, fluorite, illite, oxides, pyrite, quartz, sphene, wairakite

702-700 masl (1188-1190 m)   Microsyenite
Light grey, medium grained rock. The bulk is microcrystalline with good segregation of mafic minerals. It has large feldspar phenocrysts, which show replacement by calcite. Arfvedsonite and pyroxenes also show alteration to clays.
Alteration minerals: Calcite, chlorite, epidote, illite, oxides, pyrite, quartz, wairakite

700-608 masl   (1190-1282 m)   Basalt
Dark grey, fine-grained porphyritic rock.   The phenocrysts are made up of mainly plagioclase feldspars which show alteration to chlorite and metasomatism by calcite along the edges. Calcite occurs as vein fillings with quartz and epidote.
Alteration minerals: Adularia, albite, biotite, calcite, chlorite, swelling chlorite, epidote, illite, oxides, prehnite, pyrite, sphene, quartz, wairakite

608-600 masl (1282-1290 m)   Microsyenite
Light grey, medium grained rock. The bulk is microcrystalline with good segregation of mafic minerals. It has large feldspar phenocrysts, which show replacement by calcite. Arfvedsonite and pyroxenes also show alteration to greenish clays.
Alteration minerals: Calcite, chlorite, swelling chlorite, epidote, fluorite, illite, oxides, pyrite, wairakite

600-550 masl (1290-1340 m)   Trachyte
Grey, fine grained highly altered feldspar porphyritic rock. The poorly formed feldspar crystallites exhibit trachytic texture. The rock is altered to chlorite and calcite is deposited in veins together with well formed crystals of epidote. Pyrite cubes are disseminated in the rock matrix.
Alteration minerals: Albite, chlorite, swelling chlorite, epidote, fluorite, illite, oxides, pyrite, sphene, quartz, wairakite

550-530 masl   (1340-1360 m)   Tuff
Light grey to brown coloured, tuffaceous cuttings showing moderate alteration to green and white clays. Consist of fragments of quartz, feldspar and trachytic lava fragments cemented in a glassy to ashy matrix.
Alteration minerals: Calcite, chlorite, epidote, fluorite, illite, oxides, pyrite, sphene, quartz

530-470 masl (1360-1420 m)   Trachyte
Grey, fine grained moderately altered rock. The rock is feldspar porphyritic with stumpy feldspar phenocrysts exhibiting trachytic texture. The paragenetic sequences observed in the vesicles indicate quartz to be the earlier formed mineral followed by epidote.
Alteration minerals: Adularia, albite, calcite, chlorite, epidote, fluorite, illite, oxides, pyrite, sphene, quartz, wairakite

470-426 masl   (1420-1464 m)   Tuff
Whitish to brown coloured, tuffaceous rock dominated by glass, quartz, lava and ash particles. The rock is highly altered to light green to white clays and consists of tiny pyrite disseminations in the matrix. The rock has veins infilled with quartz and calcite. The rock shows silvery metallic luster at the edge with basaltic lava which is an indication of contact metamorphism.
Alteration minerals: Calcite, chlorite, epidote, illite, fluorite oxides, pyrite, sphene, quartz

426-404 masl   (1464-1486 m)   Basalt
Dark grey, fine grained porphyritic rock. The phenocrysts are made up of mainly plagioclase and show alteration to clays and replacement by calcite. Calcite also occurs as vein fillings in association with quartz and epidote.
Alteration minerals: Adularia, albite, calcite, chlorite, epidote, fluorite, illite, oxides, prehnite, pyrite, sphene, quartz, wairakite

404-340 masl   (1486-1550 m)   Tuff
Whitish to brown tuffaceous rock.   The rock consists of glass, quartz and trachytic fragments cemented in an ashy to glassy matrix.   The rock is highly altered to light green clays and has tiny pyrite disseminations in the matrix. The altered part of the rock shows bleaching to white patches.
NB: The cuttings exhibit a lot of mixing.
Alteration minerals: Albite, calcite, chlorite, epidote, fluorite, illite, oxides, prehnite, pyrite, sphene, quartz,

340-320 masl   (1550-1570 m)   Trachyte
Grey, fine grained feldspar porphyritic rock. The rock is moderately altered to greenish chloritic clays and has well formed pyrite cubes disseminated in the groundmass. In thin section the rock shows stumpy feldspar laths exhibiting trachytic texture.
Alteration minerals: Albite, calcite, chlorite, epidote, fluorite, garnet, illite, oxides, pyrite, sphene, quartz, wairakite

320-312 masl   (1570-1578 m)   Microsyenite
Light grey coloured medium grained rock. Then rock shows tabular phenocrysts of feldspar which have suffered alteration. Amphiboles and pyroxenes show alteration to clays. The intrusive is weakly altered to mainly opaque oxides.
Alteration minerals: Calcite, chlorite, epidote, fluorite, illite, oxides, pyrite, quartz

312-214 masl   (1578-1676 m)   Basalt
Dark grey, feldspar porphyritic rock with rare pyroxene phenocrysts. The matrix is microcrystalline and consists mainly of subhedral plagioclase laths, magnetite and clinopyroxene. Clinopyroxene crystals appear to be completely altered to greenish clays. Fractures and vesicles are generally filled with calcite, quartz, and clays. Paragenetic sequence indicates epidote to be the earlier formed mineral in vein fillings followed by quartz.
Alteration minerals: Albite, biotite, calcite, chlorite, epidote, garnet, fluorite, illite, oxides, prehnite, pyrite, sphene, quartz, wairakite

214-150 masl   (1676-1740 m)   Tuff
White to light grey, tuffaceous cuttings containing clasts of devitrified lava and angular crystals of feldspars set in a glassy to ashy matrix. Abundant chlorite occurs in the groundmass replacing some of the feldspar lithics and the matrix.
Alteration minerals: Albite, biotite, calcite, chlorite, epidote, fluorite, garnet, illite, oxides, pyrite, sphene, quartz

150-48 masl (1740-1842 m)   Trachyte
Brownish grey, fine-grained feldspar porphyritic rock. Rare quartz phenocrysts are also present in the rock.   The rock has poorly developed crystallites in a glassy groundmass oriented in preferred directions exhibiting trachytic flow texture. At 134-130 masl, the rock show metallic luster an indication of contact metamorphism. At some depths the rock shows increased oxidation.   The paragenetic sequence indicates quartz to be the earlier formed in vesicle filling followed by epidote.
Alteration minerals: Actinolite, biotite, calcite, chalcedony, chlorite, epidote, garnet, illite, oxides, pyrite, sphene, quartz

48 to -120 masl (1842-2010 m)   Trachyte
Grey, fine-grained rock consisting of anhedral but locally embayed K-feldspar and rare anhedral quartz phenocrysts set in a glassy groundmass. The mafics are made up of sodic pyroxenes and amphiboles. Needle like crystals of riebeckite are seen to enclose quartz in a devitrified groundmass. Paragenetic sequence indicates quartz to be the earlier formed vein filling mineral followed by epidote.
Alteration minerals: Actinolite, albite, biotite, chlorite, epidote, fluorite, illite, pyrite, sphene, quartz

-120 to -309 masl (2010-2199 m)   Trachyte
Grey, fine grained highly altered feldspar porphyritic rock. The feldspar phenocrysts are large and typically measure up to 4 mm in length. Rare quartz phenocrysts also occur. The poorly formed feldspar crystallites exhibit trachytic flow texture. The rock is altered to clays and has calcite and well formed crystals of epidote in veins. Pyrite cubes are embedded in the groundmass.
Alteration minerals: Actinolite, biotite, chlorite, epidote, garnet, illite, sphene, quartz

APPENDIX VI: **Lithologic description of drill cuttings and hydrothermal alteration minerals of well OW-902. The list of hydrothermal alteration minerals given for each rock type is based on binocular and petrographic microscopes, X-ray diffraction and electron microprobe analyses**

1957-1951 masl (0-6 m)   Pyroclastics
Brownish to grey colored unconsolidated pyroclastics containing lithic fragments and weathering derivatives of the rock particles.
Alteration minerals: Chalcedony, oxide

1951-1683 masl (6-274 m)   Pyroclastics
A succession of pyroclastic tuff beds of slightly varying textural compositions. At 1951 masl to 1885 masl the pyroclastics consist of pumice dominated beds with few brownish oxidized rhyolitic fragments and volcanic glass. At 1885 masl to 1803 masl the rock is composed of mainly volcanic glass (obsidian and pumice shards) and from 1803 masl to 1683 masl the depth interval consist of greenish pyroclastic beds rich in rhyolitic fragments.
Alteration minerals: Chalcedony, oxide

1683-1621 masl (274-336 m)   No cuttings   (Loss of circulation)

1621-1525 masl (336-432 m)   **Rhyolite**
Light grey, fine grained highly siliceous lava. The rock is porphyritic with quartz and tiny feldspars and shows very low alteration. The rock shows flow texture and greenish soda amphiboles (riebeckite/arfvedsonite) crystals occur along flow bands. Zeolite, fluorite, calcite and quartz are some of the hydrothermal minerals present in the rock unit.
Alteration minerals: Calcite, chalcedony, fluorite, mordenite, oxides, pyrite,

1525-1449 masl (432-508 m)   **Trachyte**
Brownish grey, fine grained, locally flow banded with low phenocryst content rock. The phenocrysts are mainly made up of rare anhedral quartz and subhedral K-feldspar. At some parts the rock shows extensive oxidation due to baking of the underlying rock. Pyrite is disseminated in the groundmass and also lines veins and vesicles. The rock is slightly altered to clays.
Alteration minerals: Calcite, chalcedony, chlorite, Illite, mordenite, oxides, pyrite

1449-1297 masl (508-660 m)   **No cuttings (Loss of circulation)**

1297-1265 masl (660-692 m)   **Tuff**
Dark grey to brown tuffaceous rock consisting of clasts of devitrified rhyolite lava and a few angular crystals of K-feldspar which show alteration to calcite. The paragenetic sequence indicates calcite to be the latest mineral to be deposited after clays in vesicles. *NB: The rock chippings exhibit a lot of mixing with tuff and rhyolitic particles.*
Alteration minerals: Calcite, chalcedony, chlorite, illite, mordenite, oxides, pyrite

1265-1225 masl (692-732 m)   **Basalt**
Dark grey, fine grained rock. The groundmass consists of plagioclase laths and abundant anhedral clinopyroxene and anhedral to subhedral magnetite partly altered to haematite. Some plagioclase phenocrysts display zoning and albatized edges which are extensively shattered. Chalcedony in vesicles has been partly transformed into quartz.
Alteration minerals: Albite, calcite, chalcedony, chlorite, fluorite, illite, oxides, pyrite, quartz

1225-1197 masl (732-760 m)   **Trachyte**
Grey, fine-grained feldspar porphyritic rock. The rock is moderately altered to greenish clays and has poorly developed crystallites in a glassy groundmass oriented in preferred directions exhibiting characteristic trachytic flow texture.
Alteration minerals: Calcite, chalcedony, chlorite, epidote, fluorite, illite, oxides, pyrite, quartz, wairakite

1197-1177 masl (760-780 m)   **Basalt**
Pale green, fine grained porphyritic rock with phenocrysts of feldspar in a matrix consisting of altered feldspar laths. Chlorite together with albite partly replaces some of the feldspar phenocrysts. Clinopyroxene shows alteration to chlorite.
Alteration minerals: Adularia, albite, calcite, chlorite, epidote, fluorite, illite, oxides, pyrite, prehnite, quartz

1177-1145 masl (780-812 m)   **Tuff**
Whitish coloured, glassy tuff cuttings showing alteration to clays. The groundmass is glassy to ashy. The rock has abundant pyrite crystals disseminated in the matrix and also in veins. Rare chalcedony which has been partly transformed into quartz occurs in veins and vesicles.
Alteration minerals: Calcite, chalcedony, chlorite, illite, epidote, oxides, pyrite, quartz

1145-1113 masl (812-844 m)   **Rhyolite**
Grey to greyish brown, high silica, quartz and feldspar porphyritic rock. The phenocrysts are set in a very fine grained groundmass. Crystals of soda amphiboles (riebeckite) show slight alteration to clays. The rock shows moderate oxidation and has fine pyrite cubes disseminated in the groundmass as well as in veins.
Alteration minerals: Adularia, albite, calcite, chlorite, epidote, illite, oxides, pyrite, wairakite, quartz

1113-1035 masl (844-922 m)   **Tuff**

Grey to brown tuffaceous cuttings having a glassy matrix. The rock is dominated by glass, quartz, rhyolite and ash particles. It is highly altered to clays with quartz, pyrite and calcite occurring in veins. *NB: 1055-1035 masl, the rock cuttings are mixed up with trachytic ones dominating.*
Alteration minerals: Adularia, calcite, chlorite, epidote, fluorite, illite, oxides, pyrite

1035-1009 masl (922-948 m)   **Trachyte**

Dark grey, fine grained feldspar porphyritic rock. The rock is porphyritic with euhedral phenocrysts of K-feldspars and sanidine. Pyrite cubes are disseminated in the groundmass.
Alteration minerals: Adularia, albite, calcite, chlorite, epidote, fluorite, illite, oxides, pyrite, sphene, wairakite, quartz

1009-989 masl (948-968 m)   **Basaltic intrusive**

Dark grey, fine to medium grained feldspar porphyritic rock. The large K-feldspars crystals are nearly 5 mm in length are strongly embayed and show alteration to greenish clays. Some of the feldspars show replacement by albite and exhibit chessboard like twinning.
Alteration minerals: Adularia, albite, calcite, chlorite, epidote, fluorite, oxides, pyrite, sphene, wairakite, quartz

989-675 masl (968-1282 m)   **Trachyte**

Grey, fine grained porphyritic rock consisting of large plagioclase phenocrysts and rare pale green clinopyroxenes in a fine grained matrix. The matrix shows trachytic flow texture and is slightly altered to clays. Pyrite is abundant from 767 masl.
Alteration minerals: Albite, calcite, chlorite, illite, epidote, oxides, pyrite, sphene, quartz

675-639 masl (1282-1318 m)   **Basalt**

Grey to greenish rock with phenocrysts of plagioclase set in a holocrystalline groundmass of lath shaped plagioclase microlites, granules of augite and minute octahedral magnetite. The rock shows high alteration to greenish chlorite and white mica. It has abundant calcite infilling veins and vugs. Paragenetic sequence in veins indicates epidote to be the earlier formed mineral followed by calcite.

Alteration minerals: Albite, adularia, calcite, chlorite, epidote, fluorite, oxides, pyrite, sphene, quartz

639-517 masl (1318-1440 m)   **Trachyte**

Grey, fine grained feldspar porphyritic rock. The phenocrysts are made up of embayed K-feldspar and the groundmass consists mainly of microlites of feldspars exhibiting trachytic flow texture and iron oxides showing alteration to sphene. The rock generally shows alteration to clays.
Alteration minerals: Albite, calcite, chlorite, epidote, fluorite, oxides, prehnite, pyrite, quartz, sphene, wairakite

517-437 masl (1440-1520 m)   **Rhyolite**

Grey to greyish brown, quartz and feldspar porphyritic rock showing flow texture. The phenocrysts are set in a glassy groundmass with fibrous crystals of amphibole exhibiting spherulitic texture. The rock shows moderate oxidation and has fine pyrite cubes disseminated in the groundmass. High oxidation noted at 497-495 masl and also at 471-465 masl which is a probable contact zone. The rock shows metallic luster an indication of contact metamorphism.
Alteration minerals: Calcite, chlorite, epidote, oxides, prehnite, pyrite, quartz, sphene

437-317 masl (1520-1640 m)   **Trachyte**

Grey, fine grained feldspar porphyritic rock. The rock is moderately altered to clays and has well formed pyrite cubes disseminated in the groundmass. The rock shows stumpy feldspar laths exhibiting trachytic flow texture. Epidote, calcite and quartz are some of the alteration minerals in veins.
Alteration minerals: Albite, calcite, chlorite, epidote, illite, oxides, pyrite, quartz, sphene

317-283 masl   (1640-1674 m)   **Basalt**
Greyish coloured, fine grained feldspar porphyritic rock. Phenocrysts of plagioclase occur in a groundmass of pyroxenes, plagioclase and interstitial glass. Plagioclase phenocrysts show polysynthetic twinning and replacement by calcite and albite along edges. The rock is highly altered to greenish and white clays.
Alteration minerals: Adularia, albite, calcite, chlorite, illite, epidote, fluorite, oxides, prehnite, pyrite, sphene, quartz

283-117 masl (1674-1840 m)   **Trachyte**
Grey, fine grained feldspar porphyritic rock. The sanidine phenocrysts show moderate alteration to complete replacement by calcite and clays. In thin section clearly formed stumpy feldspar laths exhibit trachytic flow texture. Trace calcite is observed filling vugs and pyrite is deposited in veins. The rock show intermittent oxidation.
Alteration minerals: Calcite, chlorite, epidote, illite, oxides, pyrite, quartz, sphene

117-87masl (1840-1870 m)   **No cuttings**

87-79 masl (1870-1878 m)   **Dolerite**
Dark grey, medium grained intrusive rock. The rock is crystalline with olivine, labradorite, and ophitic clinopyroxene and shows moderate to high alteration. The rock exhibits metallic luster along edges which is typical of contact metamorphism.
Alteration minerals: Albite, adularia, calcite, chlorite, epidote, illite, oxides, prehnite, pyrite, quartz

79 to -25 masl (1878-1982 m)   **Trachyte**
Grey, fine grained feldspar porphyritic rock. The phenocrysts are made up of mainly embayed K-feldspar. Pale green clinopyroxenes form subhedral to anhedral crystals and the groundmass consists of rare quartz, K-feldspar and iron oxides. The rock shows alteration to light green clays and has quartz and calcite in veins. Pyrite cubes are also deposited in veins as well as disseminated in the groundmass. Albite replaces feldspar and exhibit twinning.
Alteration minerals: Albite, calcite, chlorite, fluorite, epidote, garnet, illite, oxides, pyrite, quartz, sphene

-25 to -33 masl (1982-1990 m)   **Microsyenite**
Grey, medium grained intrusive rock with large tubular phenocrysts of feldspar. The groundmass consists of amphiboles, feldspars and pyroxenes. The rock is moderately altered to clays.
Alteration minerals: Calcite, chlorite, epidote, illite, oxides, pyrite, quartz

-33 to -81 masl (1990-2038 m)   **Trachyte**
Grey, fine grained highly altered feldspar porphyritic rock with poorly formed feldspar crystallites exhibiting trachytic flow texture. The rock is altered to greenish clays. Calcite occurs in veins in association with pyrite and epidote.
Alteration minerals: Albite, calcite, chlorite, epidote, illite, oxides, prehnite, pyrite, quartz

-81 to -117 masl (2038-2074 m)   **Tuff**
Dark grey glassy tuffaceous rock with the groundmass showing poorly developed crystallites. The rock is moderately altered to greenish clays. Feldspar lithics show alteration to clays, calcite and epidote.
Alteration minerals: Calcite, chlorite, epidote, illite, oxides, pyrite, quartz

-117 to -211 masl (2074-2168 m)   **Trachyte**
Grey, fine grained feldspar porphyritic rock. The feldspar phenocrysts show moderate to complete alteration to greenish clays. Well formed stumpy feldspar laths exhibit trachytic flow texture. Traces of calcite are observed as vug filling and pyrite is disseminated in the groundmass as well as deposited in veins. The rock shows intermittent oxidation.
Alteration minerals: Albite, chlorite, epidote, garnet, illite, oxides, pyrite, quartz, sphene

-211 to -213 masl (2168-2174)   Microsyenite
Grey, medium grained rock with large tubular phenocrysts of feldspars. The trachytic groundmass consists of amphiboles, feldspars and pyroxenes. The rock is moderately altered to clays.
Alteration minerals: Calcite (rare), chlorite, epidote, illite, oxides, pyrite, quartz, sphene

-213 to -243 masl (2174-2200 m)   Trachyte
Grey, fine grained feldspar porphyritic rock. The feldspar phenocrysts show moderate to complete alteration to greenish clays. Stumpy feldspar laths exhibit trachytic flow texture. Trace calcite is observed as vug filling and pyrite is disseminated in the groundmass as well as deposited in veins. Some doleritic rock chippings are observed at -233 to -235 masl.
Alteration minerals: Calcite (rare), chlorite, epidote, illite, oxides (rare), pyrite, quartz, sphene

APPENDIX VII: Lithologic description of drill cuttings and hydrothermal alteration minerals of well OW-903. The list of hydrothermal alteration minerals given for each rock type is based on binocular and petrographic microscopes, X-ray diffraction and electron microprobe analyses

2043-2027 masl (0-16 m)   Pyroclastics
Loose soils/pyroclastics made up of mainly weathered pumice obsidian and lithic fragments.
Alteration minerals: Chalcedony, oxides

2027-1991 masl (16-52 m)   No Cuttings   (Loss of circulation)

1991-1975 masl (52-68 m)   Rhyolite
Grey, fine-grained rock consisting of phenocrysts of anhedral quartz and anhedral but locally embayed rare K-feldspar phenocrysts set in a glassy groundmass. The mafics are made up of sodic pyroxenes and amphiboles. Needle like crystals of soda amphiboles are seen to enclose quartz in a devitrified groundmass. Pyroxenes and amphiboles show concentration along flow banding and show very little or no alteration at all.
Alteration minerals: Chalcedony, oxide, pyrite

1975-1787 masl (68-256 m)   No Cuttings   (Loss of circulation)

1787-1695 masl (256-348 m)   Rhyolite
Grey fine-grained quartz and feldspar porphyritic rock. The phenocrysts of anhedral quartz and anhedral, but locally embayed, rare K-feldspar phenocrysts are set in a glassy groundmass. The mafics consist of sodic pyroxenes and amphiboles. Needle like crystals of soda amphibole are seen to enclose quartz in a devitrified groundmass. The rock shows moderate alteration to clays.
Alteration minerals: Chalcedony, chlorite, mordenite, oxide, pyrite

1695-1663 masl (348-380 m)   Rhyolite
Grey, fine-grained lava exhibiting flow texture. In thin section the rock shows quartz and K-feldspar phenocrysts set in a glassy groundmass. Riebeckite and quartz needles exhibit spherulitic texture.
Alteration minerals: Chalcedony, illite, oxides, pyrite, chlorite

1663-1551 masl (380-492 m)   Rhyolite
Brownish grey, fine grained, locally flow banded rock with low phenocryst content. The phenocrysts are made up of anhedral quartz and subhedral feldspars. In thin section, needle like crystals of quartz, alkali feldspars and riebeckite radiate from a common nucleus exhibiting spherulitic texture. At some parts the rock shows extensive oxidation due to baking of the underlying rock. Pyrite is disseminated in the groundmass and also lining veins and infilling vesicles.
Alteration minerals: Chalcedony, calcite, illite, fluorite, mordenite, oxides, pyrite, quartz

1551-1539 masl (492-504 m)   **No Cuttings   (Loss of circulation)**

1539-1517 masl (504-526 m)   Rhyolite
Brownish-grey, fine grained quartz and feldspar porphyritic rock showing moderate alteration to clays. In thin section, crystals of both quartz and alkali feldspars radiate from a common nucleus exhibiting spherulitic texture. Calcite replaces plagioclase and is also deposited in veins in association with fluorite.
Alteration minerals: Calcite, fluorite, oxides, pyrite, quartz

1517-1381 masl (526-662 m)   Rhyolite
Grey to greyish brown quartz and feldspar porphyritic lava rock. The phenocrysts are set in a glassy groundmass with fibrous crystals of riebeckite exhibiting spherulitic texture. The rock shows moderate oxidation and has fine pyrite cubes disseminated in the groundmass. High oxidation noted at 1469-1467 masl and at 1445-1443 masl which are probably fractured zones.
Alteration minerals: Clays, oxides, pyrite, mordenite, sphene

1381-1315 masl (662-728 m)   Trachyte
Brownish grey, fine-grained feldspar porphyritic lava. The rock has poorly developed crystallites in a glassy groundmass oriented in preferred directions exhibiting trachytic flow texture.
Alteration minerals: Calcite, chlorite, fluorite, illite, oxides, pyrite, quartz

1315-1285 masl (728-758 m)   Tuff
Greyish brown, rock containing clasts of devitrified rhyolite plus a few angular crystals of K-feldspar. Abundant chlorite and tiny rhombs of adularia occur in the groundmass.
Alteration minerals: Adularia, calcite, chlorite, fluorite, oxides, pyrite, quartz, mordenite

1285-1257 masl (758-786 m)   Basalt
Dark grey, fine-grained feldspar porphyritic rock. Pyroxenes persist in some cuttings and are characterized by a variety of hydrothermal minerals that occur in vesicles and veins. Plagioclase phenocrysts show replacement by calcite.
Alteration minerals: Calcite, chlorite, fluorite, oxides, pyrite, quartz

1257-1203 masl (786-840 m)   Trachyte
Light grey to greyish brown coloured rock consisting of euhedral K-feldspars in a trachytic groundmass. Plagioclase and K-feldspar show alteration to clays, calcite and quartz. Bladed calcite occurs indicating boiling at this part of the reservoir. Paragenetic sequence of hydrothermal minerals in vesicles indicate two generations of calcite with the sequence being calcite, chlorite and calcite.
Alteration minerals: Calcite, chlorite, fluorite, illite, oxides, pyrite, quartz,

1203-1127 masl (840-916 m)   Basaltic intrusive
Greyish coloured, fine-grained feldspar porphyritic rock. Micro-phenocrysts of olivine occur in a groundmass of pyroxenes, plagioclase and interstitial glass. Plagioclase phenocrysts show polysynthetic twinning and replacement by calcite along the edges. The paragenetic sequence indicates the earlier formed mineral to be quartz followed by chlorite, then quartz and lastly oxides. Bladed calcite occurs indicating boiling must have occurred in the reservoir. At 1161-1159 masl, the rock shows some baking and exhibit metallic luster an indication contact metamorphism. Rare chalcedony crystallizing to quartz is observed in vesicles.
Alteration minerals: Adularia, albite, corrensite, chalcedony, calcite, fluorite, oxides, pyrite, quartz, wairakite

1127-1079 masl (916-964 m)   Tuff
Greyish-green tuffaceous rock with a groundmass made up of very fine-grained banded ashy matrix. It consists of flow banded rhyolite, plagioclase and quartz fragments enclosed in a fine grained matrix which could have originally been glassy. The rock exhibits contact metamorphism as indicated by grey metallic luster at 1117-1115 masl.
Alteration minerals: Calcite, chlorite, fluorite, illite, pyrite, quartz, wairakite

67

1079-1009 masl (964-1034 m)   Rhyolite
Light grey, porphyritic lava with a fine grained groundmass containing tiny plagioclase laths and short opaque magnetite grains. The rock is enriched with soda amphiboles and exhibit spherulitic texture. The groundmass is glassy and consists of microphenocrysts of aegerine, quartz, K-feldspar laths, riebeckite and magnetite which show slightly oxidation.
Alteration minerals: Albite, calcite, chlorite, illite, oxides, pyrite, quartz

1009-955 masl (1034-1088 m)   Tuff
Whitish to brownish grey tuffaceous rock showing moderate alteration to greenish clays. The rock is glassy and consists of fragments of quartz and feldspars enclosed in an ashy matrix. At 991-987 masl the rock shows extensive oxidation indicated by abundant iron oxyhydroxides. Rare chalcedony occurs at 1001 masl. Abundant bladed calcite occurs within rock unit indicating boiling in this part of the reservoir.
Alteration minerals: Chalcedony, calcite, clays, oxides, pyrite, quartz

955-915 masl (1088-1128 m)   Tuff
Brownish coloured tuffaceous cuttings showing slight alteration to greenish clays. The rock consists of sub-angular xenoliths, subhedral phenocrysts of quartz and feldspar fragments cemented in an ashy matrix. The first occurrence of well crystallized epidote occurs at 955 masl, indicating formation temperatures of over 250°C. Rare chalcedony that has been partly transformed into quartz occurs at 945-941 and at 927-923 masl.
Alteration minerals: Calcite, chalcedony, chlorite, epidote, fluorite, pyrite, quartz,

915-825 masl (1128-1218 m)   Tuff
Greyish brown, tuffaceous rock consisting of broken quartz and feldspar fragments cemented in an ashy matrix. Rare chalcedony occurs and part of it has recrystallized into quartz. The rock exhibits metallic luster indicating contact metamorphism. Well crystallized epidote occurs in veins.
Alteration minerals: Chalcedony, calcite, clays, epidote, fluorite, oxides, pyrite, quartz, sphene, wairakite

825-775 masl (1218-1268 m)   Trachyte
Greyish brown, fine-grained lava with occasional phenocrysts of embayed plagioclase feldspar in strongly oxidized trachytic groundmass. Vein minerals found are quartz, epidote and chalcedony. The paragenetic sequence indicates that chalcedony formed after oxides in the vesicles. Well formed epidote crystals fill veins.
Alteration minerals: Albite, adularia, chalcedony, calcite, chlorite, epidote, fluorite, illite, oxides, pyrite, quartz

775-737 masl   (1268-1306 m)   Tuff
Whitish coloured, tuffaceous rock showing alteration to clays. The rock has veins infilled with quartz and calcite. Epidote occurs in association with quartz. Rare chalcedony which has partly re-crystallizing into quartz occurs in vesicles.
Alteration minerals: Chalcedony, calcite, chlorite, epidote, fluorite, illite, pyrite, quartz

737-701 masl (1306-1342 m)   Tuff
Brownish coloured, tuffaceous cuttings showing moderate alteration to clays. In thin section, fragments of quartz, feldspar and trachyte are cemented in a glassy to ashy matrix.
Alteration minerals: Calcite, chlorite, epidote, fluorite, pyrite, quartz, wairakite

701-643 masl (1342-1400 m)   Trachyte
Grey to light-grey, fine-grained feldspar porphyritic rock. The rock is moderately altered to clays and has well formed pyrite cubes disseminated in the groundmass. In thin section the rock shows stumpy feldspar laths exhibiting trachytic flow texture.
Alteration minerals: Adularia, albite, calcite, chlorite, epidote, fluorite, illite, pyrite, quartz, sphene

643-549 masl (1400-1494 m)   Trachyte
Grey to greyish brown, fine grained highly altered feldspar porphyritic rock. The poorly formed feldspar crystallites exhibit trachytic flow texture. The rock is altered to clays and has bladed calcite in veins, an indication of boiling (CO_2 loss) in the reservoir. Large pyrite cubes are embedded in the rock. Well formed crystals of epidote are deposited in veins.
Alteration minerals: Albite, adularia, calcite, chlorite, epidote, fluorite, oxides, illite, pyrite, quartz, sphene

549-517 masl   (1494-1526 m)   Trachyte
Grey, fine grained feldspar phyric moderately altered rock. The rock has poorly formed short stumpy feldspar crystallites exhibiting trachytic flow texture.   Rare chalcedonic silica which is partly crystallized into quartz occurs.
Alteration minerals: Albite, calcite, chalcedony, chlorite, epidote, fluorite, illite, oxide, pyrite, quartz, sphene, wairakite

517-499 masl   (1526-1544 m)   Basalt
Dark grey, fine-grained feldspar porphyritic rock. Plagioclase phenocrysts show alteration to chlorite and metasomatism by calcite along the edges. Abundant calcite occurs as vein fillings in association with quartz and epidote. Rare chalcedony partly crystallized to quartz occurs in vesicles and veins.
Alteration minerals: Albite, biotite, chalcedony, calcite, chlorite, epidote, fluorite, illite, oxides, pyrite, quartz, sphene

499-441 masl (1544-1602 m)   Trachyte
Greyish brown, fine grained rock. The rock shows flow banding texture with poorly formed crystallites of feldspars exhibiting trachytic flow texture. The rock is altered to clays and consist of well formed quartz crystals in veins.
Alteration minerals: Adularia, albite, biotite, calcite, chlorite, epidote, fluorite, oxides, illite, pyrite, quartz, sphene

441-405 masl (1602-1638 m)   Trachyte
Dark grey fine grained feldspar porphyritic lava. The rock is altered to clays and has abundant epidote in vesicles. Stumpy feldspar phenocrysts exhibit trachytic flow texture. The paragenetic sequence indicates calcite to be the earlier deposited mineral followed by epidote.
Alteration minerals: Calcite, biotite, chlorite, garnet, epidote, fluorite, illite, pyrite, sphene, wairakite

405-385 masl   (1638-1658 m)   Trachyte
Grey, fine-grained feldspar porphyritic rock showing alteration to clays. In thin section clearly formed feldspar laths exhibit trachytic flow texture. Bladed calcite filling vugs and pyrite is disseminated in the groundmass as well as lining veins. Plagioclase is show replacement by the albite.
Alteration minerals: Albite, calcite, chlorite, epidote, fluorite, garnet, oxides, quartz, sphene

385-371 masl (1658-1672 m)   Basalt
Greyish brown to greenish lava showing generally high alteration to clays. It has abundant calcite fillings in veins and vugs. In thin section phenocrysts of plagioclase are embedded in a holocrystalline groundmass of lath shaped plagioclase microlites, granules of augite and minute octahedral magnetite. Presence of olivine is revealed by its crystal outline having undergone complete metasomatism.
Alteration minerals: Albite, adularia, biotite, calcite, chlorite, epidote, garnet, illite, pyrite, oxides, quartz

371-307 masl   (1672-1736)   Trachyte
Grey, fine grained moderately altered rock. The rock is feldspar porphyritic with stumpy feldspar laths exhibiting trachytic flow texture. The paragenetic sequence observed in the vesicles indicates the latest deposited mineral to be epidote after quartz.
Alteration minerals: Albite, calcite, chlorite, epidote, fluorite, illite, pyrite, oxides, quartz, sphene

307-247 masl (1736-1796 m)   **Trachyte**
Greyish coloured, fine grained feldspar porphyritic lava. The feldspar phenocrysts show alteration to clays and also replacement by calcite.   Some phenocrysts show complete alteration to clays. The paragenetic sequence indicates epidote to be a later mineral deposit after chlorite.
Alteration minerals: Biotite, chlorite, epidote, illite, oxides, pyrite, sphene

247-229 masl   (1796-1814 m)   **Trachyte**
Grey, fine grained feldspar porphyritic rock. The rock shows moderate alteration to clays. In thin section clearly formed feldspar laths exhibit trachytic flow texture. Little calcite is observed as fillings in vugs.
Alteration minerals: Albite, calcite, chlorite, epidote, garnet, illite, pyrite, oxides, quartz, sphene, wairakite

229-203 masl   (1814-1840 m)   **Microsyenite**
Light grey coloured, medium grained rock showing little alteration.   The bulk of the rock is microcrystalline with good segregation of mafic minerals.   It has large feldspar phenocrysts, which show replacement by calcite.   Arfvedsonite and pyroxenes also show alteration to chlorite.   Calcite and well crystallized epidote are deposited in veins.
Alteration minerals: Albite, calcite, chlorite, garnet, epidote, pyrite, oxides, quartz, sphene

203-183 masl (1840-1860 m)   **Trachyte**
Grey to light grey, fine-grained feldspar porphyritic rock. The rock is moderately altered to clays and has pyrite crystals disseminated in the groundmass. In thin section the rock shows stumpy feldspar laths exhibiting trachytic texture.   Paragenetic sequence in the rock indicates calcite to be a later deposited mineral after chlorite.
Alteration minerals: Albite, biotite, calcite, chlorite, epidote, illite, pyrite, oxides, quartz, sphene

183-171 masl (1860-1872 m)   **Trachyte**
Grey, fine grained feldspar porphyritic rock with mafics disseminated in the groundmass. The rock shows moderate alteration to clays. In thin section clearly formed stumpy feldspar laths exhibit trachytic texture. Calcite is seen replacing plagioclase and also deposited in veins. Apatite occurs as a primary mineral. The paragenetic sequence from the latest is calcite, epidote and chlorite.
Alteration minerals: Calcite, biotite, chlorite, epidote, fluorite, garnet, prehnite, pyrite, oxides, quartz, sphene

171-143 masl (1872-1900 m)   **Trachyte**
Greyish brown, feldspar porphyritic rock showing moderate alteration to clays. In thin section clearly formed stumpy feldspar laths exhibit trachytic flow texture.
Alteration minerals: Albite, calcite, chlorite, illite, epidote, pyrite, oxides

143-95 masl (1900-1948 m)   **Trachyte**
Greyish coloured, fine grained feldspar porphyritic rock. The rock has abundant quartz in association associated with epidote in veins. At 87-85 masl, the paragenetic sequence in veins indicates epidote to be an earlier deposited mineral followed by quartz.
Alteration minerals: Actinolite, adularia, albite, chlorite, epidote, illite, oxides, prehnite (rare), pyrite, quartz, sphene

95 to -53 masl   (1948-2096 m)   **Trachyte**
Grey, fine grained feldspar porphyritic rock. The sanidine phenocrysts show moderate alteration to clays. In thin section clearly formed stumpy feldspar laths exhibit trachytic flow texture. The feldspar phenocrysts show alteration to clays some almost completely replaced. Traces of calcite are observed as fillings in vugs. The rock show intermittent oxidation.
Alteration minerals: Actinolite, albite, biotite, chlorite, epidote, fluorite, garnet, illite, pyrite, oxides, quartz

-53 to -61m (2096-2104 m)   **Microsyenite**

Grey, medium grained rock with tubular phenocrysts of feldspars in a trachytic groundmass consisting of nepheline, feldspars and pyroxenes. The rock is moderately altered to clays.

Alteration minerals: Albite, chlorite, clays, epidote, fluorite, oxides, pyrite, quartz

-61 to -85 masl (2104-2128 m)   **Trachyte**

Grey, fine grained feldspar porphyritic rock with rare quartz phenocrysts. The rock is altered to clays. In vesicles, paragenesis indicates calcite as an earlier formed mineral followed by chlorite. Rare calcite occurs.

Alteration minerals: Actinolite, calcite (trace), chlorite, epidote, fluorite, garnet, illite, oxides, pyrite, quartz, sphene

-85 to -113 masl (2128-2156 m)   **No Cuttings**   **(Loss of circulation)**

-113 to -159 masl (2156-2202 m)   **Tuff**

Dark grey glassy tuffaceous rock. The groundmass show poorly developed crystallites in a glassy to ashy matrix. It is moderately altered to clays.

Alteration minerals: Actinolite, biotite, chlorite, fluorite, epidote, garnet, oxides, pyrite, sphene